

# Framework for $\exists\mathbb{R}$ -Completeness of Two-Dimensional Packing Problems

Mikkel Abrahamsen\*, Tillmann Miltzow†, Nadjia Seiferth‡

April 16, 2020

## Abstract

We show that many natural two-dimensional packing problems are algorithmically equivalent to finding real roots of multivariate polynomials. A two-dimensional packing problem is defined by the type of pieces, containers, and motions that are allowed. The aim is to decide if a given set of pieces can be placed inside a given container. The pieces must be placed so that in the resulting placement, they are pairwise interior-disjoint, and only motions of the allowed type can be used to move them there. We establish a framework which enables us to show that for many combinations of allowed pieces, containers, and motions, the resulting problem is  $\exists\mathbb{R}$ -complete. This means that the problem is equivalent (under polynomial time reductions) to deciding whether a given system of polynomial equations and inequalities with integer coefficients has a real solution.

We consider packing problems where only translations are allowed as the motions, and problems where arbitrary rigid motions are allowed, i.e., both translations and rotations. When rotations are allowed, we show that the following combinations of allowed pieces and containers result in  $\exists\mathbb{R}$ -complete problems:

- simple polygons, each of which has at most 8 corners, into a square,
- convex objects bounded by line segments and hyperbolic curves into a square,
- convex polygons into a container bounded by line segments and hyperbolic curves.

Restricted to translations, we show that the problems for the following combinations are  $\exists\mathbb{R}$ -complete:

- objects bounded by segments and hyperbolic curves into a square,
- convex polygons into a container bounded by segments and hyperbolic curves.

Two-dimensional packing problems are an active field of research both in computational geometry and operations research. The problems are very important in many industries and processes such as clothing production, sheet metal cutting, shipping, and 3D printing. Our results give an explanation for the lack of exact algorithms, as it follows that many natural attempts to discretize the problems have inherent shortcomings.

In practice, packing problems are solved with heuristics. This work explains why methods guaranteed to produce optimal solutions for problems in NP, like SAT- or IP-solvers, are not applicable without additional assumptions, unless  $\exists\mathbb{R} = \text{NP}$ .

---

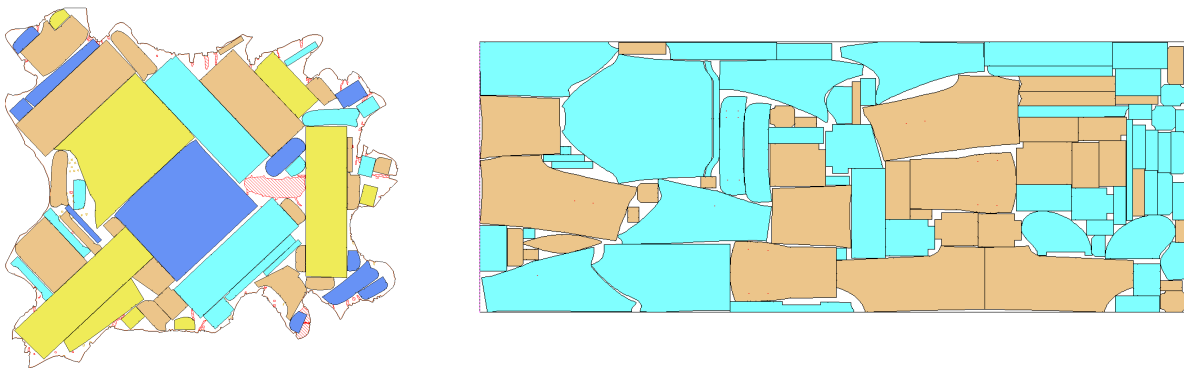
\*Basic Algorithms Research Copenhagen (BARC), University of Copenhagen. BARC is supported by the VILLUM Foundation grant 16582. [miab@di.ku.dk](mailto:miab@di.ku.dk)

†Utrecht University. Supported by the Netherlands Organisation for Scientific Research (NWO) under project no. 016.Veni.192.25 [t.miltzow@googlemail.com](mailto:t.miltzow@googlemail.com)

‡Freie Universität Berlin. [nadja.seiferth@fu-berlin.de](mailto:nadja.seiferth@fu-berlin.de)

# Contents

<b>1</b>	<b>Introduction</b>	<b>1</b>
<b>2</b>	<b>Reduction skeleton</b>	<b>6</b>
<b>3</b>	<b>Complete example</b>	<b>17</b>
<b>4</b>	<b>Preliminaries</b>	<b>18</b>
4.1	Encoding Polygons and Motions . . . . .	18
4.2	Elementary Geometry . . . . .	19
4.3	Universality . . . . .	19
<b>5</b>	<b>RANGE-ETR-INV and WIRED-INV</b>	<b>21</b>
5.1	Reduction to Conjunctive Form . . . . .	21
5.2	Reduction to Compact Semi-Algebraic Sets . . . . .	23
5.3	Reduction to ETR-AMI . . . . .	24
5.4	Reduction to ETR-SMALL . . . . .	25
5.5	Reduction to ETR-SHIFT . . . . .	27
5.6	Reduction to ETR-SQUARE . . . . .	30
5.7	Reduction to RANGE-ETR-INV . . . . .	32
5.8	Reduction to WIRED-INV . . . . .	36
<b>6</b>	<b>Fingerprinting</b>	<b>38</b>
6.1	Fingerprinting a single piece . . . . .	38
6.2	Fingerprinting more pieces at once . . . . .	40
6.3	Proof of Single Fingerprint (Lemma 45) . . . . .	43
6.4	Generalization to curved polygons . . . . .	51
<b>7</b>	<b>Linear gadgets</b>	<b>53</b>
7.1	Anchor . . . . .	53
7.2	Swap . . . . .	58
7.3	Split . . . . .	62
7.4	Adder . . . . .	63
<b>8</b>	<b>Inversion gadgets</b>	<b>68</b>
8.1	Teeter-Totter . . . . .	69
8.2	Seesaw . . . . .	73
8.3	Gramophone . . . . .	76
8.4	Concluding remarks on inversion . . . . .	81
<b>9</b>	<b>Square container</b>	<b>83</b>
<b>10</b>	<b>Universality-type theorems</b>	<b>89</b>
<b>11</b>	<b>References</b>	<b>93</b>



**Figure 1:** Real examples of nesting on a leather hide (left) and a piece of fabric (right), kindly provided by MIRISYS and produced by their software for automatic nesting, <https://www.mirisys.com/>.

## 1 Introduction

Packing problems are everywhere in our daily lives. To give a few examples, you solve packing problems when deciding where to put your furniture in your home, the manufacturer of your clothing arranges cutting patterns on a large piece of fabric in order to minimize waste, and at Christmas time you are trying to cut out as many cookies from a dough as you can. In a large number of industries, it is crucial to solve complicated instances of packing problems efficiently. In addition to clothing manufacturing, we mention leather, glass, wood, and sheet metal cutting, selective laser sintering, shipping (packing goods in containers), and 3D printing (arranging the parts to be printed in the printing volume); see Figure 1.

Packing problems can be easily and precisely defined in a mathematical manner, but many important questions are still completely elusive. In this work, we uncover a fundamental aspect of many versions of geometric packing by settling their computational difficulty.

We denote  $\mathbf{Pack}(\mathcal{P} \rightarrow \mathcal{C}, \mathcal{M})$  as the packing problem with pieces of the type  $\mathcal{P}$ , containers of type  $\mathcal{C}$ , and motions of type  $\mathcal{M}$ . In an instance of  $\mathbf{Pack}(\mathcal{P} \rightarrow \mathcal{C}, \mathcal{M})$ , we are given pieces  $p_1, \dots, p_n$  of type  $\mathcal{P}$  and a container  $C$  of type  $\mathcal{C}$ . We want to decide if there is a motion of type  $\mathcal{M}$  for each piece such that after moving the pieces by these motions, each piece is in  $C$  and the pieces are pairwise interior-disjoint. Such a placement of the pieces is called a *valid* placement.

As the allowed motions, we consider *translations* ( $\rightarrow$ ) and *rigid motions* ( $\rightarrow$ ), where a rigid motion is a combination of a translation and a rotation. As containers and pieces, we consider squares ( $\square$ ), convex polygons ( $\triangleleft$ ), simple polygons ( $\triangleright$ ), convex curved polygons ( $\triangleright$ ), and curved polygons ( $\triangleright$ ), where a *curved polygon* is a region enclosed by a simple closed curve consisting of a finite number of line segments and arcs contained in hyperbolae (such as the graph of  $y = 1/x$ ).

The problems with only translations allowed are relevant to some industries; for instance when arranging cutting patterns on a roll of fabric for clothing production, where the orientation of each piece has to follow the orientation of the weaving or a pattern printed on the fabric. In other contexts such as leather, glass, or sheet metal cutting, there are usually no such restrictions, so rotations can be used to minimize waste. As can be seen from Figure 1, it is relevant to study packing problems where the pieces as well as the containers may be non-convex and have boundaries consisting of many types of curves (not just straight line segments).

We show that many of the above mentioned variants of packing are  $\exists\mathbb{R}$ -complete. The complexity class  $\exists\mathbb{R}$  will be defined below. We call our developed techniques a *framework*, since the same techniques turn out to be applicable to prove hardness for many versions of packing.

With adjustments or additions, they can likely be used for other versions or proofs of other types of hardness as well.

**The Existential Theory of the Reals.** The term *Existential Theory of the Reals* refers ambiguously to a formal language, a corresponding algorithmic problem (ETR), and a complexity class ( $\exists\mathbb{R}$ ). Let us start with the formal logic. Let

$$\Sigma := \{\forall, \exists, 0, 1, x_1, \dots, x_n, +, \cdot, =, \leq, <, \wedge, \vee, \neg\}$$

be an alphabet for some  $n \geq 1$ . A *sentence* over  $\Sigma$  is a well-formed formula with no free variables, i.e., so that every variable is bound to a quantifier. The *Existential Theory of the Reals* is the true sentences of the form

$$\exists x_1, \dots, x_n \Phi(x_1, \dots, x_n),$$

where  $\Phi$  is a quantifier-free formula. The algorithmic problem ETR is to decide whether a sentence of this form is true or not. At last, this leads us to the complexity class *Existential Theory of the Reals* ( $\exists\mathbb{R}$ ), which consists of all those languages that are many-one reducible to ETR in polynomial time. Given a quantifier-free formula  $\Phi$ , we define the solution space of  $\Phi$  as  $V(\Phi) := \{\mathbf{x} \in \mathbb{R}^n : \Phi(\mathbf{x})\}$ . Thus in other words, ETR is to decide if  $V(\Phi)$  is empty or not. It is currently known that

$$\text{NP} \subseteq \exists\mathbb{R} \subseteq \text{PSPACE}. \quad (1)$$

To show the first inclusion is an easy exercise, whereas the second is non-trivial and was first proven by Canny [14]. A problem  $P$  is  $\exists\mathbb{R}$ -hard if ETR is many-one reducible to  $P$  in polynomial time, and  $P$  is  $\exists\mathbb{R}$ -complete if  $P$  is  $\exists\mathbb{R}$ -hard and in  $\exists\mathbb{R}$ .<sup>1</sup> None of the inclusions (1) are known to be strict, but the first is widely believed to be [12], implying that the  $\exists\mathbb{R}$ -hard problems are not in NP. As examples of  $\exists\mathbb{R}$ -complete problems, we mention problems related to realization of order-types [48, 46, 54], graph drawing [13, 21, 40, 43], recognition of geometric graphs [16, 17, 38, 45], straightening of curves [24], the art gallery problem [2], Nash-equilibria [11, 28], linkages [1, 50, 51], matrix-decompositions [20, 52, 53], and polytope theory [48]. See also the surveys [15, 44, 49].

**$\exists\mathbb{R}$ -membership.** Showing that the packing problems we are dealing with in this paper are contained in  $\exists\mathbb{R}$  is easy using the following recent result.






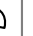




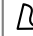

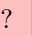

**Theorem** (Erickson, Hoog, Miltzow [25]). *For any decision problem  $P$ , there is a real verification algorithm for  $P$  if and only if  $P \in \exists\mathbb{R}$ .*





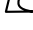
A *real verification algorithm* is like a verification algorithm for a problem in NP with the additional feature that it accepts real inputs for the witness and runs on the real RAM. (We refer to [25] for the full definition, as it is too long to include here.)




Thus in order to show that our packing problems lie in  $\exists\mathbb{R}$ , we have to specify a witness and a real verification algorithm. The witness is simply the motions that move the pieces to a valid placement. The verification algorithm checks that the pieces are pairwise interior-disjoint and contained in the container. Note that without the theorem above, we would need to describe an ETR-formula equivalent to a given packing instance in order to show  $\exists\mathbb{R}$ -membership. Although this is not difficult for packing, it would still require some work.

---

<sup>1</sup>There seems to be no general convention about how to pronounce terms such as  $\exists\mathbb{R}$ -complete. We propose to use the pronunciation *E-T-R*-complete.

motions		 							
pieces									
containers		$\exists\mathbb{R}$ *	$\exists\mathbb{R}$	$\exists\mathbb{R}$	$\exists\mathbb{R}$	$\exists\mathbb{R}$ *	$\exists\mathbb{R}$	$\exists\mathbb{R}$	$\exists\mathbb{R}$
		?	$\exists\mathbb{R}$	$\exists\mathbb{R}$	$\exists\mathbb{R}$	NP	NP	?	$\exists\mathbb{R}$
		?	$\exists\mathbb{R}$ *	$\exists\mathbb{R}$ *	$\exists\mathbb{R}$	NP	NP	?	$\exists\mathbb{R}$ *

 square  
 convex polygon  
 convex curved polygon  
 simple polygon  
 curved polygon

  rigid motion  
 translation

**Table 1:** This table displays 12 variants of the packing problem with rotations and translations, and 12 with translations only.  $\exists\mathbb{R}$  means  $\exists\mathbb{R}$ -complete and NP means NP-complete. We show that 16 of the problems are  $\exists\mathbb{R}$ -complete. The problems marked with \* are the *basic* problems. The  $\exists\mathbb{R}$ -completeness of the remaining problems follow since there is a basic problem in the table which is more restricted. The complexities of the four variants marked with ? remain elusive.

**Results.** We show that various two-dimensional packing problems are  $\exists\mathbb{R}$ -complete. A compact overview of our results is displayed in Table 1. In the table, the second row (with problems  $\text{Pack}(\mathcal{P} \rightarrow \triangleright, \mathcal{M})$ ) is in some sense redundant, since the  $\exists\mathbb{R}$ -completeness results can be deduced from the more restricted third row (the problems  $\text{Pack}(\mathcal{P} \rightarrow \square, \mathcal{M})$ ). We anyway include the row since a majority of our reduction is to establish hardness of problems with polygonal containers, and only later we reduce these problems to the case where the container is a square. For the green cells, we have constructions that work both with and without rotations allowed; for instance, we can use the same reduction to  $\text{Pack}(\square \rightarrow \triangleright, \circlearrowleft +)$  as to  $\text{Pack}(\square \rightarrow \triangleright, +)$ . For the orange cells, the reductions only work when rotations are allowed.

A strength of our reductions is that in the resulting constructions, all corners can be described with rational coordinates that require a number of bits only logarithmic in the total number of bits used to represent the instance. Therefore, we show that the problems are *strongly*  $\exists\mathbb{R}$ -hard. Another strength is that all the pieces have constant complexity, i.e., each piece can be described by its boundary as a union of  $O(1)$  straight line segments and arcs contained in hyperbolae.

It is folklore that the problems in the blue cells, i.e., the problems with polygonal pieces and containers and only translations allowed, are in NP, and in the following we sketch an argument why. We show that a valid placement can be specified as the translations of the pieces represented by a number of bits polynomial in the input size. Consider a valid placement of the pieces. For each pair of a segment  $s$  and a corner  $c$  (each of a piece or the container), we consider the line  $\ell(s)$  containing  $s$  and note which of the closed half-planes bounded by  $\ell(s)$  contains  $c$ . Then we build a linear program (LP) using that information in the natural way. Here, the translation of each piece is described by two variables and for each pair  $(s, c)$ , we have one constraint involving at most four variables, enforcing  $c$  to be on the correct side of  $\ell(s)$ . It is easy to verify that the constraint is linear. The solution of the LP gives a valid placement of every piece and as the LP is polynomial in the input, so is the number of the bits of the solution to the LP. Note that if rotations are included, the corresponding constraints become non-linear.

To sum up, we conclude that two distinct features are key for  $\exists\mathbb{R}$ -hardness of packing problems: Rotations and non-polygonal shapes. The results provide evidence that many packing problems are likely harder than problems in NP. This gives a confirmation to the operations research community that they cannot employ standard algorithm techniques (solvers for IP and SAT, etc.) that work well for many NP-complete problems like scheduling, TSP, and SAT. The main message for the theory community is that dealing with rotations or non-polygonal shapes

can probably only be done if we relax the problem considerably.

An important step in the proof of  $\exists\mathbb{R}$ -hardness of the art gallery problem [2] was the introduction of ETR-INV formulae.

**Definition 1.** An ETR-INV formula  $\Phi = \Phi(x_1, \dots, x_n)$  is a conjunction

$$\left( \bigwedge_{i=1}^n 1/2 \leq x_i \leq 2 \right) \wedge \left( \bigwedge_{i=1}^m C_i \right),$$

where  $m \geq 0$  and each  $C_i$  is of one of the forms

$$x + y = z, \quad x \cdot y = 1$$

for  $x, y, z \in \{x_1, \dots, x_n\}$ .

It was proven to be  $\exists\mathbb{R}$ -complete to decide if a given ETR-INV formula  $\Phi$  has a solution [2]. This has since then been used to prove  $\exists\mathbb{R}$ -completeness of a geometric graph drawing problem with prescribed face areas [21], completing a partially (straight-line) drawn graph [43], and the polytope nesting problem [20]. In this paper, we introduce the following promise problem which we prove is  $\exists\mathbb{R}$ -complete.

**Definition 2.** An instance  $\mathcal{I} = [\Phi, \delta, (I(x_1), \dots, I(x_n))]$  of the RANGE-ETR-INV problem consists of an ETR-INV formula  $\Phi$ , a number  $\delta := 2^{-l}$  for a positive integer  $l$ , and, for each variable  $x \in \{x_1, \dots, x_n\}$ , an interval  $I(x) \subseteq [1/2, 2]$  such that  $|I(x)| \leq 2\delta$ . For every inversion constraint  $x \cdot y = 1$ , we have either  $I(x) = I(y) = [1 - \delta, 1 + \delta]$  or  $I(x) = [2/3 - \delta, 2/3 + \delta]$  and  $I(y) = [3/2 - \delta, 3/2 + \delta]$ . We are promised that  $V(\Phi) \subset I(x_1) \times \dots \times I(x_n)$ . The goal is to decide whether  $V(\Phi) \neq \emptyset$ .

**Theorem 3.** RANGE-ETR-INV is  $\exists\mathbb{R}$ -complete, even when  $\delta = O(n^{-c})$  for any constant  $c > 0$ .

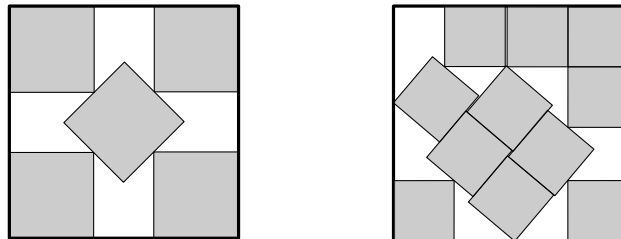
The promise that we only need to look for solutions to an ETR-INV formula in some tiny ranges of the variables will be crucial in our reduction.

**Related work.** Most papers on geometric packing problems in theoretical computer science allow translations only despite the high relevance of problems with rotations allowed. One line of research deals with packing axis-parallel rectangles into an axis-parallel rectangle with translations only [4, 7, 27, 33, 36, 37]. Most often an optimization version is studied where the rectangles also get weights and the aim is to maximize the total weight of the packed rectangles, in which case the problem is called 2-dimensional knapsack. The current best approximation factor is 1.89 using involved geometric arguments based on the idea to use an  $L$ -shaped layout [27]. There exists also a QPTAS [4].

Another line of research deals with strip-packing, where we are given a set of pieces that have to be placed inside a strip of a certain width in an axis-parallel fashion [3, 26, 31, 32, 35, 47]. Rotations by 90 degrees are sometimes allowed. The aim is to minimize the total height. The best polynomial time approximation algorithm has approximation ratio  $5/3 + \varepsilon$  [31], whereas the best pseudopolynomial time algorithm achieves an approximation ratio of  $5/4 + \varepsilon$  [32] and this is best possible [26].

Several other packing variants are known (or believed) to be NP-hard (some of the sources still lack detailed journal versions). Here we mention the problem of packing squares into a square by translation [42], packing segments into a simple polygon by translation [39], and packing circles into a square [19]. Alt [6] proves by a simple reduction from the partition

problem that packing rectangles into a rectangle is NP-hard, and this reduction works with and without rotations allowed (note that *a priori*, it is not clear that rotations make problems more difficult, and it is straightforward to define (artificial) problems that even get easier with rotations). It is easy to modify the reduction to the problem of packing rectangles into a square, so this implies NP-hardness of all problems in Table 1.



**Figure 2:** Left: The optimal packing of five unit squares already requires rotations. Right: The currently best known packing of eleven unit squares into a larger square [29].

A fundamental problem related to packing is to find the smallest square containing a given number of *unit* squares, with rotations allowed. A long line of mathematical research has been devoted to this problem, initiated by Erdős and Graham [23] in 1975, and it is still an active research area [18]. Even for *eleven* unit squares, the exact answer is unknown [29]; see Figure 2. Other packing problems have much older roots, for instance Kepler’s conjecture on the densest packings of spheres from 1611, famously proven by Hales in 2005 [30]. The 2D analog, i.e., finding the densest packings of unit disks, was solved already in 1773 by Joseph Louis Lagrange under the assumption that the disk configurations are lattices, and the general case was solved by László Fejes Tóth in 1940 [56] (Axel Thue already published a proof in 1890 which is considered incomplete).

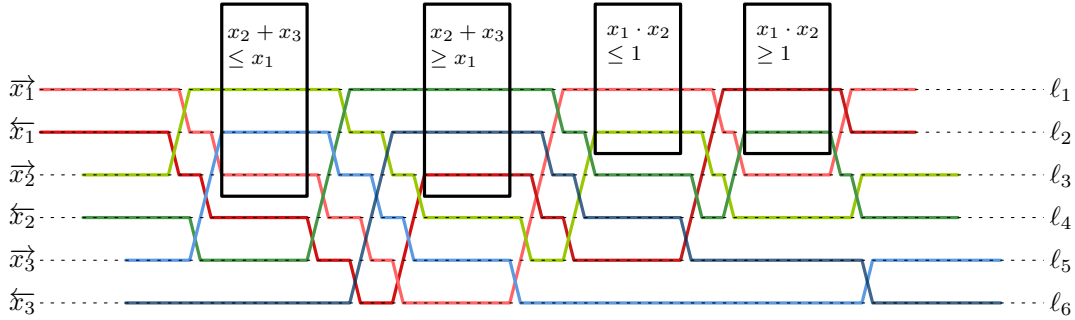
There is a staggering amount of papers in operations research on packing problems. The research is mainly experimental and focuses on the development of heuristics to solve benchmark instances efficiently. We refer to some surveys for an overview [9, 10, 22, 34, 41, 55]. In contrary to theoretical work, there is a lot of experimental work on packing pieces with irregular shapes and with arbitrary rotations allowed.

## 2 Reduction skeleton

In this section, we give an overview of the steps and concepts needed in our reductions. The rest of the paper will then fill out the details.

**RANGE-ETR-INV and WIRED-INV.** In Section 5, we prove Theorem 3, namely that the problem RANGE-ETR-INV (recall Definition 2) is  $\exists\mathbb{R}$ -complete. We also define an extension of the problem called WIRED-INV, which we also prove to be  $\exists\mathbb{R}$ -complete. An instance of WIRED-INV is an instance of RANGE-ETR-INV together with a graphical representation of the ETR-INV formula  $\Phi$ , i.e., a drawing of  $\Phi$  of a specific form, which we call a *wiring diagram*; see Figure 3 for an example. In the following, we outline the properties of a wiring diagram and refer to Section 5.8 for the details.

In a wiring diagram, each variable  $x_i$  of  $\Phi$ ,  $i \in \{1, \dots, n\}$ , is represented by two  $x$ -monotone polygonal curves  $\vec{x}_i$  and  $\overleftarrow{x}_i$ , which we call *wires*. The wires consist of segments contained in a set of  $2n$  equidistant horizontal lines  $\ell_1, \dots, \ell_{2n}$  and *jump segments* with endpoints on neighbouring lines  $\ell_j, \ell_{j+1}$ . The wires are disjoint except that each jump segment must cross another jump segment. It is important that the two wires  $\vec{x}_i, \overleftarrow{x}_i$  representing  $x_i$  start and end on the neighbouring lines  $\ell_{2i-1}, \ell_{2i}$ , respectively. We represent each constraint of  $\Phi$  as two inequalities, i.e.,  $x_i + x_j = x_k$  becomes  $x_i + x_j \leq x_k$  and  $x_i + x_j \geq x_k$  and  $x_i \cdot x_j = 1$  becomes  $x_i \cdot x_j \leq 1$  and  $x_i \cdot x_j \geq 1$ . Each inequality is represented by an axis-parallel *constraint box* intersecting the three or two topmost diagram lines; three for addition constraints and two for inversion constraints.



**Figure 3:** A wiring diagram corresponding to the ETR-INV formula  $x_2 + x_3 = x_1 \wedge x_1 \cdot x_2 = 1$ .

**Overview of geometric construction.** Let an instance  $\mathcal{I}$  of WIRED-INV be given with ETR-INV formula  $\Phi$  of variables  $x_1, \dots, x_n$  and  $\delta := n^{-300}$ . We are going to construct an instance of a packing problem with  $N = O(n^4)$  pieces, since this will be the complexity of the size of the wiring diagram of  $\mathcal{I}$ . The general idea is to build a packing instance on top of the wiring diagram. We define a polygonal container  $C := C(\mathcal{I})$  containing the wiring diagram in the interior, and a set of pieces  $\mathbf{p}$  to be placed in  $C$ . The container  $C$  is bounded from below by a line segment, from left and right by  $y$ -monotone chains, and from above by an  $x$ -monotone chain. See Figure 9 for a sketch of a complete example.

In Sections 7–8, we present reductions to the variants of the packing problem of the forms  $\mathbf{Pack}(\mathcal{P} \rightarrow \triangleright, \mathcal{M})$  and  $\mathbf{Pack}(\sqcap \rightarrow \sqcup, +)$ , i.e., where the container is a polygon or a curved polygon. Section 9 describes a reduction to the cases where the container is a square. This might however change the type of pieces: applying the reduction to a problem of the type  $\mathbf{Pack}(\mathcal{P} \rightarrow \sqcup, \mathcal{M})$  for  $\mathcal{P} \in \{\sqcap, \triangleright, \sqcup\}$  results in a problem of the type  $\mathbf{Pack}(\sqcup \rightarrow \square, \mathcal{M})$ , since pieces of type  $\sqcup$  will be added during the construction.



**Defining the construction in steps from left to right.** We define the packing instance as we sweep over the wiring diagram of  $\mathcal{I}$  with a vertical sweep line from left to right. Each step corresponds to one of the following events of the wiring diagram as we sweep over it from left to right:

- the introduction of a pair of wires  $(\vec{x}_i, \overleftarrow{x}_i)$ ,
- a crossing of two wires,
- an addition or inversion constraint,
- the termination of a pair of wires  $(\vec{x}_i, \overleftarrow{x}_i)$ .

In each step, we add one or more *gadgets*, each involving a constant number of pieces and possibly a constant number of edges to the boundary of the container  $C$ . When the sweep line passes over the right endpoints of the last wires  $(\vec{x}_n, \overleftarrow{x}_n)$ , the complete construction of the container  $C$  and all the pieces  $\mathbf{p}$  has been done.

The overall goal of the construction is to prove the following theorem.

**Theorem 4.** *Let  $C$  be the container and  $\mathbf{p}$  be the pieces of an instance of  $\mathbf{Pack}(\mathcal{P} \rightarrow \triangleright, \mathcal{M})$  or  $\mathbf{Pack}(\mathcal{P} \rightarrow \triangleleft, \mathcal{M})$  that we construct based on the instance  $\mathcal{I}$  of WIRED-INV, using the gadgets from Section 7 and Section 8. Then  $\mathcal{I}$  has a solution if and only if there is a valid placement of  $\mathbf{p}$  in  $C$ .*

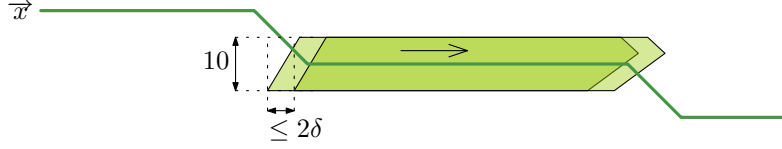
From Theorem 4, we now get the claimed results of row one and two in Table 1.

**Theorem 5.** *The problems  $\mathbf{Pack}(\sqcap \rightarrow \triangleleft, \odot +)$ ,  $\mathbf{Pack}(\triangleright \rightarrow \triangleright, \odot +)$ ,  $\mathbf{Pack}(\sqcap \rightarrow \triangleright, \odot +)$ , and  $\mathbf{Pack}(\sqcap \rightarrow \triangleleft, +)$  are  $\exists\mathbb{R}$ -hard.*

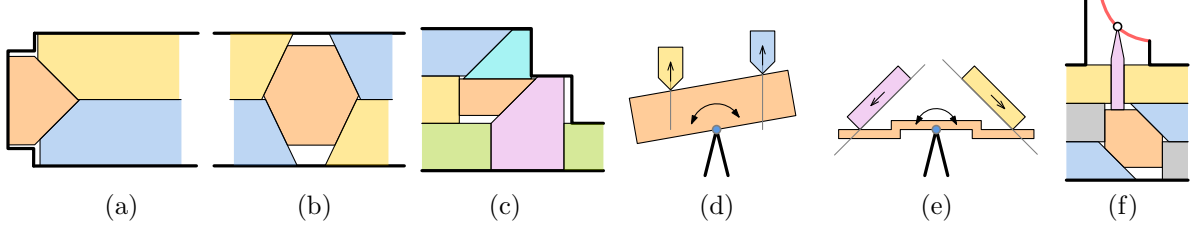
The third row in Table 1 follows from the reduction in Section 9, as described later in this section.

**Variable pieces.** Each variable  $x$  of  $\Phi$  will be represented by a number of *variable pieces* in our construction, each of which is a convex polygon. Each variable piece represents exactly one variable  $x$ , and we make a correspondance between certain placements of the piece and the values of  $x$ . Recall that  $x$  comes with an interval  $I(x) \subset [1/2, 2]$ , which we can write as  $I(x) = [m - w, m + w]$  for  $w \leq \delta$ . When adding a variable piece to our construction, we also specify the *middle placement* of the piece, which is a specific placement where it encodes the value  $m$  of  $x$ . In the middle placement, the piece will have a pair of (long) horizontal edges which have distance 10. By sliding the piece to the left or to the right from the middle placement, we obtain placements of the piece that encode all real values of  $x$ , even values outside the range  $[1/2, 2]$ . Each variable piece will be defined to be either right- or left-oriented. By sliding a right-oriented (resp. left-oriented) variable piece to the right by some amount  $t \geq 0$ , we obtain a placement that encodes the value  $m + t$  (resp.  $m - t$ ), while sliding it to the left by  $t$  results in a placement encoding  $m - t$  (resp.  $m + t$ ). If the piece is rotated in a different way or placed higher or lower than the middle placement, we do not define any value of  $x$  to be encoded by the placement. We define the *canonical placements* of a variable piece to be the placements that encode values in the interval  $I(x)$ ; see Figure 4.

On each wire  $\vec{x}_i$  or  $\overleftarrow{x}_i$  in the wiring diagram of  $\mathcal{I}$ , we will place some variable pieces representing  $x_i$ . The pieces placed on one wire are called a *lane*. The variable pieces on  $\vec{x}_i$  and  $\overleftarrow{x}_i$  are oriented to right and left, respectively. We also introduce some variable pieces which will be placed at other places than on the wires, namely above the topmost wire where they will be introduced in the steps of the construction corresponding to addition or inversion constraints.



**Figure 4:** A wire  $\vec{x}$  and a variable piece representing  $x$  placed on top, showing the leftmost and rightmost canonical placements of the piece. The large arrow in the piece indicates that the piece is right-oriented.



**Figure 5:** (a): anchor, (b): swap, (c): adder, (d): teeter-totter, (e): seesaw, (f): gramophone.

**Gadgets.** Sketches of some of the gadgets can be seen in Figure 5. In the wiring diagram, each variable  $x_i$  is represented by two wires  $\vec{x}_i$  and  $\overleftarrow{x}_i$  such that the left endpoints of  $\vec{x}_i$  and  $\overleftarrow{x}_i$  are vertically aligned at distance 10, as are the right endpoints. In each end of the wires, we build an *anchor* (Section 7.1) which ensures that the pieces placed on  $\vec{x}_i$  and those placed on  $\overleftarrow{x}_i$  encode the value of  $x_i$  consistently.

Whenever two wires cross, we build a *swap* (Section 7.2). The swap employs a central piece that can translate in all directions, so that when it is pushed by a variable piece, the push will propagate to the neighbouring variable piece on the other side of the crossing. We describe *adders* (Section 7.4) to implement the addition constraints and *inversion gadgets* (Section 8) for the inversion constraints. We describe several different inversion gadgets (see Figure 5 (d–f)), and which versions we use depends on the variant of packing we are reducing to.

Every time we add a gadget to the construction, we also introduce a constant number of new pieces. Each variable piece is introduced in one gadget where the left end of the piece is defined. The piece then extends outside the gadget to the right and the right end of the piece will be defined in another gadget added later to the construction. The piece is *exiting* the former gadget and *entering* the latter. In between the left and right end of the piece, defined in these two gadgets, the piece is bounded by a pair of horizontal edges. All pieces that are not variable pieces are contained within a single gadget.

**Canonical placements.** Recall that we define canonical placements of each variable piece. We do not define individual canonical placements of pieces that are not variable pieces, but instead we define canonical placements of all pieces of one or more gadgets: A placement of a set of pieces is canonical if (1) the placement is valid (i.e., the pieces are in  $C$  and are non-overlapping), (2) all variable pieces have a canonical placement, and (3) the pieces have certain relationships such as edge-edge contacts between each other. Part (3) will be specified for each gadget individually.

**Preservation of solutions.** The following lemma will be used to prove that for every solution to the ETR-INV formula  $\Phi$ , there is a canonical placement where the pieces encode that solution, meaning that for each variable  $x$ , all variable pieces representing  $x$  encode the same value of  $x$  as in the solution. Define  $g$  to be the total number of gadgets, and let  $\mathbf{p}_i$  denote the set of all

pieces introduced in the first  $i$  gadgets, where  $i \in \{0, \dots, g\}$ , so that  $\mathbf{p}_0 := \emptyset$ . The proof will be given in the sections describing the individual types of gadgets.

**Lemma 6** (Solution Preservation). *Consider any  $i \in \{1, \dots, g\}$  and suppose that for every solution to  $\Phi$ , there is a canonical placement of the pieces  $\mathbf{p}_{i-1}$  that encodes that solution. Then the same holds for  $\mathbf{p}_i$ .*

**Soundness of the reduction.** As mentioned, each variable  $x$  will be represented by many variable pieces in the complete construction. A difficulty is that conceivably, such a piece may not be placed in a way that encodes a value of  $x$ . Even if all the pieces happen to be placed such that they *do* encode values of  $x$ , these values could be different and therefore not represent a solution to the formula  $\Phi$ .

For a small number  $\Delta \geq \delta$ , we are going to introduce class of placements called *aligned  $\Delta$ -placements*. These are defined from the canonical placements by relaxing the requirements a bit. In an aligned  $\Delta$ -placements, each variable piece must be placed so that it encodes a value, but it may slide  $\Delta$  sideways from the middle placement instead of at most  $\delta$  as for the canonical placements. The requirements to the other pieces are likewise relaxed and will be given later. The values encoded by the variable pieces in an aligned  $\Delta$ -placement may therefore conceivably be outside the required range  $[1/2, 2]$ . The following lemma tells us that this is not the case for  $\Delta$  sufficiently small. In fact, the existence of such a placement is enough to ensure that  $\mathcal{I}$  has a solution. The number  $\mu$  is the *slack* of the construction defined as the area of the container  $C$  minus the total area of the pieces  $\mathbf{p}$ , and as will be explained later,  $\mu = O(n^{-296})$  in our construction. The number  $g = O(n^4)$  is the number of gadgets.

**Lemma 7** (Soundness). *In an aligned  $g\mu$ -placement, all pieces representing a variable  $x$  encode the value of  $x$  consistently (i.e., they all encode the same value of  $x$ ) and the value is in the range  $[1/2, 2]$ . Furthermore, these values of the variables satisfy the addition and inversion constraints of  $\Phi$ .*

In fact, it will follow from Lemma 7 that every aligned  $g\mu$ -placement is canonical, but this is not important for our proof of Theorem 4. The main work in proving the theorem will be to prove the following lemma.

**Lemma 8.** *Every valid placement is an aligned  $g\mu$ -placement.*

The proof of Theorem 4 is now straight-forward:

*Proof of Theorem 4.* If  $\mathcal{I}$  has a solution, it follows directly from repeated use of Lemma 6 that there is a valid placement. Suppose now that there is a valid placement. By Lemma 8, the placement is an aligned  $g\mu$ -placement. By Lemma 7, this placement encodes the variables consistently and in a way that respects the range  $[1/2, 2]$  and such that all addition and inversion constraints are satisfied. Therefore,  $\mathcal{I}$  has a solution.  $\square$

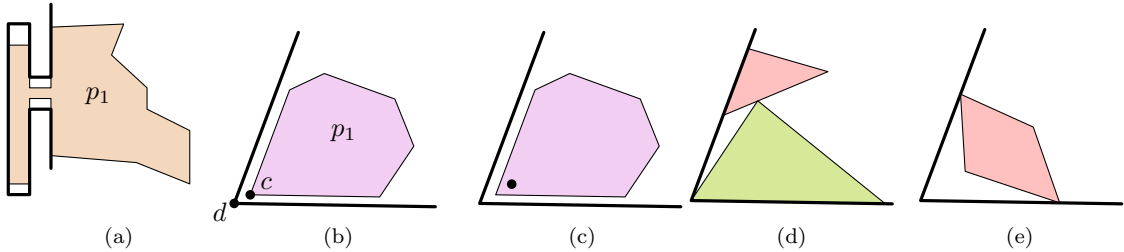
In the following we will describe the tools needed to prove Lemma 8.

**The slack of the construction.** The *slack* of an instance of a packing problem is the area of the container minus the total area of the pieces, and we denote it by  $\mu$ . and define their canonical placements. Our construction will be described as depending on the number  $\delta := n^{-300}$ . We need the slack to be very small in order to use the fingerprinting technique which will be described later.

We now give an upper bound on the slack of the complete construction. We place each variable piece so that it encodes the middle value of the interval  $I(x)$  of the variable  $x$  it

represents. By checking each type of gadget, it is straightforward to verify that this can be realized as a canonical (and thus valid) placement of the pieces in all gadgets except for the adders, where there might be a small overlap of the pieces. Therefore, the area of the empty space in this placement is at least  $\mu$ , so we bound  $\mu$  from above by bounding this area from above. The empty space in each gadget will appear as a thin layer along some of the edges of the pieces in the gadget. This layer has thickness  $O(\delta)$ , and the edges along which it appears have total length  $O(1)$ , so the area is  $O(\delta)$  in each gadget. There will be no empty space outside the gadgets because that space will be completely covered by variable pieces. Since the final construction has  $g = O(N) = O(n^4)$  gadgets, it follows that the total slack is  $\mu = O(n^4\delta) = O(n^{-296})$ . It may seem a little odd to measure the slack in this indirect way, but we found it to be the easiest way to get the bound since we do not explicitly specify the area of the container or the pieces in our construction.

**Fingerprinting.** In order to prove Lemma 8, we first show that every piece must be placed very close to a canonical placement using a technique we call *fingerprinting*. To grasp the idea of this technique, we first present another simpler technique that only works for non-convex pieces, and which we call the *jigsaw puzzle* technique for obvious reasons, see Figure 6 (a). The idea behind this technique is to force each piece  $p_1$  to be at a specific position by creating a pocket of the container and a corresponding augmentation of the piece  $p_1$  intended to be placed there. This is done in a way that only the piece  $p_1$  has an augmentation that fits into the pocket, just as the principle behind a jigsaw puzzle, and it can be done in a way that gives the piece freedom to slide back and forth by a slight amount or rotate, etc. The pocket can also be created in another piece  $p_2$  if  $p_1$  is intended to be placed next to  $p_2$ . Making enough of these pairs of pockets and extensions, we can therefore deduce where all the pieces are placed in all valid placements.



**Figure 6:** (a): A pocket and an augmentation that fit perfectly together as in a jigsaw puzzle. (b): A wedge of the empty space and a piece which fit together. (c): The corner of the piece we are fingerprinting is marked with a dot. (d) and (e): Two examples where space is wasted because a wedge is not occupied by a piece with a matching angle.

Unfortunately, the jigsaw puzzle technique is not directly realizable with convex pieces.<sup>2</sup> In *fingerprinting*, instead of a complicated augmentation, we only work with a piece  $p_1$  with a convex corner  $c$  of a specific angle  $\alpha_1$ . In the canonical placements, the empty space left by the other pieces forms a wedge with apex corner  $d$  of angle  $\alpha_1$  which can thus be covered very efficiently by  $p_1$  by placing the corner  $c$  at or very close to  $d$ , as in Figure 6 (b). We make sure that every corner of every other piece has an angle  $\alpha_2$  significantly different from  $\alpha_1$ , in the sense that  $|\alpha_2 - \alpha_1| = \Omega(N^{-2})$ . It should likewise hold that the total angle of any combination of corners of other pieces is different from  $\alpha_1$  in that sense. Furthermore, the slack

<sup>2</sup>In fact, the jigsaw puzzle technique can be used to prove  $\exists\mathbb{R}$ -hardness of packing problems with non-convex pieces in a much simpler way than the proofs of this paper, but since we anyway need to use the more involved fingerprinting technique for convex pieces, we stick to that in all cases.

$\mu$  is teeny tiny, as described above. As a result, we can show that if  $c$  is *not* placed very close to  $d$ , this will result in the empty space in a neighbourhood around  $d$  with an area exceeding  $\mu$ , because no other piece (or combination of pieces) can cover that neighbourhood efficiently, illustrated in Figure 6 (d-e). In our constructions, fingerprinted corners are marked with a dot; see Figure 6 (c). For technical reasons, the fingerprinted corners must have angles in the range from  $5\pi/180$  to  $\pi/2$ .

We add a few remarks about the use of fingerprinting. First of all, the situation shown in Figure 6 (b) is simplified. In our applications, the fat segments (bounding the empty space left by the other pieces) do not need to meet at the apex corner  $d$ , since a short portion (of length  $O(\delta)$ ) close to the corner can be missing. Furthermore, the angle between the two fat segments does not have to be exactly  $\alpha_1$  before the technique can be used; just very close to  $\alpha_1$  (this will be important when we are fingerprinting more than one piece in a row).

Second, the fingerprinting does not imply that the piece  $p_1$  *must* be placed with the corner  $c$  coincident with  $d$ , but only that the distance  $\|cd\|$  has to be small. This is used deliberately in our constructions, since it allows for the piece  $p_1$  to move slightly.

Third, when we introduce a new gadget and its  $k$  new pieces  $p_i, \dots, p_{i+k-1}$ , we use fingerprinting iteratively to argue where the new pieces must be placed. Here, the  $j$ 'th piece  $p_{i+j-1}$ ,  $j \in \{1, \dots, k\}$ , can be fingerprinted in a wedge of the empty space formed by the preceding pieces  $p_i, \dots, p_{i+j-2}$ . However, the bound on the uncertainty of where  $p_{i+j-1}$  is placed increases with  $j$ . Slightly simplified, the bound grows as  $O(n^{O(j)}\sqrt{\mu})$ , and we need the bound to be at most some small constant to be of any use. We prefer to create an instance where we need only a logarithmic number of bits to represent the coordinates of the container and the pieces, since this will prove that the packing problems are *strongly*  $\exists\mathbb{R}$ -hard. It is therefore important that we only apply fingerprinting iteratively a constant number of times, i.e., that  $k = O(1)$ , as we will otherwise need to choose the slack to smaller than  $n^{-q}$  for every constant  $q > 0$ , and then it will require a superlogarithmic number of bits to represent the coordinates of our instance. In the construction, we will always have  $k \leq 7$  and we can do with choosing  $\delta := n^{-300}$  so that  $\mu = O(n^{-296})$ .

After using fingerprinting iteratively a constant number of times for the new pieces, we use other techniques, such as the *alignment* (to be described in the sequel), to argue about their placement. In Section 6, we will develop the fingerprinting technique in detail. We consider this part the technically most challenging of the paper. The technique is versatile and can likely be used in other reductions to packing.

As the conditions for the fingerprinting technique are technical, we will list them in Section 6 in detail. We will show for each gadget that those conditions are met.

**Choosing unique angles.** As described in the previous paragraph, whenever we apply the fingerprinting technique to argue that a corner with angle  $\alpha_1$  of some piece is placed close to some specific point in the container, we need that every combination of corners of the other pieces have angles that sum to an angle  $\alpha_2$  such that  $|\alpha_2 - \alpha_1| = \Omega(N^{-2})$ . This will be called the *unique angle property*. In order to obtain this property, the construction will be designed so that each piece has a special corner where the angle can be chosen freely (within some interval of angles of size  $\Omega(1)$ ). Likewise, the wedge (where the special corner is intended to be placed) formed by the boundary of the container or the other pieces is flexible, so that the angle of the wedge can match the chosen angle of the corner. The fingerprinting technique will be applied to the special corner. In our figures, fingerprinted corners are marked with a dot, as in Figure 6 (c). The following lemma is used to choose these free angles such that we get the unique angle property.

**Lemma 9.** Let  $S_k := \{i/k + 1/2k^2 \mid i \in \{1, \dots, k\}\}$ , consider a subset  $R \subseteq S$ , and let  $x := \sum_{r \in R} r$ . If  $x \in S_k$ , then  $R = \{x\}$ .

*Proof.* If  $R$  consists of  $m$  elements, then  $x$  has the form  $j/k + m/2k^2$  for some  $j \in \mathbb{N}$ . A number of this form, for  $m \leq k$ , can only be in  $S_k$  if  $m = 1$ .  $\square$

The lemma provides a set of  $k$  numbers in a range of size  $O(1)$  and any number is  $\Omega(k^{-2})$  away from the sum of any combination of other numbers. We multiply the numbers in  $S_k$  by  $\pi$  to get a set of rational angles and choose the free angles from such a set  $\pi S_k$ , for  $k = O(N)$ . We need to use  $k > N$  since the free angles are restricted to various subintervals of  $[0, \pi]$ , so we choose  $k$  so large that  $\pi S_k$  contains enough angles for each of these subintervals. However, as each subinterval has size  $\Omega(1)$ , we can do with  $k = O(N)$ .

**Proof structure of Lemma 8.** In the proof of Lemma 8, we use the fingerprinting technique to prove that in every valid placement, the pieces are placed almost as in a canonical placement. To explain the structure of the argument in more detail, we need some notions of placements that are close to being canonical, which will be defined in the following paragraph.

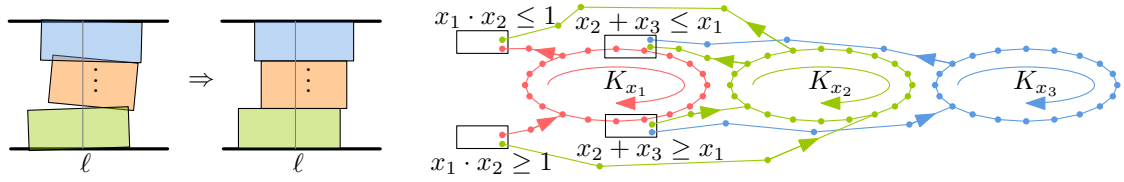
**Almost-canonical placements and aligned placements.** We say that a valid placement of the pieces of a gadget is *almost-canonical* if there exists rigid motions that move the pieces to a canonical placement such that every point in each piece is moved a distance of at most  $n^{-1}$  (in other words, the *displacement* between the actual placement and the canonical placement of each piece is  $n^{-1}$ ).

We say that a placement of the pieces of a gadget is an *aligned  $\Delta$ -placement* for  $\Delta \geq \delta$  if (i) the placement is almost-canonical, and (ii) for each variable  $x$ , each variable piece representing  $x$  is rotated and has  $y$ -coordinates as in the canonical placements and encodes a value in the range  $[m - \Delta, m + \Delta]$ , where  $m$  is the middle value of the interval  $I(x)$ . Note that since the placement is almost-canonical, we can always assume  $\Delta \leq n^{-1} + \delta = n^{-1} + n^{-300}$ .

The following lemma says that the pieces of every new gadget can be assumed to be almost-canonical if the preceding pieces have an aligned  $\Delta$ -placement. Recall that  $\mathbf{p}_i$  is the set of all pieces introduced in the first  $i$  gadgets, where  $i \in \{0, \dots, g\}$ , so that  $\mathbf{p}_0 := \emptyset$ . The lemma will follow from the use of fingerprinting, and the proof will be given in the sections describing the individual types of gadgets.

**Lemma 10** (Almost-canonical Placement). *For any  $i \in \{1, \dots, g\}$ , consider a valid placement  $P$  (of all the pieces) for which the pieces  $\mathbf{p}_{i-1}$  have an aligned  $(i-1)\mu$ -placement. It then holds for  $P$  that the pieces  $\mathbf{p}_i$  have an almost-canonical placement.*

**Aligning pieces.** Once we know that the pieces  $\mathbf{p}_i$  have an almost-canonical placement, provided by the previous lemma, we can use so-called *alignment segments* to further restrict where the new pieces  $\mathbf{p}_i \setminus \mathbf{p}_{i-1}$  introduced in gadget  $i$  can be placed. In particular, we will be able to fix the rotations of some pieces to be as in the canonical placements. The idea is sketched in Figure 7 (left). From the rough placements we get from fingerprinting, we know that a set of the pieces each has a pair parallel edges that are both cut through by an alignment segment  $\ell$ . If we sum the distance between the two parallel edges over all the pieces, we get exactly the length of  $\ell$ . Since the portions of  $\ell$  covered by the pieces must be pairwise disjoint in a valid placement, we can conclude that the pieces have to be rotated so that the parallel edges are perpendicular to  $\ell$ . This technique will be used to prove the following lemma for each gadget individually. Using the lemma repeatedly together with Lemma 10, we get that every valid placement is also an aligned  $g\mu$ -placement, proving Lemma 8.



**Figure 7:** Left: The alignment segment  $\ell$  makes us conclude that the pieces must be horizontally aligned: otherwise, they would overlap, cross the container boundary, or cover more of the alignment segment than what is available. Right: An abstract drawing of the dependency graphs of the instance we get from the wiring diagram in Figure 14 and how the graphs connect to the gadgets for addition and inversion constraints. The number of vertices on the cycles and paths are neither important nor correct.

**Lemma 11** (Aligned Placement). *For any  $i \in \{1, \dots, g\}$ , consider a valid placement  $P$  (of all the pieces) for which the pieces  $\mathbf{p}_{i-1}$  have an aligned  $(i-1)\mu$ -placement and the pieces  $\mathbf{p}_i$  have an almost-canonical placement. It then holds for  $P$  that the pieces  $\mathbf{p}_i$  have an aligned  $i\mu$ -placement.*

It now remains to prove Lemma 7.

**Proof structure of Lemma 7.** The proof of Lemma 7 goes along the following lines. In an aligned  $g\mu$ -placement, each variable piece  $p_x$  encodes a value for the variable  $x$  it is representing, which we will denote by  $\langle p_x \rangle$ . The problem is that different pieces representing the same variable  $x$  may conceivably not encode the value consistently. However, recall that we build lanes of pieces on top of the two wires  $\vec{x}, \overleftarrow{x}$ , and these meet at the left and right endpoints of the wires. We prove that the values encoded by these pieces  $p_1, \dots, p_m$  make a cycle of inequalities:  $\langle p_1 \rangle \leq \langle p_2 \rangle \leq \dots \leq \langle p_m \rangle \leq \langle p_1 \rangle$ . It thus follows that all these pieces encode a value of  $x$  consistently.

Furthermore, the anchors, which are the gadgets that we place at the left and right endpoints of the wires  $\vec{x}, \overleftarrow{x}$ , will ensure that  $\langle p_1 \rangle \in [1/2, 2]$ , so that the encoded values are in the correct range.

In our construction, we also make additional lanes of pieces going to the addition and inversion gadgets. The functionality of the specific gadgets and the inequalities we get between the encoded values of pieces in these lanes implies that the addition and inversion inequalities of  $\Phi$  are all satisfied. In order to describe the structure of the argument, we introduce a graph  $G_x$  for each variable  $x$  as described in the next paragraph.

**Dependency graph of variable pieces.** For each variable  $x$ , we introduce a directed *dependency graph*  $G_x$ . The vertices of  $G_x$  are the variable pieces representing  $x$ . Consider a gadget and two variable pieces  $p_1, p_2$  appearing in the gadget and both representing  $x$ . We add an edge from  $p_1$  to  $p_2$  in  $G_x$  if  $p_1$  is an entering right-oriented piece or an exiting left-oriented piece and  $p_2$  is an exiting right-oriented piece or an entering left-oriented piece. In crossings between the two wires  $\vec{x}, \overleftarrow{x}$  representing  $x$ , there will be a swap where this rule introduces unintended edges, so we make one exception described in Section 7.2 where the swap is described in detail.

The following lemma is going to follow trivially from the way we make the lanes on top of the wires  $\vec{x}, \overleftarrow{x}$  for each variable  $x$ , and the way we connect the gadgets representing addition and inversion inequalities to these lanes. See Figure 7 (right) for an illustration.

**Lemma 12.** *For each variable  $x$ , the graph  $G_x$  consists of a directed cycle  $K_x$  with some directed paths attached to it (oriented towards or away from  $K_x$ ). The vertices of the cycle  $K_x$  are the*

variable pieces appearing on the wire  $\overrightarrow{x}$  from left to right and the wire  $\overleftarrow{x}$  from right to left in this order. For each path attached to  $K_x$ , the vertex farthest from  $K_x$  is a piece entering a gadget representing an addition or inversion constraint.

In the following, we consider a given aligned  $g\mu$ -placement of all the pieces. Since all edges of  $G_x$  are between pieces appearing in the same gadget, the following lemma will be proven for each gadget individually.

**Lemma 13** (Edge inequality). *Consider a variable  $x$  and an edge  $(p_1, p_2)$  of  $G_x$ . Then  $\langle p_1 \rangle \leq \langle p_2 \rangle$ .*

From Lemma 12 and 13, we now get the following (except that the part about the anchor gadget will be proven in Section 7.1).

**Lemma 14.** *For each variable  $x$ , all the pieces of the cycle  $K_x$  encode the value of  $x$  consistently. Furthermore, due to the design of the anchor gadget, the value is in  $[1/2, 2]$ .*

By the above lemma, we may write  $\langle K_x \rangle$  to denote the value represented by all pieces of  $K_x$ .

**Addition and inversion gadgets work.** We will show in Section 7.4 and Section 8 that the addition and inversion gadgets actually enforce addition and inversion constraints as they are supposed to. This entails showing that the gadgets implement the addition or inversion operations in a geometric sense and also that the variable pieces of the gadgets are correctly connected to the cycles in the respective dependency graphs. In particular, we will show the following two lemmas.

**Lemma 15** (addition). *For every addition constraint  $x + y = z$  of  $\Phi$ , we have  $\langle K_x \rangle + \langle K_y \rangle = \langle K_z \rangle$ .*

**Lemma 16** (inversion). *For every inversion constraint  $x \cdot y = 1$  of  $\Phi$ , we have  $\langle K_x \rangle \cdot \langle K_y \rangle = 1$ .*

From the proofs of the lemmas, we get that not only the variable pieces of the cycles  $K_x$  encode the value of  $x$  consistently, but also the pieces of the directed paths that lead to the addition and inversion gadgets. Together with the statement of Lemma 14 that the values  $\langle K_x \rangle$  are in  $[1/2, 2]$ , we then have a proof of Lemma 7.

**Square container.** In Section 9, we describe a reduction from problems of type  $\mathbf{Pack}(\mathcal{P} \rightarrow \triangleright, \mathcal{M})$  to  $\mathbf{Pack}(\mathcal{P} \rightarrow \square, \mathcal{M})$  and from  $\mathbf{Pack}(\sqcap \rightarrow \sqcup, \mathcal{M})$  to  $\mathbf{Pack}(\sqcup \rightarrow \square, \mathcal{M})$ .<sup>3</sup> It will be crucial that the container  $C$  is 4-monotone, as defined below.<sup>4</sup>

**Definition 17.** *A simple closed curve  $\gamma$  is 4-monotone if  $\gamma$  can be partitioned into four parts  $\gamma_1, \dots, \gamma_4$  in counterclockwise order that move monotonically down, to the right, up, and to the left, respectively. A (curved) polygon  $Q$  is 4-monotone if the boundary of  $Q$  is a 4-monotone curve.*

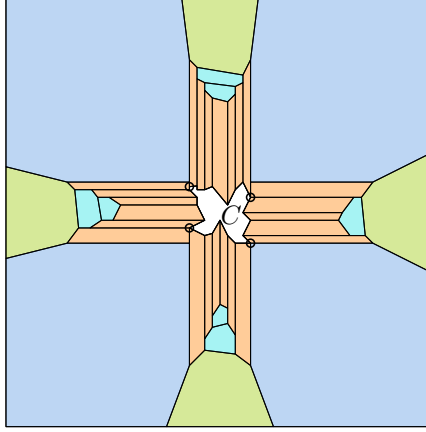
**Lemma 18.** *In the reductions to each problem mentioned in Theorem 5, the resulting container is 4-monotone.*

---

<sup>3</sup>There is in fact a much simpler reduction from  $\mathbf{Pack}(\sqcap \rightarrow \sqcup, \mathcal{M})$  to  $\mathbf{Pack}(\sqcup \rightarrow \square, \mathcal{M})$ , but it requires pieces of non-constant complexity: We simply introduce a huge square piece and remove a hole from it with a shape as the original container of type  $\sqcup$ . We also remove a thin corridor from that hole to the boundary to make the piece simply-connected. Then the hole in the piece will act as the container for the other pieces.

<sup>4</sup>In some cases, the gadgets that we describe might at first appear slightly more convoluted than necessary because we want  $C$  to have this property.





**Figure 8:** Construction used in the reduction to packing problems with a square container. The space left by the exterior pieces (blue, green, orange, and turquoise) is exactly the 4-monotone container  $C$  of the instance we are reducing from.

*Proof.* The boundary of the resulting container has a left and a right staircase,  $\gamma_1$  and  $\gamma_3$ , created by the left and right anchors, respectively, and these staircases are  $y$ -monotone, and their upper and lower endpoints are horizontally aligned. The lower endpoints of the staircases  $\gamma_1$  and  $\gamma_3$  are connected by a single horizontal line segment  $\gamma_2$  bounding the bottom lane from below. The upper endpoints of the staircases are connected by a curve  $\gamma_4$  which bounds the topmost lane and the addition and inversion gadgets from above. The curve  $\gamma_4$  is  $x$ -monotone, as can easily be verified by inspecting the boundary added due to each type of constraint gadget. Hence, the container is 4-monotone.  $\square$

We get from the lemma that the packing problems are even  $\exists\mathbb{R}$ -hard for 4-monotone containers. Let  $\mathcal{I}_1$  be an instance of a packing problem where the container  $C := C(\mathcal{I}_1)$  is 4-monotone. We place  $C$  in the middle of a larger square and fill out the area around  $C$  with pieces in a careful way; the details are given in Section 9 and Figure 8 shows an example of the construction. We call these new pieces the *exterior* pieces, whereas we call the pieces of  $\mathcal{I}_1$  the *inner* pieces. Using fingerprinting and other arguments, we are able to prove that if there exists a valid packing of the resulting instance, then there exists one where the exterior pieces are placed as they are intended to. Then the space left for the inner pieces is exactly the container  $C$ . Therefore, there exists a valid placement of the pieces in the resulting instance if and only if there is one of the inner pieces in  $C$ . We get the results in the third row of Table 1 as expressed by the following theorem.

**Theorem 19.** *The problems  $\text{Pack}(\mathcal{P} \rightarrow \square, \mathcal{M})$  are  $\exists\mathbb{R}$ -hard, where*

$$(\mathcal{P}, \mathcal{M}) \in \{(\mathbb{L}, \odot +), (\mathbb{D}, \odot +), (\mathbb{L}, +)\}.$$

**Universality.** Our reductions imply so-called Mnëv-universality type results. They show algebraic and topological equivalence of packing problems to compact semi-algebraic sets.

As we will argue about the entire solution space, we will show the following lemma, which will be proven for each gadget individually and in Section 9. The proof builds upon Lemma 7 and Lemma 8.

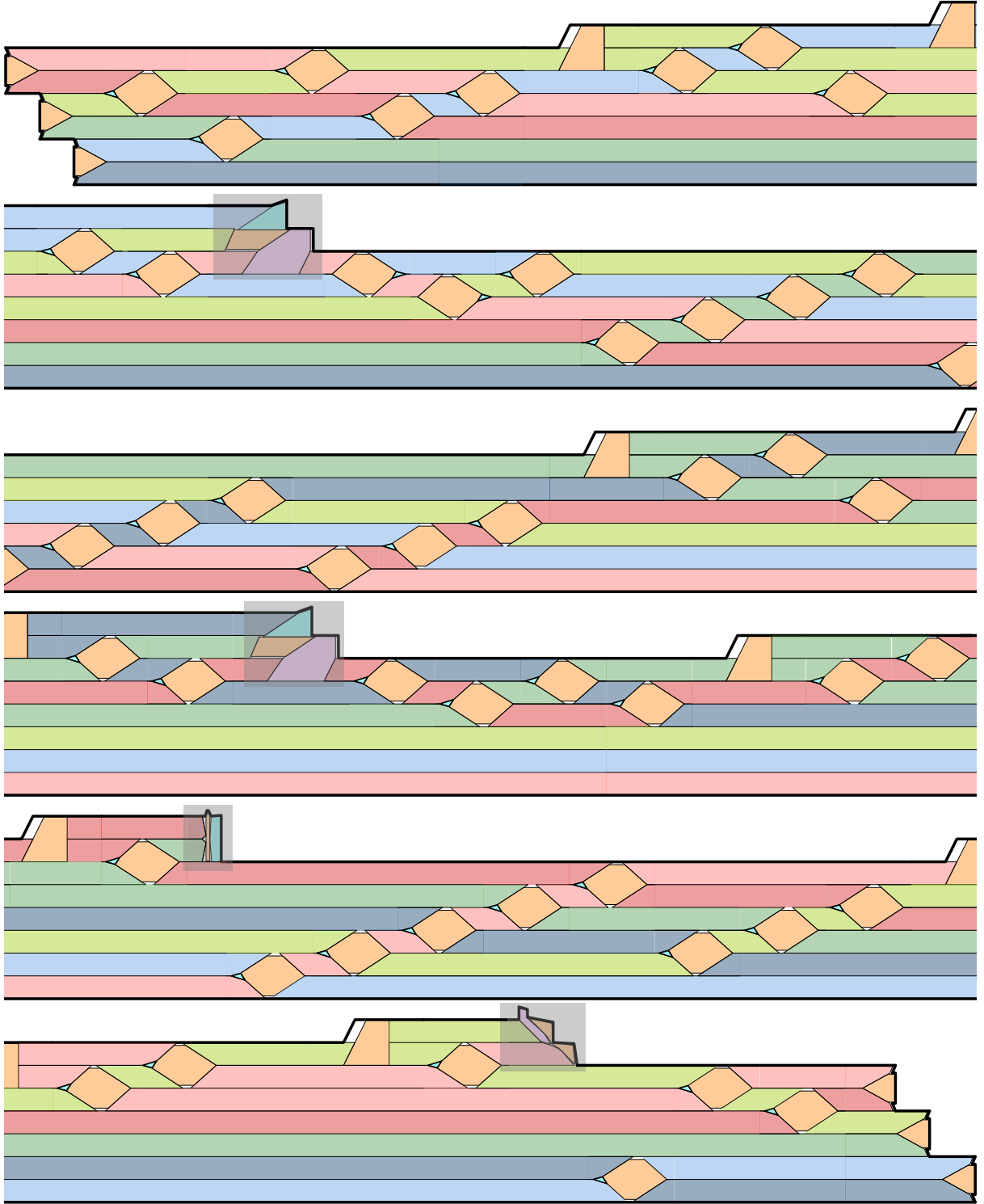
**Lemma 20.** *Every valid placement is canonical.*

In Section 10, we will show the following two theorems.

**Theorem 21.** *Let  $P$  be one of the packing problems indicated as  $\exists\mathbb{R}$ -complete in Table 1. Let  $\mathbb{F}_1, \mathbb{F}_2$  be algebraic field extensions of  $\mathbb{Q}$  such that  $\mathbb{Q} \subseteq \mathbb{F}_1 \subsetneq \mathbb{F}_2 \subset \mathbb{R}$ . Then there exists an instance  $(\mathbf{p}, C)$  of  $P$  that has a solution in  $\mathbb{F}_2$ , but none in  $\mathbb{F}_1$ .*

**Theorem 22.** *Let  $T$  be a compact semi-algebraic set, and let  $P$  be one of the packing problems indicated as  $\exists\mathbb{R}$ -complete in Table 1. Then there is an instance  $(\mathbf{p}, C)$  of  $P$  such that  $T$  is homotopy equivalent to the solution space  $V(\mathbf{p}, C)$ .*

### 3 Complete example



**Figure 9:** A sketch of the instance of  $\mathbf{Pack}(\triangleright \rightarrow \triangleright, \odot \oplus)$ , broken over six lines, we get from the wiring diagram in Figure 3 (except that the order of the inversion gadgets has been swapped to decrease the number of crossings). The addition and inversion gadgets are marked with gray boxes.

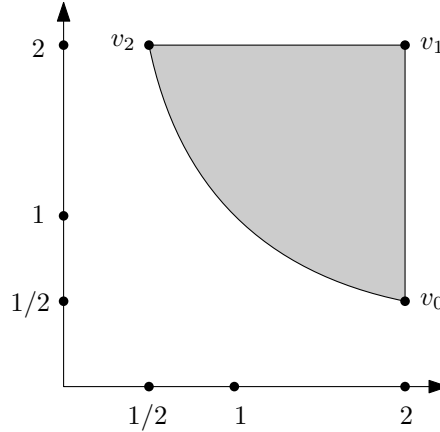
## 4 Preliminaries

This section contains three parts with definitions and conventions used in the rest of the paper. The first part concerns the way we encode geometric objects and motions. The second part defines some general geometric definitions, which we will use heavily in Section 6 about fingerprinting. The third part is concerned with different notions of equivalence of solution spaces and become relevant in Section 5 about RANGE-ETR-INV and Section 10 about universality.

### 4.1 Encoding Polygons and Motions

**Orientation of polygons.** We always consider a simple polygon (or a curved polygon) to be oriented in counterclockwise direction, which makes it well-defined to talk about the edge preceding or succeeding a given corner, etc.

**Representation of curved segments.** Recall that the convex ( $\sqsupset$ ) or curved polygons ( $\curvearrowright$ ) pieces or containers that we use have boundaries which are a finite union of line segments and curves contained in hyperbolae. We assume that these curved parts will be given implicitly, by a polynomial equation and two endpoints, see Figure 10.



**Figure 10:** The shape can be encoded by  $v_0 = (2, 0.5)$ ,  $v_1 = (2, 2)$ ,  $v_2 = (0.5, 2)$ ,  $x \cdot y = 1$ ,  $v_0$ .

**Motion and Placement.** We encode a rotation by a *rotation matrix*, which is a matrix  $M$  of the form

$$M = \begin{pmatrix} a & -b \\ b & a \end{pmatrix},$$

with  $\det M = 1$ . From a translation  $t \in \mathbb{R}^2$  and a rotation  $M$ , we get a *motion*  $m := (t, M)$ . If only translations are allowed, we require that  $M$  is the identity.

When we define the solution space  $V(\mathcal{I})$ , then we also allow rotations  $M$  such that  $\det M > 0$ . Note that we can normalize a matrix by simply multiplying every entry with  $\sqrt{\det M}$ . The reason we do not require the rotation to be normalized is related to the algebraic universality, which we will show in Section 10. The introduction of square-roots would destroy this algebraic-universality.

Given a piece  $p$  and a motion  $m = (M, t)$ , then we denote by  $p^m$  the piece  $p$  after moving  $p$  according to  $m$ , i.e.,

$$p^m := \{Mx + t : x \in p\}.$$

The set  $p^m$  is the *placement* of  $p$  by  $m$ . Given a tuple of  $\mathbf{p} = (p_1, \dots, p_k)$  of pieces and a tuple  $\mathbf{m} = (m_1, \dots, m_k)$  of motions, then we denote by

$$\mathbf{p}^{\mathbf{m}} = (p_1^{m_1}, \dots, p_k^{m_k})$$

the *placement* of  $\mathbf{p}$  by  $\mathbf{m}$ . We may write  $p_i^{\mathbf{m}}$  instead of  $p_i^{m_i}$ .

Given a container  $C$  and pieces  $\mathbf{p} = (p_1, \dots, p_k)$  and a motion  $\mathbf{m}$ , we say  $\mathbf{m}$  and  $\mathbf{p}^{\mathbf{m}}$  are a *valid* motion and placement, respectively, if  $p_i^{\mathbf{m}} \subset C$  for all  $i$  and  $p_i^{\mathbf{m}}$  and  $p_j^{\mathbf{m}}$  are interior-disjoint for all  $i \neq j$ .

## 4.2 Elementary Geometry

Let  $ab$  and  $cd$  be two (oriented) line segments. The *angle between*  $ab$  and  $cd$  is the minimum angle the  $ab$  can be turned such that  $ab$  and  $cd$  become parallel and point in the same direction, i.e.,  $(b - a) \cdot (d - c) > 0$ .

Consider two motions  $m_1$  and  $m_2$  of a piece  $p$ . The *displacement* between  $m_1$  and  $m_2$  is  $\sup_{x \in p} \|x^{m_1} - x^{m_2}\|$ . The *displacement angle* is the absolute difference in how much  $m_1$  and  $m_2$  rotate  $p$  in the interval  $[0, \pi]$ .

Given a compact set  $S$  in the plane, we denote by  $\text{area}(S)$  the area of  $S$ . All sets that we consider will be compact.

Given a container  $C$  and pieces  $\mathbf{p}$ , we define the *slack* as  $\mu(C, \mathbf{p}) = \text{area}(C) - \sum_{p \in \mathbf{p}} \text{area}(p)$ .

Given a compact set  $S$  in the plane, the *diameter* of  $S$  is defined as  $\text{diam}(S) := \max_{a, b \in S} \|ab\|$ .

Let  $A \subset \mathbb{R}^2$ . Then  $A^c = \{x \in \mathbb{R}^2 \mid x \notin A\}$ . Let  $A, B \subset \mathbb{R}^2$ . Then we denote the Minkowski sum as  $A \oplus B := \{a + b \mid a \in A, b \in B\}$  and the Minkowski difference as  $A \ominus B := (A^c \oplus B)^c$ .

## 4.3 Universality

A universality statement says that for every object of type A, there exists an object of type B such that A and B are equivalent in some sense C. In Theorem 29, to be stated and proved in the next section, we have compact solution spaces of ETR formulae (i.e., compact semi-algebraic sets) as objects of type A, solution spaces of ETR-INV formulas are objects of type B, and we preserve algorithmic, topological and algebraic properties. Specifically, we show rational equivalence between the solution spaces and that those of ETR-INV formulae are linear extensions of those of ETR formulae. In Section 10, we will show some weaker forms of equivalence for all our packing problems.

**Definition 23.** Given a packing instance  $\mathcal{I} = (C, \mathbf{p})$ , we define  $V(\mathcal{I}) := \{\mathbf{m} \in \mathbb{R}^{6n} : \mathbf{m} \text{ is a valid motion}\}$  to be the solution space of  $\mathcal{I}$ .

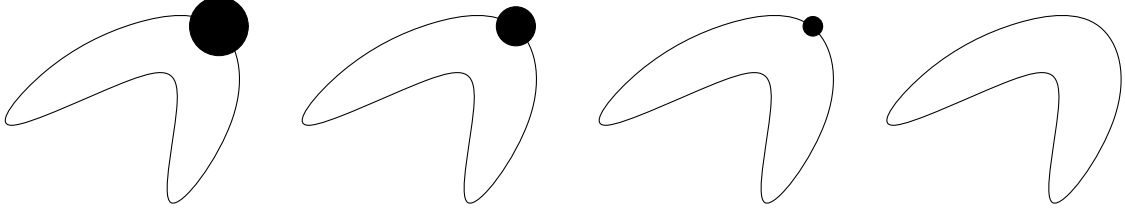
For the definition of solution space we explicitly also allow *non-normalized rotation matrices*  $M$ , which are matrices of the form  $M = \lambda M'$  for a scalar  $\lambda > 0$  and a rotation matrix  $M'$ . To see how this can be useful consider the rotation matrix  $M'$  of a  $45^\circ$  rotation, which has irrational entries:

$$M' := \begin{pmatrix} \cos 45^\circ & -\sin 45^\circ \\ \sin 45^\circ & \cos 45^\circ \end{pmatrix} = \begin{pmatrix} \frac{1}{\sqrt{2}} & -\frac{1}{\sqrt{2}} \\ \frac{1}{\sqrt{2}} & \frac{1}{\sqrt{2}} \end{pmatrix}.$$

We can also easily express this rotation by the rational matrix

$$M := \begin{pmatrix} 1 & -1 \\ 1 & 1 \end{pmatrix}$$

Note that if we want to rotate a vector  $v$ , we have to normalize the matrix first, which is possible if we allow taking square-roots in our model of computation.



**Figure 11:** A continuous deformation from left to right. The two shapes are not homeomorphic, but homotopy equivalent.

**Definition 24.** Given a polynomial  $p \in \mathbb{Z}[x_1, \dots, x_n]$ , we define  $V(p) := V(p = 0) = \{\approx \in \mathbb{R}^n : p(\approx) = 0\}$  to be the variety or the solution space of  $p$ .

**Definition 25** (Rational Equivalence). Consider two sets  $V \subseteq \mathbb{R}^n$  and  $W \subseteq \mathbb{R}^m$  and a function  $f : V \rightarrow W$ . We say that  $f$  is a homeomorphism if  $f$  is bijective, continuous, and the inverse  $f^{-1}$  is continuous as well.

Write  $f$  as its components  $(f_1, \dots, f_m)$ , where  $f_i : V \rightarrow \mathbb{R}$  for each  $i \in \{1, \dots, m\}$ . Then  $f$  is rational if each function  $f_i$  is the ratio of two polynomials.

The sets  $V$  and  $W$  are rationally equivalent if there exists a homeomorphism  $f : V \rightarrow W$  such that both  $f$  and  $f^{-1}$  are rational functions. In that case, we write  $V \simeq W$ .

Be aware that the term linear extension, that we define below, has other meanings in other contexts.

**Definition 26** (Linear Extension). Given two sets  $V \subseteq \mathbb{R}^n$  and  $W \subseteq \mathbb{R}^m$ , we say that  $W$  is a linear extension of  $V$  if there is an orthogonal projection  $\pi : \mathbb{R}^m \rightarrow \mathbb{R}^n$  and two vectors  $\mathbf{a}, \mathbf{b} \in \mathbb{Q}^n$  such that the mapping  $l : W \rightarrow V$  defined by

$$l(x) := \mathbf{a} \odot \pi(\mathbf{x}) + \mathbf{b}$$

is a continuous bijection. Here,  $\mathbf{c} \odot \mathbf{y}$  denotes the elementwise product  $(c_1 d_1, \dots, c_n d_n) \in \mathbb{R}^n$  for  $\mathbf{c} = (c_1, \dots, c_n)$  and  $\mathbf{d} = (d_1, \dots, d_n)$ . We denote that  $W$  is a linear extension of  $V$  as  $V \leq_{\text{lin}} W$ .

Rational equivalence and linear extension are both transitive relations, i.e., if  $U \simeq V$  and  $V \simeq W$ , then  $U \simeq W$ , and if  $U \leq_{\text{lin}} V$  and  $V \leq_{\text{lin}} W$ , then  $U \leq_{\text{lin}} W$ .

Furthermore, for a compact set  $V$ , if  $V \simeq W$  or  $V \leq_{\text{lin}} W$ , then  $W$  is compact as well.

**Example 27.** Let  $V := [1, 2]$  and  $W := \{(x, y) : x \in [1, 2], x = y^2\}$ . Then  $W$  is not a linear extension of  $V$ , and  $V$  and  $W$  are not rationally equivalent, as  $W$  has two connected components.

Unfortunately, in the geometric reduction from RANGE-ETR-INV to  $\mathbf{Pack}(\mathcal{P} \rightarrow \mathcal{C}, \mathcal{M})$ , our geometric reductions give neither rational equivalence, nor a linear extension. The reason is that some pieces have room to move in the valid placements of the constructed instances. Such pieces are sometimes called *rattlers* in the literature on packing problems. We are still preserving some topological properties and also some algebraic properties. To state these, we define homotopy equivalence. Informally, two spaces are homotopy equivalent if one can be continuously deformed into the other; see Figure 11 for an illustration.

**Definition 28** (Homotopy). We say two functions  $f, g : X \rightarrow Y$  are homotopic if there exists a continuous map  $G : [0, 1] \times X \rightarrow Y$  such that  $G(0, x) = f(x)$  and  $G(1, x) = g(x)$ , for all  $x \in X$ .

We say two topological spaces  $S, T$  are homotopy equivalent if there are continuous maps  $f : S \rightarrow T$  and  $g : T \rightarrow S$  such that  $f \circ g$  is homotopic to  $\text{id}_T$  and  $g \circ f$  is homotopic to  $\text{id}_S$ .

Note that if  $U \simeq V$  or  $U \leq_{\text{lin}} V$ , then  $U$  and  $V$  are homotopy equivalent.

## 5 RANGE-ETR-INV and WIRED-INV

First recall the definition of ETR-INV formulae and the problem RANGE-ETR-INV, repeated below.

**Definition 1.** An ETR-INV formula  $\Phi = \Phi(x_1, \dots, x_n)$  is a conjunction

$$\left( \bigwedge_{i=1}^n 1/2 \leq x_i \leq 2 \right) \wedge \left( \bigwedge_{i=1}^m C_i \right),$$

where  $m \geq 0$  and each  $C_i$  is of one of the forms

$$x + y = z, \quad x \cdot y = 1$$

for  $x, y, z \in \{x_1, \dots, x_n\}$ .

**Definition 2.** An instance  $\mathcal{I} = [\Phi, \delta, (I(x_1), \dots, I(x_n))]$  of the RANGE-ETR-INV problem consists of an ETR-INV formula  $\Phi$ , a number  $\delta := 2^{-l}$  for a positive integer  $l$ , and, for each variable  $x \in \{x_1, \dots, x_n\}$ , an interval  $I(x) \subseteq [1/2, 2]$  such that  $|I(x)| \leq 2\delta$ . For every inversion constraint  $x \cdot y = 1$ , we have either  $I(x) = I(y) = [1 - \delta, 1 + \delta]$  or  $I(x) = [2/3 - \delta, 2/3 + \delta]$  and  $I(y) = [3/2 - \delta, 3/2 + \delta]$ . We are promised that  $V(\Phi) \subset I(x_1) \times \dots \times I(x_n)$ . The goal is to decide whether  $V(\Phi) \neq \emptyset$ .

The goal of this section is to prove the following extension of Theorem 3.

**Theorem 29.** RANGE-ETR-INV is  $\exists\mathbb{R}$ -complete, even when  $\delta = O(n^{-c})$  for any constant  $c > 0$ . Furthermore, for every instance  $\Phi$  of ETR where  $V(\Phi)$  is compact, there is an instance  $\mathcal{I}$  of RANGE-ETR-INV with ETR-INV formula  $\Psi$  such that  $V(\Phi)$  and  $V(\Psi)$  are rationally equivalent and  $V(\Psi)$  is a linear extension of  $V(\Phi)$ .

We give a self-contained proof of the theorem except that we will need a few results from real algebraic geometry. The reductions in Sections 5.1–5.4 rely on well-known techniques and can be considered folklore, but we need to phrase them differently than done earlier to obtain the latter part of Theorem 29. The reductions in Sections 5.5–5.7 are new.

**Naming the variables.** We typically denote a new variable with a multi-character symbol such as  $\llbracket v \rrbracket$ . Here,  $v$  is an expression involving already known quantities, and  $\llbracket v \rrbracket$  should be thought of as a placeholder with that value. In the case that  $v$  is a constant, e.g.,  $v = 2$  such that the variable is  $\llbracket 2 \rrbracket$ , then we say that  $\llbracket v \rrbracket$  is a *constant variable*. By *constructing* a constant variable  $\llbracket v \rrbracket$  in an ETR formula  $\Phi$ , we mean introducing variables and constraints to  $\Phi$  such that it follows that in every solution to  $\Phi$ , we have  $\llbracket v \rrbracket = v$ .

The expression  $v$  of a variable  $\llbracket v \rrbracket$  can also involve other parameters such as for instance  $\llbracket x^2 + 2x + 1 \rrbracket$ . In that case  $\llbracket x^2 + 2x + 1 \rrbracket$  should be thought of as a variable holding the value  $x^2 + 2x + 1$ , where  $x$  is another variable or a parameter of the problem. It should follow from the assumptions or constraints introduced in the concrete case that  $\llbracket x^2 + 2x + 1 \rrbracket$  indeed has the value  $x^2 + 2x + 1$  in any solution to  $\Phi$ .

### 5.1 Reduction to Conjunctive Form

**Definition 30.** An ETR-CONJ formula  $\Phi := \Phi(x_1, \dots, x_n)$  is a conjunction  $C_1 \wedge \dots \wedge C_m$ , where  $m \in \mathbb{N}$  and each  $C_i$  is of one of the two forms

$$x \geq 0, \quad p(y_1, \dots, y_l) = 0$$

for  $x, y_1, \dots, y_l \in \{x_1, \dots, x_n\}$  and  $p$  is a polynomial.

Note that since there are no strict inequalities in a formula  $\Phi$  in ETR-CONJ, the set  $V(\Phi)$  is closed.

We show how to reduce a general ETR formula to an ETR-CONJ formula. The reduction preserves rational equivalence and runs in linear time. A similar reduction has been described by Schaefer and Štefankovič [51].

**Lemma A.** *Given an ETR formula  $\Phi$ , we can in  $O(|\Phi|)$  time compute an ETR-CONJ formula  $\Psi$  such that  $V(\Phi) \simeq V(\Psi)$  and  $V(\Phi) \leq_{lin} V(\Psi)$ .*

*Proof.* We start with an ETR formula  $\Phi$  and modify it repeatedly to attain an ETR-CONJ formula  $\Psi$ . Each modification leads to an equivalent formula. Our modifications can be summarized in four steps. (1) Delete “ $\neg$ ”. (2) Delete “ $>$ ”. (3) Move “ $\geq$ ” to variables only. (4) Delete “ $\vee$ ”. In the rest of this proof  $p$  and  $q$  denote polynomials.

Step (1): Here, we merely “pull” every negation  $\neg$  in front of every atomic predicate. For instance  $\neg(A \vee B \vee C)$  becomes  $(\neg A \wedge \neg B \wedge \neg C)$ . To see that this can be done in linear time, note that the length of  $\Phi$  is at least the number of atomic predicates. In the end of this process, every atomic predicate is preceded by either a negation or not. It may be that  $\wedge$  and  $\vee$  symbols are swapped, but we count both as one symbol.

Thereafter each atomic predicate preceded by  $\neg$  is replaced as follows:

$$\begin{aligned} \neg(q > 0) &\mapsto -q \geq 0 \\ \neg(q = 0) &\mapsto (q > 0) \vee (-q > 0) \\ \neg(q \geq 0) &\mapsto -q > 0 \end{aligned}$$

Those replacements are done repeatedly until there are no occurrence of “ $\neg$ ” left in the formula.

Step (2): We replace each inequality as follows:

$$q > 0 \mapsto (q \cdot z - 1 = 0) \dots \wedge z \geq 0.$$

The dots indicate that the predicate  $z \geq 0$  does not immediately follow after  $(q \cdot z - 1 = 0)$ , but will be adjoined at the end of the new formula. Furthermore,  $z$  denotes a new variable. Those replacements are done repeatedly until there are no occurrence of “ $>$ ” left in the formula.

Step (3): We replace all atomic predicates of the form  $q \geq 0$  by the predicate  $q - z = 0$  and adjoin a new predicate  $z \geq 0$  at the the end of the formula. Again  $z$  denotes a new variable.

Step (4): We delete disjunctions as follows. It will also be necessary to replace some conjunctions. Let  $\Phi$  be the formula after Step (1)–(3). Suppose that there is a disjunction somewhere in  $\Phi$ , and write it as  $\Phi_1 \vee \Phi_2$  for two sub-formulas  $\Phi_1$  and  $\Phi_2$ . Note that  $\Phi_1 \vee \Phi_2$  might just be a small part of  $\Phi$  – there will in general be more of  $\Phi$  to the right and left of this part.

We want to reduce each of  $\Phi_i$  to a single polynomial equation, as follows. Note that since we have already performed Step (1)–(3), there are no inequalities in  $\Phi_i$ . Suppose that  $\Phi_i$  is not already a single polynomial equation. Then there must somewhere in  $\Phi_i$  be either (i) a disjunction  $p = 0 \vee q = 0$  or (ii) a conjunction  $p = 0 \wedge q = 0$ . We now explain how to reduce each of these cases to a simpler case.

- **Case (i):** We make the replacement

$$p = 0 \vee q = 0 \mapsto p \cdot q = 0.$$

- **Case (ii):** We make the replacement

$$p = 0 \wedge q = 0 \mapsto x \cdot x + y \cdot y = 0 \dots \wedge p - x = 0 \wedge q - y = 0.$$

Here,  $x$  and  $y$  are new variables. As in Step (2), the part following the dots is appended at the end of the complete formula  $\Phi$ .



Eventually, we have reduced each  $\Phi_i$  to a single polynomial equation. Thus the original disjunction  $\Phi_1 \vee \Phi_2$  has the form as in Case (i), and we apply the replacement rule described there.

At first, it might seem easier in Case (ii) to replace  $p = 0 \wedge q = 0$  by  $p \cdot p + q \cdot q = 0$ . However, we want our reduction to be linear and the simplified step could, if done repeatedly, lead to very long formulas.

With the replacement rules we have suggested, each iteration reduces the number of disjunctions and conjunctions by one and increases the length of the formula by at most a constant. Those replacements are done repeatedly until there are no disjunctions left in the formula.

This reduction takes linear time and the final formula  $\Psi$  is in conjunctive form. We need to describe a rational function

$$f : V(\Phi) \rightarrow V(\Psi).$$

Note that  $\Psi$  has all the original variables  $x_1, \dots, x_n$  of  $\Phi$  plus some additional variables, which we denote by  $z_1, \dots, z_k$ . If  $z \in \{z_1, \dots, z_k\}$  is introduced in step (2), it is assigned the value  $z = \frac{1}{q}$  and if it is introduced in step (3) or (4), it is assigned the value  $z = q$  for some polynomial  $q$ . This defines  $f$ . Assume that  $\Psi$  has the free variables  $x_1, \dots, x_n, z_1, \dots, z_k$ , where  $z_1, \dots, z_k$  are the variables introduced by the reduction. Then

$$f^{-1} : (x_1, \dots, x_n, z_1, \dots, z_k) \mapsto (x_1, \dots, x_n).$$

Thus  $f$  and  $f^{-1}$  are rational bijective functions. Thus  $f$  is a homeomorphism. The description of  $f^{-1}$  implies that  $V(\Psi)$  is a linear extension of  $V(\Phi)$ .  $\square$

**Remark 31.** *Note that the standard way to remove strict inequalities is*

$$q > 0 \mapsto q \cdot y \cdot y - 1 = 0.$$

*However, this implies that  $y = \pm\sqrt{1/q}$ . This transformation has two issues. First, the number of solutions in a sense doubles, as the sign of  $y$  is not fixed. Second, irrational solutions are introduced where before may have been only rational solutions.*

## 5.2 Reduction to Compact Semi-Algebraic Sets

**Definition 32.** *In the problem ETR-COMPACT, we are given an ETR-CONJ formula  $\Phi$  with the promise that  $V(\Phi)$  is compact. The goal is to decide if  $V(\Phi)$  is non-empty.*

In this section, we describe a reduction from ETR-CONJ to ETR-COMPACT. We need a tool from real algebraic geometry. The following corollary has been pointed out by Schaefer and Štefankovič [51] in a simplified form.

**Corollary 33** (Basu and Roy [8] Theorem 2). *Let  $\Phi$  be an instance of ETR of complexity  $L \geq 4$  such that  $V(\Phi)$  is a non-empty subset of  $\mathbb{R}^n$ . Let  $B$  be the set of points in  $\mathbb{R}^n$  at distance at most  $2^{L^{8n}} = 2^{2^{8n \log L}}$  from the origin. Then  $B \cap V(\Phi) \neq \emptyset$ .*

**Lemma B.** *Given an ETR-CONJ formula  $\Phi := \Phi(x_1, \dots, x_n)$ , we can in  $O(|\Phi| + n \log |\Phi|)$  time create an ETR-CONJ formula  $\Psi$  such that  $V(\Psi)$  is compact and  $V(\Phi) \neq \emptyset \Leftrightarrow V(\Psi) \neq \emptyset$ . In other words, there is a reduction from ETR-CONJ to ETR-COMPACT in near-linear time.*

*Proof.* Let an instance  $\Phi$  of ETR-CONJ be given and define  $k := \lceil 8n \log L \rceil$ . To make an equivalent formula  $\Psi$  such that  $V(\Psi)$  is compact, we start by including all the variables and

constraints of  $\Phi$  in  $\Psi$ . We then construct a large constant variable  $\llbracket 2^{2^k} \rrbracket$  using *exponentiation by squaring*.

$$\begin{aligned} \llbracket 2^{2^0} \rrbracket - 1 - 1 &= 0 \\ \llbracket 2^{2^1} \rrbracket - \llbracket 2^{2^0} \rrbracket \cdot \llbracket 2^{2^0} \rrbracket &= 0 \\ &\vdots \\ \llbracket 2^{2^k} \rrbracket - \llbracket 2^{2^{k-1}} \rrbracket \cdot \llbracket 2^{2^{k-1}} \rrbracket &= 0 \end{aligned}$$

For each variable  $x$  of  $\Phi$ , we now introduce the variables  $\llbracket x - 2^{2^k} \rrbracket$  and  $\llbracket x - 2^{2^k} - x \rrbracket$  and the constraints

$$\begin{aligned} \llbracket x + 2^{2^k} \rrbracket - x - \llbracket 2^{2^k} \rrbracket &= 0 \\ \llbracket x + 2^{2^k} \rrbracket &\geq 0 \\ \llbracket 2^{2^k} - x \rrbracket - \llbracket 2^{2^k} \rrbracket + x &= 0 \\ \llbracket 2^{2^k} - x \rrbracket &\geq 0. \end{aligned}$$

Note that this corresponds to introducing the constraint  $-2^{2^k} \leq x \leq 2^{2^k}$  in  $\Psi$ .

It now follows by Corollary 33 that

$$V(\Phi) \neq \emptyset \Leftrightarrow V(\Psi) \neq \emptyset.$$

Note that  $V(\Psi)$  is compact since  $\Psi$  contains no strict inequalities and each variable is bounded. This finishes the proof.  $\square$

**Remark 34.** *Unfortunately, we do not have  $V(\Phi) \simeq V(\Psi)$  in the above reduction. That is not possible as it would imply, together with Lemma A, that an open subset of  $\mathbb{R}^n$  is homeomorphic to a compact set. We can also not hope for the reduction to yield a linear extension, as a bounded set cannot be a linear extension of an unbounded one.*

### 5.3 Reduction to ETR-AMI

ETR-AMI is an abbreviation for **E**xistential **T**heory of the **R**eals with **A**ddition, **M**ultiplication, and **I**nequalities.

**Definition 35.** *An ETR-AMI formula  $\Phi := \Phi(x_1, \dots, x_n)$  is a conjunction  $C_1 \wedge \dots \wedge C_m$ , where  $m \geq 0$  and each  $C_i$  is a constraint of one of the forms*

$$x + y = z, \quad x \cdot y = z, \quad x \geq 0, \quad x = 1$$

for  $x, y, z \in \{x_1, \dots, x_n\}$ .

**Lemma C** (ETR-AMI Reduction). *Given an instance of ETR-COMPACT defined by a formula  $\Phi$ , we can in  $O(|\Phi|)$  time construct an ETR-AMI formula  $\Psi$  such that  $V(\Phi) \simeq V(\Psi)$  and  $V(\Phi) \leq_{lin} V(\Psi)$ .*

*Proof.* Recall that  $\Phi$  is a conjunction of atomic formulas of the form  $p = 0$  for a polynomial  $p$  and  $x \geq 0$  for a variable  $x$ . Each polynomial  $p$  may contain minuses, zeros, and ones. The reduction has four steps. In each step, we make changes to  $\Phi$ . In the end,  $\Phi$  has become a formula  $\Psi$  with the desired properties. In step (1)–(3), we remove unwanted ones, zeros and minuses by replacing them by constants. In step (4), we eliminate complicated polynomials.

Step (1): We introduce the constant variable  $\llbracket 1 \rrbracket$  and the constraint  $\llbracket 1 \rrbracket = 1$  to  $\Phi$ . We then replace all appearances of 1 with  $\llbracket 1 \rrbracket$  in the atomic formulas of the form  $p = 0$ .

Step (2): We introduce the constant variable  $\llbracket 0 \rrbracket$  and the constraint  $\llbracket 1 \rrbracket + \llbracket 0 \rrbracket = \llbracket 1 \rrbracket$  to  $\Phi$ . We then replace all appearances of 0 with  $\llbracket 0 \rrbracket$  except in the constraints of the form  $x \geq 0$ .

Step (3): We introduce the constant variable  $\llbracket -1 \rrbracket$  and the constraint  $\llbracket 1 \rrbracket + \llbracket -1 \rrbracket = \llbracket 0 \rrbracket$  to  $\Phi$ . We then replace all appearances of minus with a multiplication by  $\llbracket -1 \rrbracket$  in  $\Phi$ . To be precise, we replace  $-p$  with  $+\llbracket -1 \rrbracket \cdot p$ .

Step (4): We replace bottom up every occurrence of multiplication and addition by a new variable and an extra addition or multiplication constraint, which will be adjoined at the end of the formula. Here are two examples of such replacements:

$$\begin{aligned} x_1 + x_2 \cdot x_4 + x_5 + x_6 = \llbracket 0 \rrbracket &\mapsto x_1 + z_1 + x_5 + x_6 = \llbracket 0 \rrbracket \dots \wedge z_1 = x_2 \cdot x_4 \\ x_1 + z_1 + x_5 + x_6 = \llbracket 0 \rrbracket &\mapsto z_2 + x_5 + x_6 = \llbracket 0 \rrbracket \dots \wedge z_2 = x_1 + z_1 \end{aligned}$$

In this way every atomic predicate is eventually transformed to atomic predicates of ETR-AMI or is of the form  $x = \llbracket 0 \rrbracket$ . In the latter case, we replace  $x = \llbracket 0 \rrbracket$  by  $x + \llbracket 0 \rrbracket = \llbracket 0 \rrbracket$ .

To see that the reduction is linear, note that every replacement adds a constant to the length of the formula. Furthermore, at most linearly many replacements will be done.

Let us show that this reduction preserves rational equivalence and linear extension. This is trivial for steps (1)–(3), as these just introduce constants in order to rewrite polynomials without using zeros, ones, and minuses. In Step (4), we repeatedly make one of two types of steps, replacing either a multiplication or an addition. Thus it is sufficient to show that one such step preserves all of those properties. Consider a step where we go from  $\Phi_1$  to  $\Phi_2$  and  $\Phi_1$  has the variables  $x_1, \dots, x_n$  and  $\Phi_2$  has the variables  $x_1, \dots, x_n, z$ , with  $z = x_i \diamond x_j$ . Here  $\diamond$  is either multiplication or addition. This defines  $f$  as

$$(x_1, \dots, x_n) \mapsto (x_1, \dots, x_n, x_i \odot x_j),$$

and  $f^{-1}$  is defined by

$$(x_1, \dots, x_n, z) \mapsto (x_1, \dots, x_n).$$

Both functions are rational and bijective, and  $f^{-1}$  is an orthogonal projection. This implies both rational equivalence and linear extension between  $V(\Phi)$  and  $V(\Psi)$ .  $\square$

## 5.4 Reduction to ETR-SMALL

**Definition 36.** For a number  $\delta > 0$ , an ETR-SMALL- $\delta$  formula  $\Phi := \Phi(x_1, \dots, x_n)$  is a conjunction  $C_1 \wedge \dots \wedge C_m$ , where  $m \geq 0$  and each  $C_i$  is a constraint of one of the forms

$$x + y = z, \quad x \cdot y = z, \quad x \geq 0, \quad x = \delta$$

for  $x, y, z \in \{x_1, \dots, x_n\}$ .

An instance  $\mathcal{I} := [\Phi, \delta]$  of the ETR-SMALL problem is a number  $\delta := 2^{-l}$  for a positive integer  $l$  and an ETR-SMALL- $\delta$  formula  $\Phi$ . We are promised that  $V(\Phi) \subset [-\delta, \delta]^n$ . The goal is to decide whether  $V(\Phi) \neq \emptyset$ .

We are going to present a reduction from the problem ETR-AMI to ETR-SMALL. As a preparation, we present another tool from real algebraic geometry. Schaefer [50] made the following simplification of a result from [8], which we will use. More refined statements can be found in [8].

**Corollary 37** (Basu and Roy [8]). *If a bounded semi-algebraic set in  $\mathbb{R}^n$  has complexity at most  $L \geq 5n$ , then all its points have distance at most  $2^{2^{L+5}}$  from the origin.*

**Lemma D** (ETR-SMALL Reduction). *Given an ETR-AMI formula  $\Phi$  such that  $V(\Phi)$  is compact and a number  $\delta := 2^{-L}$ , we can in  $O(|\Phi| + l)$  time construct an instance  $\mathcal{I} := [\Psi, \delta]$  of ETR-SMALL such that  $V(\Phi) \simeq V(\Psi)$  and  $V(\Phi) \leq_{\text{lin}} V(\Psi)$ .*

*Proof.* Let  $\Phi$  be an instance of ETR-AMI with  $n$  variables  $x_1, \dots, x_n$ . We construct an instance  $\Psi$  of ETR-SMALL.

We set  $\varepsilon := \delta \cdot 2^{-2^{L+5}}$ , where  $L := |\Phi|$ . In  $\Psi$ , we first define a constant variable  $\llbracket \varepsilon \rrbracket$ . This is obtained by exponentiation by squaring, using  $O(L)$  new constant variables and constraints. We first define  $\llbracket \delta \rrbracket$ ,  $\llbracket 0 \rrbracket$ , and  $\llbracket \delta \cdot 2^{-2^0} \rrbracket$  by the equations

$$\begin{aligned} \llbracket \delta \rrbracket &= \delta \\ \llbracket 0 \rrbracket + \llbracket \delta \rrbracket &= \llbracket \delta \rrbracket \\ \llbracket \delta \cdot 2^{-2^0} \rrbracket + \llbracket \delta \cdot 2^{-2^0} \rrbracket &= \llbracket \delta \rrbracket. \end{aligned}$$

We then use the following equations for all  $i \in \{0, \dots, L+4\}$ ,

$$\begin{aligned} \llbracket \delta \cdot 2^{-2^i} \rrbracket \cdot \llbracket \delta \cdot 2^{-2^i} \rrbracket &= \llbracket \delta^2 \cdot 2^{-2^{i+1}} \rrbracket \\ \llbracket \delta \cdot 2^{-2^{i+1}} \rrbracket \cdot \llbracket \delta \rrbracket &= \llbracket \delta^2 \cdot 2^{-2^{i+1}} \rrbracket. \end{aligned}$$

Finally, we define  $\llbracket \varepsilon \rrbracket$  by the constraint  $\llbracket \varepsilon \rrbracket + \llbracket 0 \rrbracket = \llbracket \delta \cdot 2^{-2^{L+5}} \rrbracket$ .

In  $\Psi$ , we use the variables  $\llbracket \varepsilon x_1 \rrbracket, \dots, \llbracket \varepsilon x_n \rrbracket$  instead of  $x_1, \dots, x_n$ . An equation of  $\Phi$  of the form  $x = 1$  is transformed to the equation  $\llbracket \varepsilon x \rrbracket + \llbracket 0 \rrbracket = \llbracket \varepsilon \rrbracket$  in  $\Psi$ . An equation of  $\Phi$  of the form  $x + y = z$  is transformed to the equation  $\llbracket \varepsilon x \rrbracket + \llbracket \varepsilon y \rrbracket = \llbracket \varepsilon z \rrbracket$  of  $\Psi$ . For an equation of  $\Phi$  of the form  $x \cdot y = z$ , we also introduce a variable  $\llbracket \varepsilon^2 z \rrbracket$  of  $\Psi$  and the equations

$$\begin{aligned} \llbracket \varepsilon x \rrbracket \cdot \llbracket \varepsilon y \rrbracket &= \llbracket \varepsilon^2 z \rrbracket \\ \llbracket \varepsilon \rrbracket \cdot \llbracket \varepsilon z \rrbracket &= \llbracket \varepsilon^2 z \rrbracket. \end{aligned}$$

At last, constraints of the form  $x \geq 0$  become  $\llbracket \varepsilon x \rrbracket \geq 0$ .

We now describe a function  $f : V(\Phi) \rightarrow V(\Psi)$  in order to show that  $\Psi$  has the properties stated in the lemma. Let  $\mathbf{x} := (x_1, \dots, x_n) \in V(\Phi)$ . In order to define  $f$ , it suffices to specify the values of the variables of  $\Psi$  depending on  $\mathbf{x}$ . For all the constant variables  $\llbracket c \rrbracket$ , we define  $\llbracket c \rrbracket := c$ . Note that these are all *rational* constants. For all  $i \in \{1, \dots, n\}$ , we now define  $\llbracket \varepsilon x_i \rrbracket := \varepsilon x_i$  and (when  $\llbracket \varepsilon^2 x_i \rrbracket$  appears in  $\Psi$ )  $\llbracket \varepsilon^2 x_i \rrbracket = \varepsilon^2 x_i$ . Since  $\mathbf{x}$  is a solution to  $\Phi$ , it follows from the constraints of  $\Psi$  that these assignments are a solution to  $\Psi$ .

We need to verify that  $\Psi$  defines an ETR-SMALL problem, i.e., that  $\Psi$  satisfies the promise that  $V(\Psi) \subset [-\delta, \delta]^m$ , where  $m$  is the number of variables of  $\Psi$ . To this end, consider an assignment of the variables of  $\Psi$  that satisfies all the constraints. Note first that the constant variables are non-negative and at most  $\delta$ . For the other variables, we consider the inverse  $f^{-1}$ , which is given by the assignment  $x_i := \llbracket \varepsilon x_i \rrbracket / \varepsilon$  for all  $i \in \{1, \dots, n\}$ . It follows that this yields

a solution to  $\Phi$ . Since  $V(\Phi)$  is compact, it follows from Corollary 37 that  $|\llbracket \varepsilon x_i \rrbracket|/\varepsilon \leq 2^{2^{L+5}}$ . Hence  $|\llbracket \varepsilon x_i \rrbracket| \leq \varepsilon \cdot 2^{2^{L+5}} = \delta \cdot 2^{-2^{L+5}} \cdot 2^{2^{L+5}} = \delta$ . Similarly, when  $\llbracket \varepsilon^2 x_i \rrbracket$  is a variable of  $\Psi$ , we get  $|\llbracket \varepsilon^2 x_i \rrbracket| \leq \varepsilon \cdot \delta < \delta$ .

By the definitions of  $f$  and  $f^{-1}$ , we have now established that  $V(\Phi) \simeq V(\Psi)$  and  $V(\Phi) \leq_{\text{lin}} V(\Psi)$ . The length of  $\Psi$  is  $O(L)$  longer than the length of  $\Phi$ , and  $\Psi$  can thus be computed in  $O(|\Phi|)$  time.  $\square$

**Corollary 38.** *ETR-SMALL is  $\exists\mathbb{R}$ -complete, even when  $\delta = O(n^{-c})$  for any constant  $c > 0$ , where  $n$  is the number of variables in the ETR-SMALL- $\delta$  formula.*

*Proof.* Let an ETR-AMI formula  $\Phi$  with  $n$  variables be given. Let  $l \in \mathbb{N}$  be such that  $2^{-l} \leq n^{-c}$  and define  $\delta := 2^{-l}$ . The reduction of Lemma D gives an equivalent instance  $\mathcal{I} := [\Psi, \delta]$  of ETR-SMALL in time  $O(|\Phi| + l)$ . Since  $l = O(\log n)$ , the reduction takes polynomial time.  $\square$

## 5.5 Reduction to ETR-SHIFT

**Definition 39.** *An ETR-SHIFT formula  $\Phi := \Phi(x_1, \dots, x_n)$  is a conjunction*

$$\left( \bigwedge_{i=1}^n 1/2 \leq x_i \leq 2 \right) \wedge \left( \bigwedge_{i=1}^m C_i \right),$$

where  $m \geq 0$  and each  $C_i$  is of one of the forms

$$x + y = z, \quad x \cdot y = z$$

for  $x, y, z \in \{x_1, \dots, x_n\}$ .

An instance  $\mathcal{I} := [\Phi, \delta, (I(x_1), \dots, I(x_n))]$  of the ETR-SHIFT problem is an ETR-SHIFT formula  $\Phi$ , a number  $\delta := 2^{-l}$  for a positive integer  $l$ , and, for each variable  $x \in \{x_1, \dots, x_n\}$ , an interval  $I(x) \subseteq [1/2, 2]$  such that  $|I(x)| \leq 2\delta$ . For each multiplication constraint  $x \cdot y = z$ , we have  $I(x) \subset [1 - \delta, 1 + \delta]$  and  $I(y) \subset [1 - \delta, 1 + \delta]$ .

We are promised that  $V(\Phi) \subset I(x_1) \times \dots \times I(x_n)$ . The goal is to decide whether  $V(\Phi) \neq \emptyset$ .

We will now present a reduction from the problem ETR-SMALL to ETR-SHIFT. The following technical lemma is a handy tool to show that all variables  $x$  of the constructed ETR-SHIFT problem are in the ranges  $I(x)$  we are going to specify.

**Lemma 40.** *Let  $g(x, y) := \frac{p(x, y)}{q(x, y)}$  be a rational function such that*

$$\begin{aligned} p(x, y) &:= a_1 x^2 + a_2 xy + a_3 y^2 + a_4 x + a_5 y + a_6, \quad \text{and} \\ q(x, y) &:= b_1 x^2 + b_2 xy + b_3 y^2 + b_4 x + b_5 y + b_6, \end{aligned}$$

where  $a_6, b_6 > 0$ . Let  $\alpha := |b_1| + \dots + |b_5|$  and  $\beta := |b_1| + \dots + |b_5|$ , and let  $\delta \in [0, 1]$  be such that  $a_6 > \alpha\delta$  and  $b_6 > \beta\delta$ .

Then for all  $x, y \in [-\delta, \delta]$ , we have

$$g(x, y) \in \left[ \frac{-\alpha\delta + a_6}{\beta\delta + b_6}, \frac{\alpha\delta + a_6}{-\beta\delta + b_6} \right]. \quad (2)$$

In particular,

(a) if  $q(x, y) = b_6 = 1$  and  $a_1, \dots, a_5 \in [0, c]$  for some  $c \geq 0$ , then

$$g(x, y) \in [a_6 - 5c\delta, a_6 + 5c\delta],$$

and

(b) if  $a_1, \dots, a_5, b_1, \dots, b_5 \in [-c, c]$  for some  $c \geq 0$  and  $\delta \leq \frac{\varepsilon b_6^2}{5c(a_6 + (1+\varepsilon)b_6)}$  for a given  $\varepsilon > 0$ , then

$$g(x, y) \in [a_6/b_6 - \varepsilon, a_6/b_6 + \varepsilon].$$

*Proof.* We bound each term in each polynomial from below and above and get

$$\begin{aligned} p(x, y) &\in [-(|a_1| + |a_2| + |a_3|)\delta^2 - (|a_4| + |a_5|)\delta + a_6, \\ &\quad + (|a_1| + |a_2| + |a_3|)\delta^2 + (|a_4| + |a_5|)\delta + a_6], \quad \text{and} \\ q(x, y) &\in [-(|b_1| + |b_2| + |b_3|)\delta^2 - (|b_4| + |b_5|)\delta + b_6, \\ &\quad + (|b_1| + |b_2| + |b_3|)\delta^2 + (|b_4| + |b_5|)\delta + b_6]. \end{aligned}$$

Since  $\delta \in [0, 1]$ , we have  $\delta^2 \leq \delta$ , so that  $p(x, y) \in [-\alpha\delta + a_6, \alpha\delta + a_6]$  and  $q(x, y) \in [-\beta\delta + b_6, \beta\delta + b_6]$ . The bounds (2) now follows since both of these intervals are positive by assumption.

For part (a), note that  $\beta = 0$  and  $\alpha \in [0, 5c]$ . For part (b), we get that

$$g(x, y) \in \left[ \frac{-5c\delta + a_6}{5c\delta + b_6}, \frac{5c\delta + a_6}{-5c\delta + b_6} \right].$$

One can then check that if  $\delta \leq \frac{\varepsilon b_6^2}{5c(a_6 + (1+\varepsilon)b_6)}$ , that range is contained in  $[a_6/b_6 - \varepsilon, a_6/b_6 + \varepsilon]$ .  $\square$

**Lemma E** (ETR-SHIFT Reduction). *Let  $\delta_2 := 2^{-l}$  for  $l \geq 3$ , and let  $\delta_1 := 2^{-l-3}$ . Consider an instance  $\mathcal{I}_1 := [\Phi_1, \delta_1]$ . We can in  $O(|\mathcal{I}_1|) = O(|\Phi_1| + l)$  time compute an instance  $\mathcal{I}_2$  of the ETR-SHIFT problem with  $\delta(\mathcal{I}_2) = \delta_2$  and formula  $\Phi_2 := \Phi(\mathcal{I}_2)$  such that  $V(\Phi_1) \simeq V(\Phi_2)$  and  $V(\Phi_1) \leq_{lin} V(\Phi_2)$ .*

*Proof.* In the following, we specify the variables and constraints we add to  $\Phi_2$ . Define  $\Delta := 1 - \delta_1$ . As a first step, we construct constant variables  $\llbracket c \rrbracket$  for each of  $c \in \{1/2, 3/4, 1, 3/2\}$ , as follows. We first use the constraint  $\llbracket 1 \rrbracket \cdot \llbracket 1 \rrbracket = \llbracket 1 \rrbracket$ . Note that the solutions to this are  $\llbracket 1 \rrbracket \in \{0, 1\}$ , but since we are restricted to  $[1/2, 2]$ , we conclude that  $\llbracket 1 \rrbracket = 1$ . We observe that  $\llbracket 1 \rrbracket$  is in the promised range  $[1 - \delta_2, 1 + \delta_2]$  of variables involved in multiplication constraints.

We can then construct the other constants as follows.

$$\begin{aligned} \llbracket 1/2 \rrbracket + \llbracket 1/2 \rrbracket &= \llbracket 1 \rrbracket \\ \llbracket 1 \rrbracket + \llbracket 1/2 \rrbracket &= \llbracket 3/2 \rrbracket \\ \llbracket 3/4 \rrbracket + \llbracket 3/4 \rrbracket &= \llbracket 3/2 \rrbracket \end{aligned}$$

We now show how to construct a constant variable  $\llbracket \Delta \rrbracket$ . To this end, we construct constant variables  $\llbracket 1 - 2^{-i} \rrbracket$  for  $i \in \{1, \dots, l\}$ , so that  $\llbracket \Delta \rrbracket$  is a synonym for  $\llbracket 1 - 2^{-l} \rrbracket$ . For the base case  $i = 1$ , note that this is just the already constructed  $\llbracket 1/2 \rrbracket$ . Suppose inductively that we have constructed the constant variable  $\llbracket 1 - 2^{-i} \rrbracket$ . In order to construct  $\llbracket 1 - 2^{-(i+1)} \rrbracket$ , we proceed as follows.

$$\begin{aligned} \llbracket 1 - 2^{-i} \rrbracket + \llbracket 1 \rrbracket &= \llbracket 2 - 2^{-i} \rrbracket \\ \llbracket 1 - 2^{-(i+1)} \rrbracket + \llbracket 1 - 2^{-(i+1)} \rrbracket &= \llbracket 2 - 2^{-i} \rrbracket \end{aligned}$$

Thus we can generate a variable with the value  $\llbracket \Delta \rrbracket$  in  $O(l)$  steps.

For each of the constant variables  $\llbracket c \rrbracket$  thus created, we define  $I(\llbracket c \rrbracket) := [c - \delta_2, c + \delta_2] \cap [1/2, 2]$ . Note that it follows from the constraints that in any solution to  $\Phi_2$ , we must have  $\llbracket c \rrbracket = c$ .

For each each variable  $x \in [-\delta_1, \delta_1]$  of  $\Phi_1$ , we make a corresponding variable  $\llbracket x + 1 \rrbracket$  of  $\Phi_2$ . As we shall see, for every solution  $\mathbf{x} := (x_1, \dots, x_n)$  of  $\Phi_1$ , there will be a corresponding solution to  $\Phi_2$  with  $\llbracket x_i + 1 \rrbracket = x_i + 1$ , and vice versa.

For each variable  $x$  of  $\Phi_1$ , we construct the variables  $\llbracket x + 3/2 \rrbracket$ ,  $\llbracket x + 3/4 \rrbracket$ , and  $\llbracket x + \Delta \rrbracket$  as follows.

$$\begin{aligned}\llbracket x + 1 \rrbracket + \llbracket 1/2 \rrbracket &= \llbracket x + 3/2 \rrbracket \\ \llbracket x + 3/4 \rrbracket + \llbracket 3/4 \rrbracket &= \llbracket x + 3/2 \rrbracket \\ \llbracket x + 3/4 \rrbracket + \llbracket \Delta \rrbracket &= \llbracket x + 3/4 + \Delta \rrbracket \\ \llbracket x + \Delta \rrbracket + \llbracket 3/4 \rrbracket &= \llbracket x + 3/4 + \Delta \rrbracket.\end{aligned}$$

For each of these of the form  $\llbracket x + b \rrbracket$ ,  $b \in \{3/4, \Delta, 3/2\}$ , it holds that if  $\llbracket x + 1 \rrbracket = x + 1$ , then  $\llbracket x + b \rrbracket = x + b$ .

We now go through the constraints of  $\Phi_1$  and create equivalent constraints in  $\Phi_2$ . For each equation  $x = \delta_1$  of  $\Phi_1$ , we add the equation

$$\llbracket x + \Delta \rrbracket \cdot \llbracket 1 \rrbracket = \llbracket 1 \rrbracket$$

to  $\Phi_2$ . The equation implies that if  $\llbracket x + 1 \rrbracket = x + 1$ , then  $x = \delta_1$ .

For each equation  $x + y = z$  of  $\Phi_1$ , we add

$$\llbracket x + 3/4 \rrbracket + \llbracket y + 3/4 \rrbracket = \llbracket z + 3/2 \rrbracket \tag{3}$$

to  $\Phi_2$ . This equation implies that if  $\llbracket x + 1 \rrbracket = x + 1$  and  $\llbracket y + 1 \rrbracket = y + 1$ , then  $\llbracket z + 1 \rrbracket = x + y + 1$ .

For each equation  $x \cdot y = z$  of  $\Phi_1$ , we have the following set of equations in  $\Phi_2$ .

$$\begin{aligned}\llbracket x + 1 \rrbracket \cdot \llbracket y + 1 \rrbracket &= \llbracket xy + x + y + 1 \rrbracket \\ \llbracket xy + x + y + 1 \rrbracket + \llbracket 1/2 \rrbracket &= \llbracket xy + x + y + 3/2 \rrbracket \\ \llbracket xy + x + 3/4 \rrbracket + \llbracket y + 3/4 \rrbracket &= \llbracket xy + x + y + 3/2 \rrbracket \\ \llbracket xy + x + 3/4 \rrbracket + \llbracket 3/4 \rrbracket &= \llbracket xy + x + 3/2 \rrbracket \\ \llbracket z + 3/4 \rrbracket + \llbracket x + 3/4 \rrbracket &= \llbracket xy + x + 3/2 \rrbracket\end{aligned}$$

These equations imply that if  $\llbracket x + 1 \rrbracket = x + 1$  and  $\llbracket y + 1 \rrbracket = y + 1$ , then  $\llbracket z + 1 \rrbracket = xy + 1$ .

At last, for each constraint  $x \geq 0$  of  $\Phi_1$ , we introduce the variable  $\llbracket x + 1/2 \rrbracket$  of  $\Phi_2$  and the equation  $\llbracket x + 1/2 \rrbracket + \llbracket 1/2 \rrbracket = \llbracket x + 1 \rrbracket$ . The constraint  $\llbracket x + 1/2 \rrbracket \geq 1/2$ , which holds for all variables of  $\Phi_2$  by definition of ETR-SHIFT, then corresponds to  $x \geq 0$ .

For the variables  $\llbracket x + \Delta \rrbracket$ , we define  $I(\llbracket x + \Delta \rrbracket) := [1 - \delta_2, 1 + \delta_2]$ , since the variable takes part in a multiplication constraint. For all the other variables, we define the intervals as follows. Note that each of the introduced variables has the form  $\llbracket p(x, y) \rrbracket$ , where  $p(x, y)$  is a polynomial of degree at most 2 and with constant term  $c := p(0, 0) \in \{1/2, 3/4, 1, 3/2\}$ . We now define  $I(\llbracket p(x, y) \rrbracket) := [c - \delta_2, c + \delta_2] \cap [1/2, 2]$ .

The construction of  $\Phi_2$  is now finished, and we need to check that it has the claimed properties. Let the variables of  $\Phi_1$  be  $x_1, \dots, x_n$  and the variables of  $\Phi_2$  be

$$\llbracket x_1 + 1 \rrbracket, \dots, \llbracket x_n + 1 \rrbracket, \llbracket y_1 \rrbracket, \dots, \llbracket y_m \rrbracket.$$

For each variable  $\llbracket y_i \rrbracket$ ,  $i \in \{1, \dots, m\}$ , the expression  $y_i$  is a polynomial of degree at most two in two variables among  $x_1, \dots, x_n$  (this includes the case that  $y_i$  is a constant). Consider any solution  $\mathbf{x} := (x_1, \dots, x_n) \in [-\delta_1, \delta_1]^n$  to  $\Phi_1$ . We get a corresponding solution  $f(\mathbf{x})$  to  $\Phi_2$  as follows. We set  $\llbracket x_i + 1 \rrbracket := x_i + 1$  for every  $i \in \{1, \dots, n\}$ . For every  $i \in \{1, \dots, m\}$ ,  $y_i$  is a

(possibly constant) polynomial in two variables among  $x_1, \dots, x_n$ , and we assign  $\llbracket y_i \rrbracket$  the value we get when evaluating this polynomial.

In order to show that this yields a solution to  $\Phi_2$ , we consider the constraint (3) introduced to  $\Phi_2$  due to an addition  $x + y = z$  of  $\Phi_1$ . The other constraints can be verified in a similar way. Due to the construction of  $\llbracket x + 3/4 \rrbracket$ , it follows from  $\llbracket x + 1 \rrbracket := x + 1$  that  $\llbracket x + 3/4 \rrbracket = x + 3/4$ , and similarly that  $\llbracket y + 3/4 \rrbracket = y + 3/4$  and  $\llbracket z + 3/2 \rrbracket = z + 3/2$ . Hence we have

$$\llbracket x + 3/4 \rrbracket + \llbracket y + 3/4 \rrbracket = x + 3/4 + y + 3/4 = z + 3/2 = \llbracket z + 3/2 \rrbracket,$$

so indeed the constraint is satisfied.

Note that the inverse of  $f$  is

$$f^{-1} : (\llbracket x_1 + 1 \rrbracket, \dots, \llbracket x_n + 1 \rrbracket, \llbracket y_1 \rrbracket, \dots, \llbracket y_m \rrbracket) \mapsto (\llbracket x_1 + 1 \rrbracket - 1, \dots, \llbracket x_n + 1 \rrbracket - 1).$$

We now show that  $f^{-1}$  is a map from  $V(\Phi_2)$  to  $V(\Phi_1)$ , i.e., that given any solution to  $\Phi_2$ ,  $f^{-1}$  yields a solution to  $\Phi_1$ . Consider a constraint of  $\Phi_1$  of the form  $x + y = z$ . We then have

$$\begin{aligned} x + y &= \llbracket x + 1 \rrbracket - 1 + \llbracket y + 1 \rrbracket - 1 = \llbracket x + 3/4 \rrbracket + 1/4 - 1 + \llbracket y + 3/4 \rrbracket + 1/4 - 1 \\ &= \llbracket z + 3/2 \rrbracket - 3/2 = z. \end{aligned}$$

In a similar way, the other constraints of  $\Phi_1$  can be shown to hold due to the constraints of  $\Phi_2$ .

It follows that  $f$  is a rational homeomorphism so  $V(\Phi_1) \simeq V(\Phi_2)$ , and since  $f^{-1}$  merely subtracts 1 from some variables, we also have  $V(\Phi_1) \leq_{\text{lin}} V(\Phi_2)$ .

At last, we need to verify that  $\Phi_2$  satisfies the promise that in every solution, each variable  $\llbracket p(x, y) \rrbracket$  is in the interval  $I(\llbracket p(x, y) \rrbracket)$ . Here,  $p(x, y)$  is a polynomial of degree at most 2 and with constant term  $c := p(0, 0) \in \{1/2, 3/4, 1, 3/2\}$ . By the map  $f^{-1}$ , we get a solution to  $\Phi_1$  by the assignments  $x := \llbracket x + 1 \rrbracket - 1$  and  $y := \llbracket y + 1 \rrbracket - 1$  (and similarly for the remaining variables of  $\Phi_1$ ). It then follows from the constraints of  $\Phi_2$  that  $\llbracket p(x, y) \rrbracket = p(x, y)$ . By the promise of  $\Phi_1$ , we get that  $x, y \in [-\delta_1, \delta_1]$ . The coefficients of the non-constant terms of  $p(x, y)$  are all either 0 or 1. We therefore get by Lemma 40 that since  $x, y \in [-\delta_1, \delta_1]$ , then  $p(x, y) \in [c - 5\delta_1, c + 5\delta_1] \subset [c - \delta_2, c + \delta_2]$ .

Recall that  $I(\llbracket p(x, y) \rrbracket) := [c - \delta_2, c + \delta_2] \cap [1/2, 2]$  and that  $\delta_2 < 1/4$ . With the exception of the case  $c = 1/2$ , we therefore have that  $I(\llbracket p(x, y) \rrbracket) = [c - \delta_2, c + \delta_2]$ , so it follows that  $\llbracket p(x, y) \rrbracket \in I(\llbracket p(x, y) \rrbracket)$ . Note that the case  $c = 1/2$  only occurs when  $p(x, y) = x + 1/2$  and  $I(\llbracket x + 1/2 \rrbracket) = [1/2, 1/2 + \delta_2]$ . In this case, there is a constraint  $x \geq 0$  in  $\Phi_1$ . Hence  $x \in [0, \delta_1]$ , so that  $\llbracket x + 1/2 \rrbracket = x + 1/2 \in [1/2, 1/2 + \delta_1] \subset [1/2, 1/2 + \delta_2] = I(\llbracket x + 1/2 \rrbracket)$ .

In order to construct  $\llbracket \Delta \rrbracket$  in  $\Phi_2$ , we introduce  $O(l)$  variables and constraints. For each of the  $O(|\Phi_1|)$  variables and constraints of  $\Phi_1$ , we make a constant number of variables and constraints in  $\Phi_2$ . It thus follows that the running time is  $O(|\Phi_1| + l)$ . This completes the proof.  $\square$

## 5.6 Reduction to ETR-SQUARE

In this and the following section, we show that the problem ETR-SHIFT remains essentially equally hard even when we only allow more specialized types of multiplications in our formulas. In this section, we require every multiplication to be a *squaring* of the form  $x^2 = y$ , and in the following section, we only allow *inversion* of the form  $x \cdot y = 1$ . The result that these two restricted types of constraints preserve the full expressibility of ETR-SHIFT is related to the result of Aho et al. [5, Section 8.2] that squaring and taking reciprocals of integers require work proportional to that of multiplication.



**Definition 41.** An ETR-SQUARE formula  $\Phi := \Phi(x_1, \dots, x_n)$  is a conjunction

$$\left( \bigwedge_{i=1}^n 1/2 \leq x_i \leq 2 \right) \wedge \left( \bigwedge_{i=1}^m C_i \right),$$

where  $m \geq 0$  and each  $C_i$  is of one of the forms

$$x + y = z, \quad x^2 = y$$

for  $x, y, z \in \{x_1, \dots, x_n\}$ .

An instance  $\mathcal{I} = [\Phi, \delta, (I(x_1), \dots, I(x_n))]$  of the ETR-SQUARE problem is an ETR-SQUARE formula  $\Phi$ , a number  $\delta := 2^{-l}$  for a positive integer  $l$ , and, for each variable  $x \in \{x_1, \dots, x_n\}$ , an interval  $I(x) \subseteq [1/2, 2]$  such that  $|I(x)| \leq 2\delta$ . For every squaring constraint  $x^2 = y$ , we have  $I(x) \subset [1 - \delta, 1 + \delta]$ .

We are promised that  $V(\Phi) \subset I(x_1) \times \dots \times I(x_n)$ . The goal is to decide whether  $V(\Phi) \neq \emptyset$ .

Below, we present a reduction from the problem ETR-SHIFT to ETR-SQUARE.

**Lemma F** (ETR-SQUARE Reduction). Let  $\delta_2 := 2^{-l}$  be given for  $l \geq 3$ , and let  $\delta_1 := 2^{-l-4}$ . Consider an instance  $\mathcal{I}_1$  of the ETR-SHIFT problem such that  $\delta(\mathcal{I}_1) = \delta_1$ , and let  $\Phi_1 := \Phi(\mathcal{I}_1)$ . We can in  $O(|\mathcal{I}_1|)$  time compute an instance  $\mathcal{I}_2$  of the ETR-SQUARE problem with  $\delta(\mathcal{I}_2) = \delta_2$  and formula  $\Phi_2 := \Phi(\mathcal{I}_2)$  such that  $V(\Phi_1) \simeq V(\Phi_2)$  and  $V(\Phi_1) \leq_{lin} V(\Phi_2)$ .

*Proof.* As in the proof of Lemma E, we first construct constant variables  $\llbracket b \rrbracket$  for each of  $b \in \{1/2, 3/4, 1, 3/2\}$ . The only difference is that we now construct  $\llbracket 1 \rrbracket$  using the constraint  $\llbracket 1 \rrbracket^2 = \llbracket 1 \rrbracket$ . The other constants are then constructed in exactly the same way as before.

We include each variable  $x$  of  $\Phi_1$  in  $\Phi_2$  as well, and reuse the interval  $I(x)$  from  $\mathcal{I}_1$  in  $\mathcal{I}_2$ . We also reuse all constraints from  $\Phi_1$  of the form  $a + b = c$  in  $\Phi_2$ , but we have to do something different for the constraints  $a \cdot b = c$ . The idea is very simple and was also used by Aho et al. [5, Section 8.2], and can be expressed by the equations

$$\begin{aligned} x &= (a + b)/2 \\ y &= (a - b)/2 \\ u &= x^2 \\ v &= y^2 \\ c &= u - v = a \cdot b. \end{aligned}$$

If there were no range constraints, we could just replace each multiplication  $a \cdot b = c$  of  $\Phi_1$  by equations as above (after rewriting the subtractions as additions, etc.). However, in our situation all intermediate variables  $w$  need to be in a range  $I(w) \subset [1/2, 2]$  in any solution. While this makes the description more involved, careful shifting will work for us.

Let  $a \cdot b = c$  be a multiplication constraint in  $\Phi_1$ . Let us rename the variables as  $\llbracket x + 1 \rrbracket := a$ ,  $\llbracket y + 1 \rrbracket := b$ , and  $\llbracket xy + x + y + 1 \rrbracket := c$ , so that  $a \cdot b = c$  becomes

$$\llbracket x + 1 \rrbracket \cdot \llbracket y + 1 \rrbracket = \llbracket xy + x + y + 1 \rrbracket. \quad (\dagger)$$

Consider two numbers  $x, y \in \mathbb{R}$  and the two conditions

$$\llbracket x + 1 \rrbracket = x + 1 \quad \text{and} \quad \llbracket y + 1 \rrbracket = y + 1, \quad (\star)$$

$$\llbracket xy + x + y + 1 \rrbracket = xy + x + y + 1. \quad (\star\star)$$

We claim that  $(\dagger)$  is equivalent to

$$(\star) \text{ implies } (\star\star). \quad (\ddagger)$$

To show this claim, suppose first that  $(\dagger)$  holds. Define  $x := \llbracket x + 1 \rrbracket - 1$  and  $y := \llbracket y + 1 \rrbracket - 1$ . Then  $\llbracket xy + x + y + 1 \rrbracket = \llbracket x + 1 \rrbracket \cdot \llbracket y + 1 \rrbracket = (x+1) \cdot (y+1) = xy + x + y + 1$ , so that  $(\star\star)$  holds. Hence we have  $(\ddagger)$ . On the other hand, suppose that  $(\ddagger)$  holds, and define  $x := \llbracket x + 1 \rrbracket - 1$  and  $y := \llbracket y + 1 \rrbracket - 1$  so that  $(\star)$  holds. Our assumption implies that  $(\star\star)$  holds, and we thus have  $\llbracket xy + x + y + 1 \rrbracket = xy + x + y + 1 = (x+1) \cdot (y+1) = \llbracket x + 1 \rrbracket \cdot \llbracket y + 1 \rrbracket$ , so that  $(\dagger)$  holds. Our aim is therefore to make constraints in  $\Phi_2$  that ensure  $(\ddagger)$ .

For every variable  $\llbracket q \rrbracket$  of  $\Phi_2$ , we can construct  $\llbracket q/2 \rrbracket$  using the constraint  $\llbracket q/2 \rrbracket + \llbracket q/2 \rrbracket = \llbracket q \rrbracket$ . Similarly, we can construct  $\llbracket 2q \rrbracket$  by  $\llbracket q \rrbracket + \llbracket q \rrbracket = \llbracket 2q \rrbracket$ .

The construction of  $\llbracket xy + x + y + 1 \rrbracket$  is shown in Figure 12. The diagram should be understood in the following way. We start with the original variables  $\llbracket x + 1 \rrbracket$  and  $\llbracket y + 1 \rrbracket$ . Each arrow is labeled with the operation that leads to the new variable. It is straightforward to check that the construction ensures condition  $(\ddagger)$ .

Note that each of the constructed auxilliary variables has the form  $\llbracket p(x, y) \rrbracket$ , where  $p(x, y)$  is a second degree polynomial with constant term  $c := p(0, 0) \in \{3/4, 1, 3/2\}$ . We define  $I(\llbracket p(x, y) \rrbracket) := [c - \delta_2, c + \delta_2]$ . This finishes the construction of  $\mathcal{I}_2$ . Note that since  $\delta_2 \leq 1/4$  and  $c \in \{3/4, 1, 3/2\}$ , we get that  $I(\llbracket p(x, y) \rrbracket) \subset [1/2, 2]$ , as required.

We now verify that  $\mathcal{I}_2$  has the claimed properties. Consider a solution  $\mathbf{x} \in V(\Phi_1)$ . We point out an equivalent solution to  $\Phi_2$ . For all the variables of  $\Phi_2$  that also appear in  $\Phi_1$ , we use the same value as in the solution  $\mathbf{x}$ . Each auxilliary variable has the form  $\llbracket p(x, y) \rrbracket$ , where  $p(x, y)$  is a second degree polynomial, and  $\Phi_1$  contains the multiplication constraint  $(\dagger)$ . We then get from the promise of  $\Phi_1$  that  $\llbracket 1 + x \rrbracket = 1 + x$  and  $\llbracket 1 + y \rrbracket = 1 + y$  for  $x, y \in [-\delta_1, \delta_1]$ . From the construction shown in Figure 12, it follows that in order to get a solution to  $\Phi_2$ , we must define  $\llbracket p(x, y) \rrbracket := p(x, y)$ . Recall that the constant term  $c := p(0, 0)$  satisfies  $c \in \{3/4, 1, 3/2\}$ , and note that all the coefficients of the non-constant terms of  $p(x, y)$  are in the interval  $[0, 2]$ . We then get from Lemma 40 that  $\llbracket p(x, y) \rrbracket \in [c - 10\delta_1, c + 10\delta_1] = [c - \delta_2, c + \delta_2] = I(\llbracket p(x, y) \rrbracket) \subset [1/2, 2]$ . The variables are thus in the range  $[1/2, 2]$ , so we have described a solution to  $\Phi_2$ .

Similarly, we see that any solution to  $\Phi_2$  corresponds to a solution to  $\Phi_1$ . Using the promise of  $\mathcal{I}_1$  and Lemma 40 as above, we then also confirm the promise of  $\mathcal{I}_2$  that each variable  $u$  of  $\Phi_2$  is in  $I(u)$ .

The correspondance described implies that  $V(\Phi_1) \simeq V(\Phi_2)$  and  $V(\Phi_1) \leq_{\text{lin}} V(\Phi_2)$ . For each constraint of  $\Phi_1$ , we introduce  $O(1)$  variables and constraints of  $\Phi_2$ , so the reduction takes  $O(|\Phi_1|)$  time.  $\square$

## 5.7 Reduction to RANGE-ETR-INV

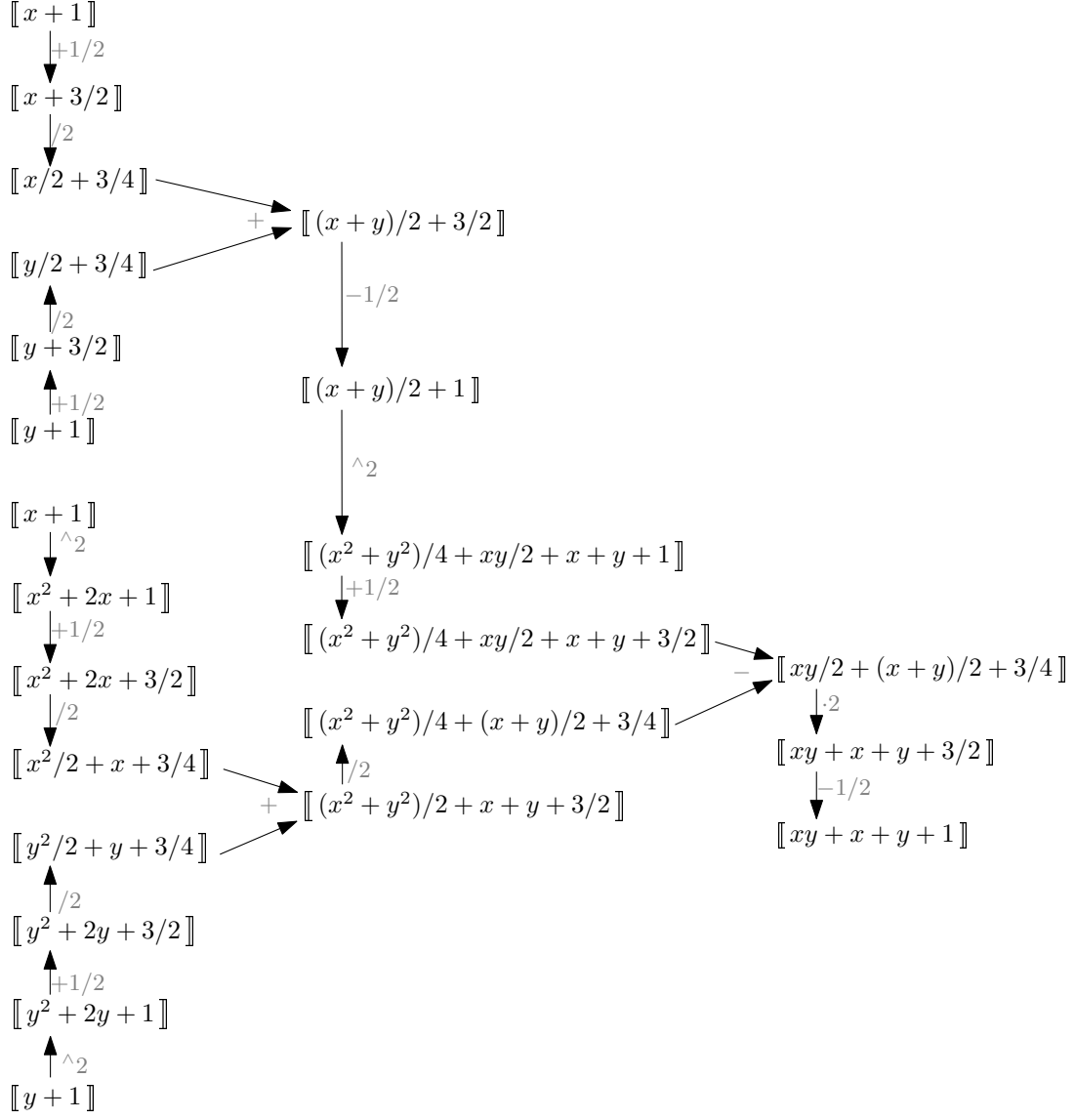
**Definition 1.** An ETR-INV formula  $\Phi = \Phi(x_1, \dots, x_n)$  is a conjunction

$$\left( \bigwedge_{i=1}^n 1/2 \leq x_i \leq 2 \right) \wedge \left( \bigwedge_{i=1}^m C_i \right),$$

where  $m \geq 0$  and each  $C_i$  is of one of the forms

$$x + y = z, \quad x \cdot y = 1$$

for  $x, y, z \in \{x_1, \dots, x_n\}$ .



**Figure 12:** The construction of  $\llbracket xy + x + y + 1 \rrbracket$  from  $\llbracket x + 1 \rrbracket$  and  $\llbracket y + 1 \rrbracket$ . Squaring a variable is denoted by  $\wedge 2$ .

**Definition 2.** An instance  $\mathcal{I} = [\Phi, \delta, (I(x_1), \dots, I(x_n))]$  of the RANGE-ETR-INV problem consists of an ETR-INV formula  $\Phi$ , a number  $\delta := 2^{-l}$  for a positive integer  $l$ , and, for each variable  $x \in \{x_1, \dots, x_n\}$ , an interval  $I(x) \subseteq [1/2, 2]$  such that  $|I(x)| \leq 2\delta$ . For every inversion constraint  $x \cdot y = 1$ , we have either  $I(x) = I(y) = [1 - \delta, 1 + \delta]$  or  $I(x) = [2/3 - \delta, 2/3 + \delta]$  and  $I(y) = [3/2 - \delta, 3/2 + \delta]$ . We are promised that  $V(\Phi) \subset I(x_1) \times \dots \times I(x_n)$ . The goal is to decide whether  $V(\Phi) \neq \emptyset$ .

We will now present a reduction from the problem ETR-SQUARE to RANGE-ETR-INV.

**Lemma G** (RANGE-ETR-INV Reduction). Let  $\delta_2 := 2^{-l}$  be given for  $l \geq 3$ , and let  $\delta_1 := 2^{-l-11}$ . Consider an instance  $\mathcal{I}_1$  of the ETR-SQUARE problem such that  $\delta(\mathcal{I}_1) = \delta_1$ , and let  $\Phi_1 := \Phi(\mathcal{I}_1)$ . We can in  $O(|\mathcal{I}_1|)$  time compute an instance  $\mathcal{I}_2$  of the RANGE-ETR-INV problem with  $\delta(\mathcal{I}_2) = \delta_2$  and formula  $\Phi_2 := \Phi(\mathcal{I}_2)$  such that  $V(\Phi_1) \simeq V(\Phi_2)$  and  $V(\Phi_1) \leq_{lin} V(\Phi_2)$ .

*Proof.* As in the proof of Lemma E, we first construct constant variables  $\llbracket b \rrbracket$  for each of  $b \in \{1/2, 3/4, 1, 3/2\}$ . The only difference is that we now construct  $\llbracket 1 \rrbracket$  using the constraint  $\llbracket 1 \rrbracket \cdot \llbracket 1 \rrbracket = 1$ . It follows from this constraint that  $\llbracket 1 \rrbracket \in \{-1, 1\}$ , and since  $\llbracket 1 \rrbracket \in [1/2, 2]$ , we must have  $\llbracket 1 \rrbracket = 1$  in every valid solution. The other constants are then constructed in exactly the same way as before. For this reduction we also need the constant variable  $\llbracket 2/3 \rrbracket$  which is constructed as  $\llbracket 2/3 \rrbracket \cdot \llbracket 3/2 \rrbracket = 1$ .

We include each variable  $x$  of  $\Phi_1$  in  $\Phi_2$  as well, and reuse the interval  $I(x)$  from  $\mathcal{I}_1$  in  $\mathcal{I}_2$ . We also reuse all constraints from  $\Phi_1$  of the form  $a + b = c$  in  $\Phi_2$ , but we have to do something different for the squaring constraints  $a^2 = b$ . In  $\Phi_2$ , we rename the variables as  $\llbracket x + 1 \rrbracket := a$  and  $\llbracket x^2 + 2x + 1 \rrbracket := b$ , so that  $a^2 = b$  becomes

$$\llbracket x + 1 \rrbracket^2 = \llbracket x^2 + 2x + 1 \rrbracket. \quad (\dagger)$$

Consider a number  $x \in \mathbb{R}$  and the two conditions

$$\llbracket x + 1 \rrbracket = x + 1, \quad (\star)$$

$$\llbracket x^2 + 2x + 1 \rrbracket = x^2 + 2x + 1. \quad (\star\star)$$

As in the proof of Lemma F, one can prove that  $(\dagger)$  is equivalent to

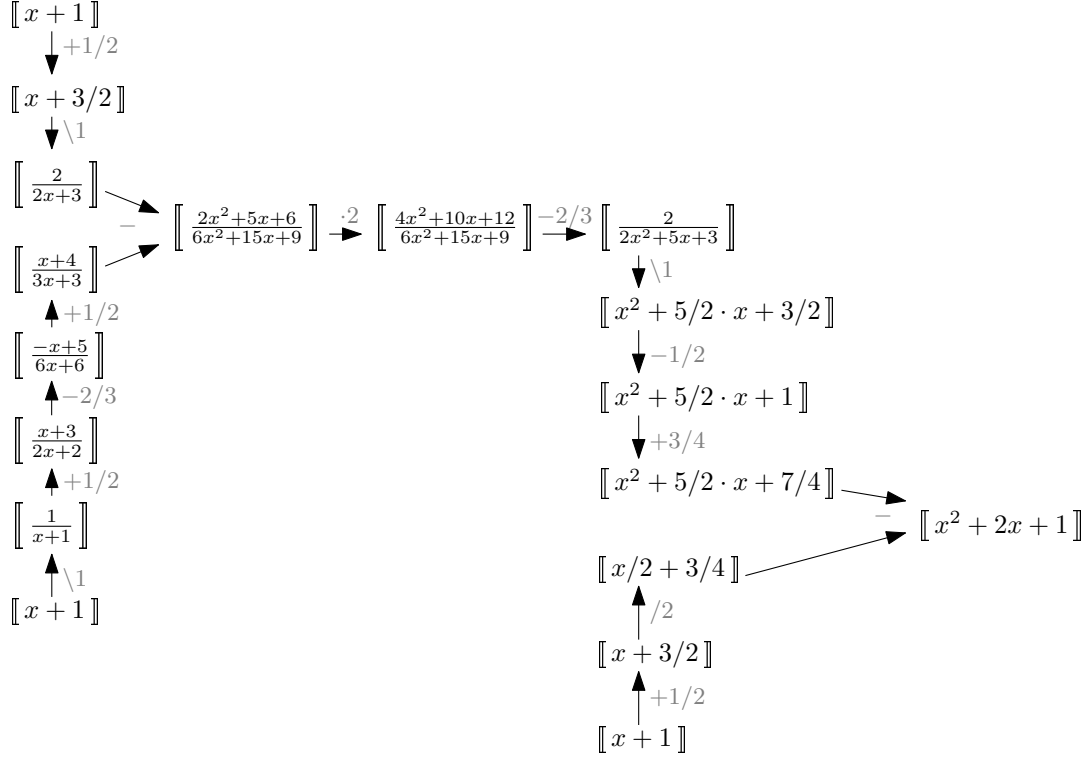
$$(\star) \text{ implies } (\star\star). \quad (\ddagger)$$

Our aim is therefore to make constraints in  $\Phi_2$  that ensure  $(\ddagger)$ .

In the same way as described in Section 5.5 and Section 5.6, we can add values, subtract values, half and double variables. Figure 13 shows the construction of  $\llbracket x^2 + 2x + 1 \rrbracket$  using these tricks as well as inversions. It is straightforward to check that the construction ensures condition  $(\ddagger)$ .

For all the variables  $x$  of  $\Phi_2$  that also appear in  $\Phi_1$ , we define the interval  $I(x)$  in  $\mathcal{I}_2$  as it is in  $\mathcal{I}_1$ . Each of the auxiliary variables has the form  $\llbracket \frac{p(x)}{q(x)} \rrbracket$ , where  $p(x)$  and  $q(x)$  are polynomials of degree 2. We define  $c := \frac{p(0)}{q(0)}$  and note that  $c \in [2/3, 7/4]$ . We define  $I\left(\llbracket \frac{p(x)}{q(x)} \rrbracket\right) := [c - \delta_2, c + \delta_2]$ . This finishes the construction of  $\mathcal{I}_2$ . Note that since  $\delta_2 \leq 1/6$  and  $c \in [2/3, 7/4]$ , we get that  $I\left(\llbracket \frac{p(x)}{q(x)} \rrbracket\right) \subset [1/2, 2]$ .

We now verify that  $\mathcal{I}_2$  has the claimed properties. Consider a solution  $\mathbf{x} \in V(\Phi_1)$ . For all the variables of  $\Phi_2$  that also appear in  $\Phi_1$ , we use the same value as in the solution  $\mathbf{x}$ . Each auxiliary variable has the form  $\llbracket \frac{p(x)}{q(x)} \rrbracket$ , where  $p(x)$  and  $q(x)$  are polynomials of degree 2, and  $\Phi_1$  contains the squaring constraint  $(\dagger)$ . We then get from the promise of  $\Phi_1$  that  $\llbracket 1 + x \rrbracket = 1 + x$



**Figure 13:** The sequence above enforces  $y = x^2$ , using only addition and inversion. Inversion is denoted by  $\setminus 1$ .

for  $x \in [-\delta_1, \delta_1]$ . From the construction shown in Figure 13, it follows in order to get a solution to  $\Phi_2$ , we must define  $\llbracket \frac{p(x)}{q(x)} \rrbracket := \frac{p(x)}{q(x)}$ . We are going to apply case (b) of Lemma 40 to show that this solution stays in the required range  $[1/2, 2]$ . The coefficients of the non-constant terms of  $p(x)$  and  $q(x)$  are in the range  $[-1, 15]$ . Denote by  $a_6$  and  $b_6$  the constant terms of  $p(x)$  and  $q(x)$ , respectively. We observe that  $b_6^2 \geq 1$  and  $a_6 + (1 + \delta_2)b_6 \leq 6 + 2 \cdot 9 = 24$ . We therefore get that since  $\delta_1 < \delta_2/1800 = \frac{\delta_2}{5 \cdot 15 \cdot 24} < \frac{\delta_2 b_6^2}{5 \cdot 15 (a_6 + (1 + \delta_2)b_6)}$ , then  $\llbracket \frac{p(x)}{q(x)} \rrbracket \in [c - \delta_2, c + \delta_2] \subset [1/2, 2]$ .

Similarly, we see that any solution to  $\Phi_2$  corresponds to a solution to  $\Phi_1$ . Using the promise of  $\mathcal{I}_1$  and Lemma 40 as above, we then also confirm the promise of  $\mathcal{I}_2$  that each variable  $u$  of  $\Phi_2$  is in  $I(u)$ .

The correspondance described implies that  $V(\Phi_1) \simeq V(\Phi_2)$  and  $V(\Phi_1) \leq_{\text{lin}} V(\Phi_2)$ . For each constraint of  $\Phi_1$ , we introduce  $O(1)$  variables and constraints of  $\Phi_2$ , so the reduction takes  $O(|\Phi_1|)$  time.  $\square$

We can now prove Theorem 29.

**Theorem 29.** *RANGE-ETR-INV is  $\exists\mathbb{R}$ -complete, even when  $\delta = O(n^{-c})$  for any constant  $c > 0$ . Furthermore, for every instance  $\Phi$  of ETR where  $V(\Phi)$  is compact, there is an instance  $\mathcal{I}$  of RANGE-ETR-INV with ETR-INV formula  $\Psi$  such that  $V(\Phi)$  and  $V(\Psi)$  are rationally equivalent and  $V(\Psi)$  is a linear extension of  $V(\Phi)$ .*

*Proof.* That RANGE-ETR-INV is  $\exists\mathbb{R}$ -complete follows from Lemmata A–G. That this holds even when  $\delta = O(n^{-c})$  follows from Corollary 38 and Lemmata F–G. For a given instance  $\Phi$  of ETR where  $V(\Phi)$  is compact, all the reductions preserve rational equivalence and result in linear extensions. Hence the final claim.  $\square$

## 5.8 Reduction to WIRED-INV

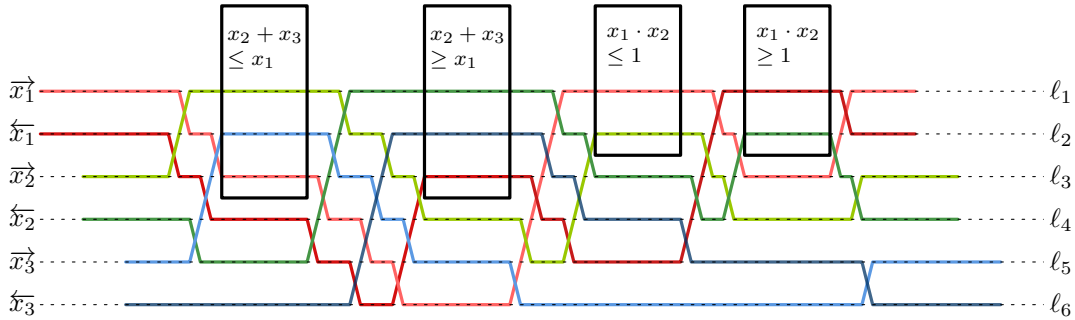
In our reduction to packing problems, we reduce from an auxiliary problem called *WIRED-INV*. An instance of *WIRED-INV* is an instance of *RANGE-ETR-INV* together with a graphical representation of the *ETR-INV* formula  $\Phi$ , i.e., a drawing of  $\Phi$  of a specific form, which we call a *wiring diagram*; see Figure 14.

The term “wiring diagram” is often used about drawings of a similar appearance used to represent electrical circuits or pseudoline arrangements. We define equidistant horizontal *diagram lines*  $\ell_1, \dots, \ell_{2n}$  so that  $\ell_1$  is the topmost one and  $\ell_{2n}$  is bottommost. The distance between consecutive lines is 10. In a wiring diagram, each variable  $x_i$  in  $\Phi$  is represented by two  $x$ -monotone polygonal curves  $\vec{x}_i$  and  $\overleftarrow{x}_i$ , which we call *wires*. We think of  $\vec{x}_i$  as oriented to the right and  $\overleftarrow{x}_i$  as oriented to the left. The wire  $\vec{x}_i$  starts and ends on  $\ell_{2i-1}$ , and  $\overleftarrow{x}_i$  starts and ends on  $\ell_{2i}$ . Each wire consists of horizontal segments contained in the diagram lines and *jump segments*, which are line segments connecting one diagram line  $\ell_j$  to a neighbouring diagram line  $\ell_{j\pm 1}$ . The wires are disjoint except that each jump segment must cross exactly one other jump segment. Thus, the jump segments are used when two wires following neighbouring diagram lines swap lines.

The left and right endpoints of  $\vec{x}_i$  and  $\overleftarrow{x}_i$  are vertically aligned, and the wires appear and disappear in the order  $(\vec{x}_1, \overleftarrow{x}_1), \dots, (\vec{x}_n, \overleftarrow{x}_n)$  from left to right in a staircase-like fashion.

In the wiring diagram, we represent each constraint of  $\Phi$  as two inequalities, i.e.,  $x_i + x_j = x_k$  becomes  $x_i + x_j \leq x_k$  and  $x_i + x_j \geq x_k$  and  $x_i \cdot x_j = 1$  becomes  $x_i \cdot x_j \leq 1$  and  $x_i \cdot x_j \geq 1$ . Each inequality is represented by an axis-parallel *constraint box* intersecting the three or two topmost diagram lines; three for addition constraints and two for inversion constraints. These boxes are pairwise disjoint. For a constraint  $x_i + x_j \leq x_k$ , the right-oriented wires  $\vec{x}_i, \vec{x}_j, \vec{x}_k$  must inside the box occupy the lines  $\ell_1, \ell_2, \ell_3$ , respectively. For  $x_i + x_j \geq x_k$ , we need the left-oriented wires  $\overleftarrow{x}_i, \overleftarrow{x}_j, \overleftarrow{x}_k$  instead. For the inversion inequalities  $x_i \cdot x_j \leq 1$  and  $x_i \cdot x_j \geq 1$ , we need one of the wires of  $x_i$  and one of the wires of  $x_j$  to occupy  $\ell_1$  and  $\ell_2$ . Which combination and which order depends on the particular variant of packing that we are reducing to.

Each vertical line is allowed to cross either zero or two jump segments and in the latter case, these two must cross each other. A vertical line crossing a constraint box must not cross any jump segment.



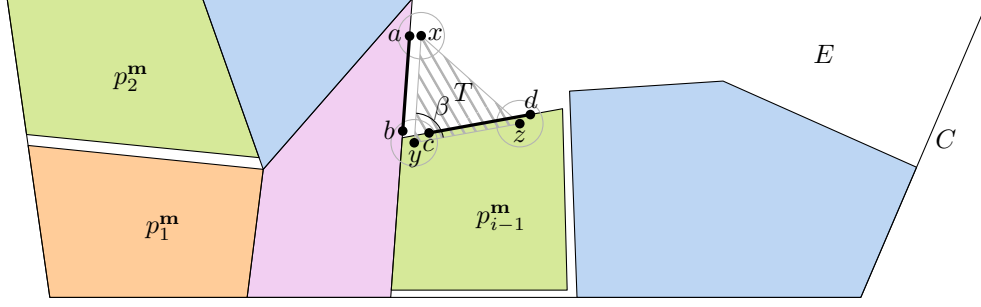
**Figure 14:** A wiring diagram corresponding to the *ETR-INV* formula  $x_2 + x_3 = x_1 \wedge x_1 \cdot x_2 = 1$ .

**Definition 42.** An instance  $\mathcal{I} := [\mathcal{I}', D]$  of the *WIRED-INV* problem consists of an instance  $\mathcal{I}'$  of *RANGE-ETR-INV* together with a wiring diagram  $D$  of the *ETR-INV* formula  $\Phi(\mathcal{I}')$ .

**Lemma 43** (*WIRED-INV Reduction*). Given an *ETR-INV* formula  $\Phi$  with variables  $x_1, \dots, x_n$ , we can in  $O(n^4)$  time construct a wiring diagram of  $\Phi$ .

*Proof.* We may assume that  $\Phi$  has  $O(n^3)$  constraints, since there will otherwise be duplicates of some constraints. We construct a wiring diagram as follows; refer to Figure 14. We construct

all the curves simultaneously from left to right, so that the  $x$ -coordinates of their left endpoints are all identical, as are the  $x$ -coordinates of their right endpoints. We handle the constraints in order and define the curves as we go along. For instance, for a constraint such as  $x_i + x_j \leq x_k$ , we route  $\vec{x}_i$  to the line  $\ell_1$  using jump segments. This defines how all other curves should behave in the same range of  $x$ -coordinates where we have routed  $\vec{x}_i$ . We then route  $\vec{x}_j$  to the line  $\ell_2$ , and then route  $\vec{x}_k$  to  $\ell_3$ . Each time we route a curve to a specific line, we introduce  $O(n)$  crossings. Therefore, we make  $O(n^4)$  crossings in total.  $\square$



**Figure 15:** We are considering the placement of the pieces  $p_1, \dots, p_{i-1}$  according to a valid motion  $\mathbf{m}$ . The white area is the empty space  $E$  available for the remaining pieces  $p_i, \dots, p_N$ . The gray circles centered at  $x, y, z$  have radius  $u$ . The first must contain  $a$ , the second  $b$  and  $c$ , and the third  $d$  such that  $ab$  and  $cd$  are segments on the boundary of  $E$ .

## 6 Fingerprinting

In this section, we develop a technique to argue that pieces are roughly at the position where we intend them to be. The high level idea is based on a few properties. First, the slack  $\mu$ , i.e., the difference between the area of the container and the total area of the pieces, is very small. Second, every piece  $p$  has a specific corner  $v$  with a unique angle that fits precisely at one position. If we were to place another piece there, we would create an empty space which is larger than  $\mu$ .

### 6.1 Fingerprinting a single piece

Now let us go one level deeper into the details of the technique, see also Figure 15. We consider a case where we already know the position of some pieces (possibly with some uncertainty), and we consider the empty space  $E$  where the remaining pieces must be placed. Ideally, we could identify a corner  $w$  of the empty space and a corner  $v$  of a remaining piece  $p$  which has exactly the same angle as  $w$  and deduce that  $p$  must be placed with  $v$  at  $w$ . Unfortunately, this is not the case, for two reasons. First, we want to give most pieces some tiny but non-zero amount of wiggle room. This is important as pieces are meant to represent variables. Second, we do not know the precise position of the other pieces as previous fingerprinting steps could only infer approximate and not exact positions of those pieces. Thus, we will identify for each piece  $p$  a triangle  $T$ , which has a corner  $y$  with the same angle as  $v$ . The edges adjacent to  $y$  will be very close to but not exactly on the boundary of the empty space  $E$ . The triangle  $T$  will be our main protagonist in the forthcoming proofs and formal definitions. It may partially overlap existing pieces or have some distance to already placed pieces. Another key player is the uncertainty value  $\lambda \geq 0$ , which is a measure of how much  $T$  is off from the ideal. We are now ready to go into the full details of the fingerprinting.

**Setup.** We are given a container  $C$  and pieces  $\mathbf{p} = (p_1, \dots, p_N)$ . Each piece  $p \in \mathbf{p}$  is a simple polygon with the following properties.

- Each segment of  $p$  has length at least 1.
- The diameter of  $p$  is at most some number  $d_{\max}$ .
- The polygon  $p$  is *fat* in the following sense. For any two points  $v, w$  on different and non-neighbouring segments of  $p$ , we have  $\|vw\| \geq \mu := 1/100$ .



Recall that the slack  $\mu$  is the area of  $C$  minus the total area of the pieces  $\mathbf{p}$ .

In Section 6.4, we will show that the results developed in the following for polygonal pieces also hold when the pieces are allowed to be curved polygons (provided that the curvature is sufficiently small and the curved part of each segment is sufficiently short).

**The empty space  $E$ .** We consider an arbitrary valid motion  $\mathbf{m}$  and analyze how we can infer something about the placement of the pieces  $p_i, \dots, p_N$  from the placement of the first  $i - 1$  pieces  $p_1, \dots, p_{i-1}$ . We can think of this situation as if we have already decided where to place the first  $i - 1$  pieces  $p_1, \dots, p_{i-1}$  in  $C$  so that they are interior-disjoint, and we are now reasoning about where to place the next piece.

Let

$$E := C \setminus \bigcup_{j=1}^{i-1} p_j^{\mathbf{m}}$$

be the uncovered space available for the remaining pieces  $p_i, \dots, p_N$ , see Figure 15. Then  $E$  is a subset of  $C$  bounded by a finite number of line segments. Note that all segments on the boundary of  $E$  are contained in edges of the pieces  $p_1^{\mathbf{m}}, \dots, p_{i-1}^{\mathbf{m}}$  or  $C$ .

**Covering a wedge of  $E$ .** Assume that there is a special triangle  $T \subset C$  with corners  $x, y, z$  and with the following properties. We have  $\|xy\| = \|yz\| = 1$ . Let  $\lambda \geq 0$  be a (small) number that will be defined whenever we are going to apply the fingerprinting. The value  $\lambda$  can be thought of as a measure of uncertainty of the already placed pieces and the distance from the boundary of  $T$  to the boundary of  $E$ . Let  $T^{\text{in}} = x^{\text{in}}y^{\text{in}}z^{\text{in}}$  denote the triangle  $T \ominus \text{disk}(\lambda)$ , such that  $x^{\text{in}}, y^{\text{in}}, z^{\text{in}}$  are on the angular bisectors from  $x, y, z$ , respectively.

**Definition 44.** We say that  $E$  is  $\lambda$ -bounding  $T$  at  $y$  if the following two conditions hold:

- There are segments  $ab$  and  $cd$  on the boundary of  $E$  such that each of the distances  $\|ax\|, \|by\|, \|cy\|, \|dz\|$  is at most  $\lambda$ .
- The interior of  $T^{\text{in}}$  is a subset of  $E$ .

The second requirement means that no piece among  $p_1, \dots, p_{i-1}$  covers anything of  $T^{\text{in}}$  when placed according to  $\mathbf{m}$ . The triangle  $T^{\text{in}}$  will have an area much larger than  $\mu$ , which implies that almost all of  $T^{\text{in}}$  must be covered by the pieces  $p_i^{\mathbf{m}}, \dots, p_N^{\mathbf{m}}$ .

**Unique angle property.** We assume that the pieces  $p_i, \dots, p_N$  have the following property, which we denote as the *unique angle property*. Let  $\beta$  be the interior angle of  $T$  at  $y$ . We require that  $\beta \in [\alpha_{\min}, \pi/2]$ , where  $\alpha_{\min} := 5\pi/180$ .

For the a (small) number  $\sigma$ , we require the following. Consider any set  $S := \{v_1, \dots, v_m\}$  of at most one corner from each piece  $p_i, \dots, p_N$ . If the sum of angles of corners in  $S$  is in the interval  $[\beta - \sigma, \beta + \sigma]$ , then  $S$  consists of only one corner  $v$ , i.e.,  $S = \{v\}$ .

In most applications of the fingerprinting technique, there will be only one such set  $S = \{v\}$ . In other words, the angle range  $[\beta - \sigma, \beta + \sigma]$  uniquely identifies a specific piece and a specific corner  $v$  of the piece. However, in Section 9, we are going to consider a special case where the container is a square where there will be more such sets.

We will argue that almost all of  $T^{\text{in}}$  must be covered by a piece with a corner  $v$  with an angle in the range  $[\beta - \sigma, \beta + \sigma]$ , and the corner  $v$  must be placed close to  $y$ . Informally, since  $\mu$  is much smaller than the area of  $T^{\text{in}}$ , almost all of  $T^{\text{in}}$  must be covered by the pieces  $p_i, \dots, p_N$ . Because of the unique angle property, it is only possible to cover a sufficient amount of  $T^{\text{in}}$  by placing a piece with such a corner  $v$  close to  $y$  and with the adjacent edges close to parallel to  $yx$  and  $yz$ , since the edges  $ab$  and  $cd$  of  $\partial E$  are preventing  $T^{\text{in}}$  to be covered in another way.

**Main lemma.** To sum up, we have made these assumptions:

- We consider a valid placement  $\mathbf{m}$  of the pieces  $\mathbf{p}$ .
- The empty space  $E$  is  $\lambda$ -bounding the triangle  $T$  at the corner  $y$  of  $T$ .
- The pieces  $p_i, \dots, p_N$  have the unique angle property with respect to the angle  $\beta$  of the corner  $y$ .

In Section 6.3, we are going to prove the following lemma in the setting described above.

**Lemma 45** (Single Fingerprint). *There is a piece  $p \in \{p_i, \dots, p_N\}$ , with a corner  $v$  such that the angle of  $v$  is in  $[\beta - \sigma, \beta + \sigma]$  and  $\|yv^{\mathbf{m}}\| = O(\lambda/\sigma + \sqrt{\mu/\sigma})$ .*

*Furthermore, let  $u, w$  be the corners preceding and succeeding  $v$ , respectively. Then the angle between  $v^{\mathbf{m}}u^{\mathbf{m}}$  and  $yx$  is  $O(\lambda/\sigma + \sqrt{\mu/\sigma})$ , as is the angle between  $v^{\mathbf{m}}w^{\mathbf{m}}$  and  $yz$ .*

## 6.2 Fingerprinting more pieces at once

In this section, we consider the iterated use of the finger printing technique (in particular Lemma 45) for some number of times. This describes the situation whenever we have introduced the pieces of a new gadget to the construction. More precisely, we consider the situation where we know how the pieces  $p_1, \dots, p_{i-1}$  must be placed, and we want to deduce how the following  $k$  pieces  $p_i, \dots, p_{i+k-1}$ , for some  $k \geq 1$ , must then be placed. To this end, consider an arbitrary valid motion  $\mathbf{m}$ . For each  $j \in \{1, \dots, i-1\}$ , define the motion  $s_j := m_j$ . Consider a set of *intended* motions  $s_i, \dots, s_{i+k-1}$  of the pieces  $p_i, \dots, p_{i+k-1}$ . We are going to define what it means for the intended motions to be *sound*, and then we prove that if they are sound, then the valid motion  $\mathbf{m}$  must place the pieces  $p_i, \dots, p_{i+k-1}$  in a way similar to the intended motions.

To define soundness of the intended motions, we first define the empty space  $E_j^s$  as

$$E_j^s := C \setminus \overline{\bigcup_{l=1}^{j-1} p_l^{s_l}}.$$

**Definition 46.** *We say that the intended motion  $s_j$ ,  $j \in \{i, \dots, i+k-1\}$ , is  $\lambda$ -sound, for a value  $\lambda \geq 0$ , if exists a triangle  $T_j = x_j y_j z_j$  and a corner  $v_j$  of  $p_j$  such that the following holds.*

- the angle  $\beta_j$  of  $T_j$  at  $y_j$  is in the range  $[\alpha_{\min}, \pi/2]$ ,
- $\|x_j y_j\| = 1$  and  $\|y_j z_j\| = 1$ ,
- $E_j^s$  is  $\lambda$ -bounding  $T_j$  at  $y_j$  (recall Definition 44),
- the following stronger version of the unique angle property holds: among all corners of all pieces  $p_j, \dots, p_N$ , only the corner  $v_j$  of  $p_j$  has an angle in the range  $[\beta_j - \sigma, \beta_j + \sigma]$ .
- $T_j \subset p_j^{s_j}$ ,
- $v_j^{s_j} = y_j$  and  $x_j y_j, y_j z_j \subset \partial p_j^{s_j}$ .

We likewise define the placement  $p_j^{s_j}$  to be  $\lambda$ -sound if the motion  $s_j$  is  $\lambda$ -sound.

**Lemma 47.** *There exists an absolute constant  $c > 0$  such that the following holds. Define*

$$\begin{aligned} \Lambda_i &:= 0, \quad \text{and} \\ \Lambda_j &:= cd_{\max}/\sigma \cdot \Lambda_{j-1} + cd_{\max}(\lambda/\sigma + \sqrt{\mu/\sigma}), \end{aligned}$$

for  $j > i$ . If the motions  $s_i, \dots, s_{i+k-1}$  are  $\lambda$ -sound, then for each  $j \in \{i, \dots, i+k-1\}$ , the displacement between  $m_j$  and  $s_j$  is at most  $\Lambda_{j+1}$ . It holds that

$$\Lambda_{k+1} \leq (k+1)(cd_{\max}/\sigma)^{k+1}(\lambda/\sigma + \sqrt{\mu/\sigma}),$$

which is a bound on all the mentioned displacements.

*Proof.* We proceed by induction on  $j$ . For  $j = i$ , we apply Lemma 45. We get that  $\|y_i v_i^{\mathbf{m}}\| \leq O(\lambda/\sigma + \sqrt{\mu/\sigma})$ . Furthermore, the second half of the lemma implies that the displacement angle between the motions  $m_i$  and  $s_i$  is likewise  $O(\lambda/\sigma + \sqrt{\mu/\sigma})$ . We therefore get that the displacement between  $m_i$  and  $s_i$  is

$$cd_{\max}(\lambda/\sigma + \sqrt{\mu/\sigma}) = \Lambda_{i+1}$$

for some constant  $c$ .

Suppose now that the statement holds for indices  $i, i+1, \dots, j-1$ . Define

$$E_j^{\mathbf{m}} := C \setminus \overline{\bigcup_{l=1}^{j-1} p_l^{m_l}}.$$

Since  $E_j^{\mathbf{s}}$  is  $\lambda$ -bounding  $T_j$  at  $y_j$  and the displacement between  $m_{j-1}$  and  $s_{j-1}$  is at most  $\Lambda_j$ , we get that  $E_j^{\mathbf{m}}$  is  $(\Lambda_j + \lambda)$ -bounding  $T_j$  at  $y_j$ . Therefore, Lemma 45 gives that the displacement between  $m_j$  and  $s_j$  is at most

$$cd_{\max}((\Lambda_j + \lambda)/\sigma + \sqrt{\mu/\sigma}) = cd_{\max}/\sigma \cdot \Lambda_j + cd_{\max}(\lambda/\sigma + \sqrt{\mu/\sigma}) = \Lambda_{j+1},$$

for the constant  $c$  introduced above. Unfolding the expression, we get

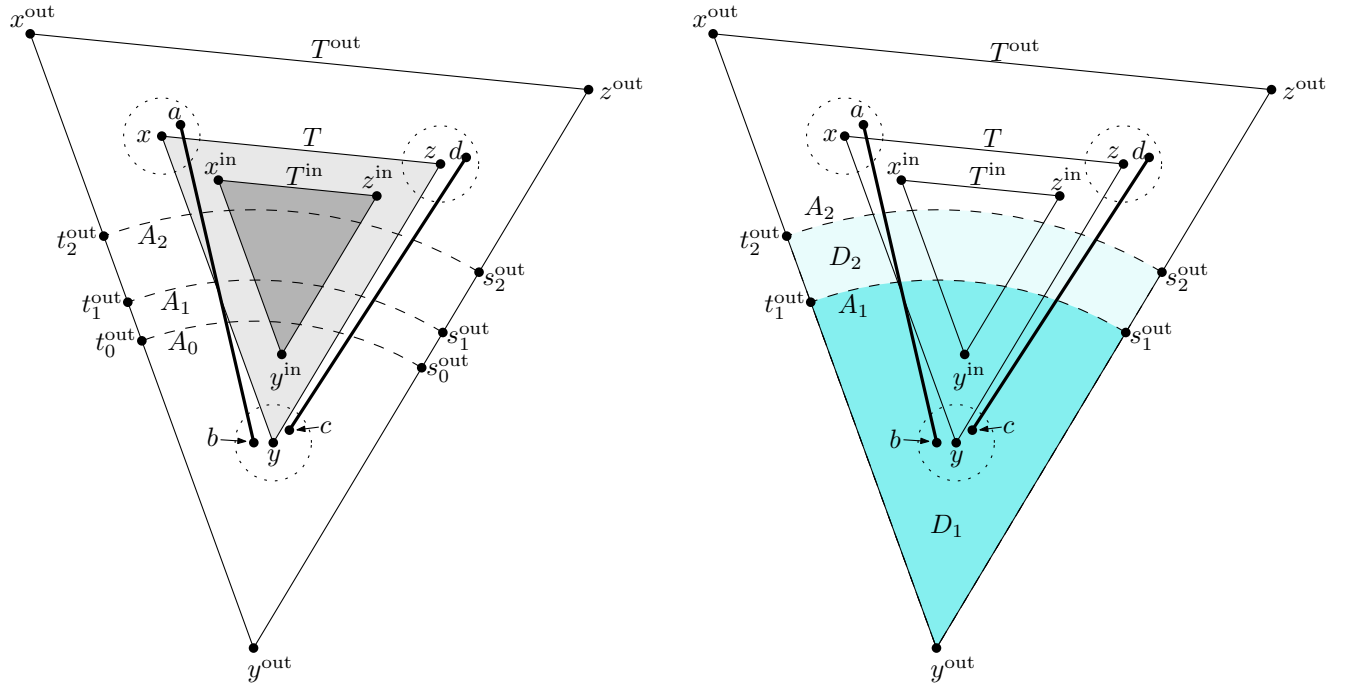
$$\begin{aligned} \Lambda_{k+1} &= \sum_{j=0}^k (cd_{\max}/\sigma)^j \cdot cd_{\max}(\lambda/\sigma + \sqrt{\mu/\sigma}) \\ &\leq \sum_{j=0}^k (cd_{\max}/\sigma)^{j+1} \cdot (\lambda/\sigma + \sqrt{\mu/\sigma}) \\ &\leq (k+1)(cd_{\max}/\sigma)^{k+1}(\lambda/\sigma + \sqrt{\mu/\sigma}). \end{aligned} \quad \square$$

The following lemma will be used to fingerprint the pieces in each gadget individually.

**Lemma 48** (Multiple Fingerprints). *Consider a gadget and its pieces  $p_i, \dots, p_{i+k-1}$ , for  $k \leq 7$ , which are introduced in some step of the construction. Suppose that there exists a valid motion  $\mathbf{m}$  of the complete construction that moves the pieces  $p_1, \dots, p_{i-1}$  to a canonical placement. Furthermore, suppose that there exists intended motions  $s_i, \dots, s_{i+k-1}$  which are  $g\mu$ -sound. Then the displacement between the intended motion  $s_j$  and the actual motion  $m_j$  is  $O(n^{-48})$ .*

*Proof.* In our construction, we have  $d_{\max} = O(n^4)$ ,  $\delta := n^{-300}$ ,  $\mu = O(\delta n^4) = O(n^{-296})$ ,  $\sigma = \Omega(N^{-2}) = \Omega(n^{-8})$ , and  $g = O(n^4)$ , so we get from Lemma 47 that the displacement is at most

$$8(cd_{\max}/\sigma)^8(\lambda/\sigma + \sqrt{\mu/\sigma}) = O((n^4 n^8)^8(n^{-292} n^8 + \sqrt{n^{-296} n^8})) = O(n^{96} n^{-144}) = O(n^{-48}). \quad \square$$



**Figure 16:** Setup in the proof of Lemma 45. The circles centered at  $x^r, y^r, z^r$  bound the disks of radius  $\lambda$  in which the points  $a, b, c, d$  are known to be. The figure is not to scale. In practice,  $\lambda$  is very small so that the triangles  $T^{\text{out}}, T, T^{\text{in}}$  are almost equally large. Furthermore, the radius of  $A_2$  is much larger than the radius of  $A_1$ , which in turn is much larger than the radius of  $A_0$ . The right figure shows the regions  $D_1$  and  $D_2$ , that together make up  $D$ . The segments  $ab$  and  $cd$  are drawn with thick lines to indicate that these act as a restriction to where the next piece can be placed.

### 6.3 Proof of Single Fingerprint (Lemma 45)

**Proof setup.** See Figure 16. Let  $\zeta(\theta) := \frac{1}{\sin(\theta/2)}$ . The function  $\zeta$  is important when computing the distances between corresponding corners of offset versions of the same triangle, as the following lemma makes clear.

**Lemma 49.** (1) Consider a triangle  $U = efg$  and define for some  $s > 0$  the triangle  $U^{\text{in}} := U \ominus \text{disk}(s) = e^{\text{in}} f^{\text{in}} g^{\text{in}}$ , so that  $e^{\text{in}}, f^{\text{in}}, g^{\text{in}}$  are on the angular bisectors of  $e, f, g$ , respectively. Then  $\|ee^{\text{in}}\| = s\zeta(\theta)$ , where  $\theta$  is the angle of  $U$  at  $e$ .

(2) Let  $e, f, g$  be points such that the distances from a point  $e^{\text{in}}$  to each of the segments  $ef$  and  $eg$  is at most  $s$ . Then  $\|ee^{\text{in}}\| \leq s\zeta(\theta)$ , where  $\theta \in [0, \pi)$  is the angle between  $ef$  and  $eg$ .

*Proof.* Proof of (1): Let  $p$  be the projection of  $e^{\text{in}}$  on  $ef$ . Then  $\|ee^{\text{in}}\| = \|pe^{\text{in}}\| / \sin(\theta/2) = s\zeta(\theta)$ .

Proof of (2): For a given angle  $\theta$ , the distance  $\|ee^{\text{in}}\|$  is maximum if the distances from  $e^{\text{in}}$  to each segment  $ef$  and  $eg$  are both  $s$ , so that, in particular,  $e^{\text{in}}$  is on the angular bisector between the segments  $ef$  and  $eg$ . We then proceed as in the proof for (1).  $\square$

Lemma 49 gives that  $\|yy^{\text{in}}\| = \lambda\zeta(\beta)$ .

Let  $T^{\text{out}} = x^{\text{out}}y^{\text{out}}z^{\text{out}}$  be the triangle we get by offsetting the edges of  $T$  outwards in a parallel fashion by distance  $\lambda\zeta(\alpha_{\min})$ , i.e.,  $T^{\text{out}}$  is the triangle such that  $T^{\text{out}} \ominus \text{disk}(\lambda\zeta(\alpha_{\min})) = T$ . The corners  $x^{\text{out}}, y^{\text{out}}, z^{\text{out}}$  are on the angular bisectors of  $x, y, z$ , respectively.

Define  $\psi := \zeta(\alpha_{\min}) + \zeta(\alpha_{\min})^2 = O(1)$ . By Lemma 49, we have  $\|yy^{\text{out}}\| = \lambda\zeta(\alpha_{\min})\zeta(\beta) \leq \lambda\zeta(\alpha_{\min})^2$ , and  $\|y^{\text{out}}y^{\text{in}}\| = \lambda(\zeta(\beta) + \zeta(\alpha_{\min})\zeta(\beta)) \leq \lambda\psi$ .

**Subdividing  $T^{\text{out}}$  by arcs.** Define three radii as

$$\begin{aligned} r_0 &:= \lambda\psi = \Omega(\lambda), \\ r_1 &:= \Omega\left(\lambda/\sigma + \sqrt{\mu/\sigma}\right), \\ r_2 &:= \Omega(r_1/\sigma). \end{aligned}$$

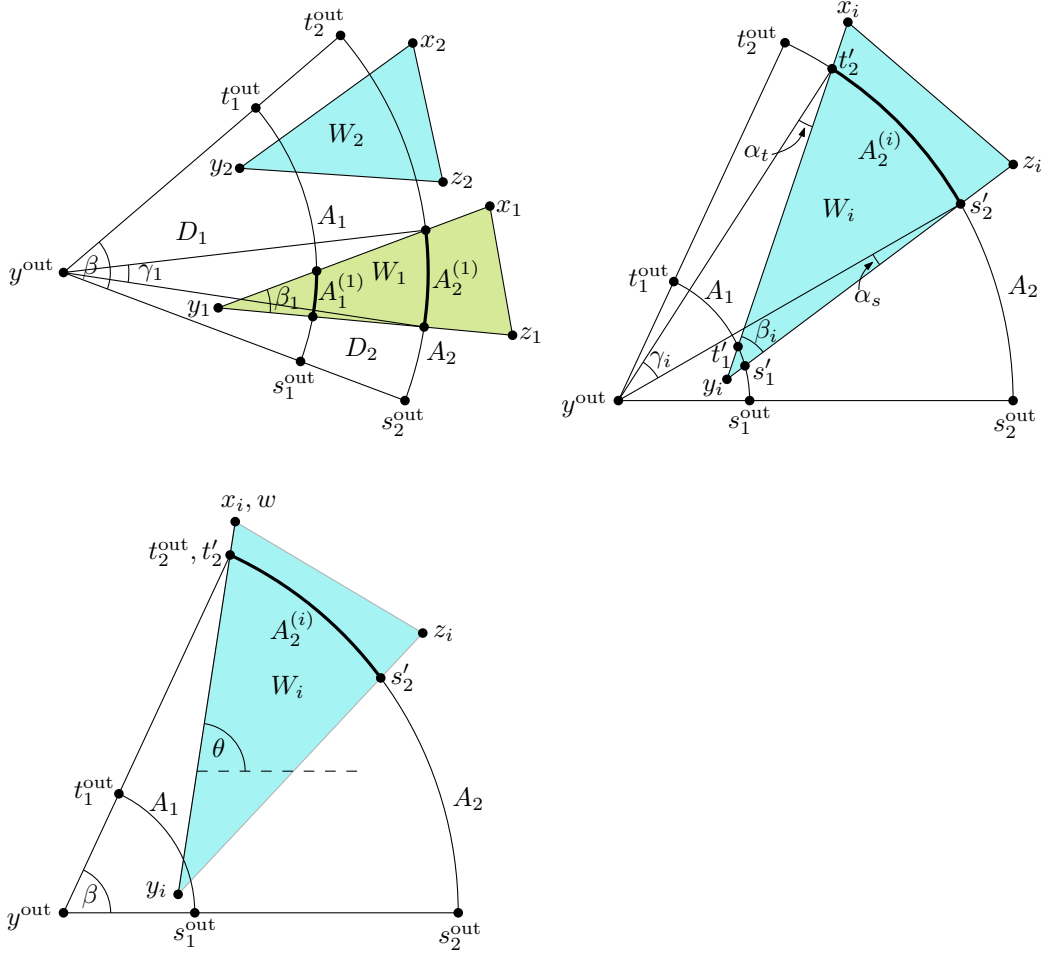
We furthermore require that  $r_2$  is much smaller than 1, say  $r_2 < 1/10$  (as it turns out, by choosing  $\delta$  small enough, we can make  $\mu$  so small that  $r_2$  is below any desired constant). For the ease of presentation, we will not specify the constants that should be chosen for  $r_1$  and  $r_2$ , but it will follow from the analysis that constants exist that will make the arguments work. Note that in our application Lemma 48, we will have  $\sigma = \Theta(n^{-8})$ , one should think of  $r_1$  as much larger than  $r_0$  and  $r_2$  as much larger than  $r_1$ .

Let  $A_i$  be the arc with center  $y^{\text{out}}$  and radius  $r_i$  from the point  $s_i^{\text{out}}$  on segment  $y^{\text{out}}z^{\text{out}}$  counterclockwise to the point  $t_i^{\text{out}}$  on segment  $x^{\text{out}}y^{\text{out}}$ .

Let  $D$  be the region bounded by segments  $t_2^{\text{out}}y^{\text{out}}$  and  $y^{\text{out}}s_2^{\text{out}}$  and the arc  $A_2$ . The arc  $A_1$  separates  $D$  into two regions  $D_1$  and  $D_2$ , where  $A_2$  appears on the boundary of  $D_2$ .

**Geometric core lemma.** The following lemma is the geometric core of our argument and the setup is shown in Figure 17 (top left). We use this lemma to conclude that if a set  $Q$  of pieces cover most of  $D_1$ , then they have corners whose angles sum to a number close to  $\beta$ . It then follows from the unique angle property that  $Q$  consists of just one piece.

**Lemma 50.** Let  $W_1, \dots, W_m$  be a collection of triangles each of which  $W_i = x_i y_i z_i$  has one corner  $y_i$  in  $D_1$  and the segment  $x_i z_i$  disjoint from  $D$ . Let  $\beta_i$  be the angle of  $W_i$  at  $y_i$  and suppose that  $\beta_i \in [\alpha_{\min}, \alpha_{\max}]$ . Suppose that  $W_1, \dots, W_m$  are pairwise interior disjoint and that



**Figure 17:** Top left: The setup of Lemma 50. Top right: In the shown example,  $\beta_i = \gamma_i - \alpha_s + \alpha_t$ . Since  $\alpha_s = O(r_1/r_2)$  and  $\alpha_t = O(r_1/r_2)$ , we always have  $\beta_i = [\gamma_i - O(r_1/r_2), \gamma_i + O(r_1/r_2)]$ . Bottom: The angle  $\theta$  is an argument of the segment  $y_i w$ . The argument is bounded by  $\beta + O(r_1/r_2)$ .

the interior of each  $W_j$  is disjoint from  $t_2^{\text{out}} y^{\text{out}}$  and  $y^{\text{out}} s_2^{\text{out}}$ . Let  $\mathcal{W} := \bigcup_{j=1}^m W_j$ . Let  $\rho \in [0, 1]$  be the fraction of  $A_2$  covered by  $\mathcal{W}$ . Then

$$\frac{\text{area}(D_1 \cap \mathcal{W})}{\text{area}(D_1)} \leq \rho + O(r_1/r_2), \text{ and} \quad (4)$$

$$\sum_{i=1}^m \beta_i \in [\beta\rho - O(r_1/r_2), \beta\rho + O(r_1/r_2)] \quad (5)$$

*Proof.* We first analyze just a single triangle  $W_i$  and then generalize to all of  $W_1, \dots, W_m$ . For  $j \in \{1, 2\}$ , let  $A_j^{(i)} := A_j \cap W_i$  be the arc on  $A_j$  contained in  $W_i$ , and let  $\gamma_i \in (0, \beta]$  be the angle spanned by  $A_2^{(i)}$ . We claim that

$$\beta_i \in [\gamma_i - O(r_1/r_2), \gamma_i + O(r_1/r_2)], \text{ and} \quad (6)$$

$$\text{area}(D_1 \cap W_i) \leq r_1^2 \gamma_i / 2 + O(r_1^3 / r_2). \quad (7)$$

Before proving (6) and (7), we show how (4) and (5) follow. We get from (7) that

$$\frac{\text{area}(D_1 \cap W_i)}{\text{area}(D_1)} \leq \frac{r_1^2 \gamma_i / 2 + O(r_1^3 / r_2)}{r_1^2 \beta / 2} = \gamma_i / \beta + O(r_1 / r_2).$$

Note that by (6) and since  $\beta_i \in [\alpha_{\min}, \alpha_{\max}]$  for all  $i$ , we know that  $m = O(1)$ . We now have that

$$\frac{\text{area}(D_1 \cap \mathcal{W})}{\text{area}(D_1)} = \sum_{i=1}^m \frac{\text{area}(D_1 \cap W_i)}{\text{area}(D_1)} \leq \sum_{i=1}^m (\gamma_i / \beta + O(r_1 / r_2)) = \rho + O(r_1 / r_2),$$

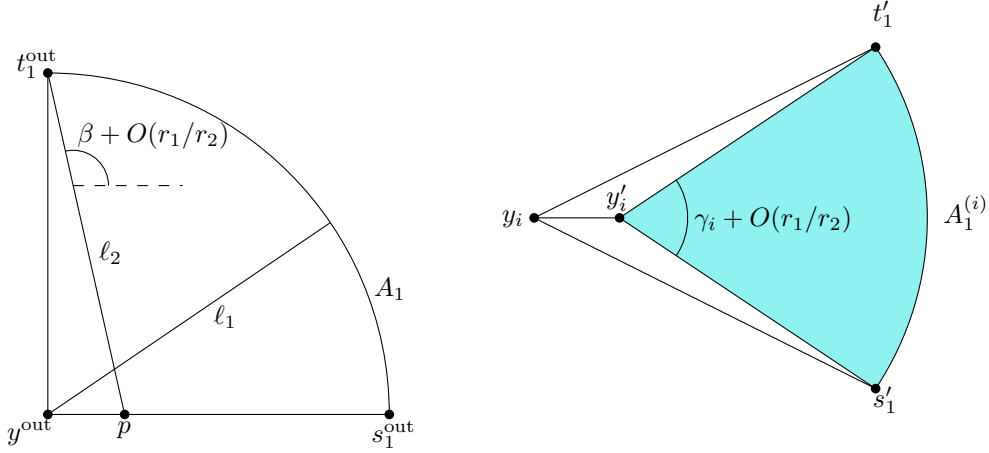
which proves (4). Likewise, (5) follows from (6) using that  $m = O(1)$  as

$$\sum_{i=1}^m \beta_i \in \left[ \sum_{i=1}^m (\gamma_i - O(r_1 / r_2)), \sum_{i=1}^m (\gamma_i + O(r_1 / r_2)) \right] = [\rho\beta - O(r_1 / r_2), \rho\beta + O(r_1 / r_2)].$$

Let  $s'_1 \in y_i z_i$  and  $t'_1 \in y_i x_i$  be the endpoints of  $A_1^{(i)}$  and define  $s'_2$  and  $t'_2$  similarly as the endpoints of  $A_2^{(i)}$ . For the following proof of (6), we refer to Figure 17 (top right). Note first that if  $y_i = y^{\text{out}}$ , we have  $\beta_i = \gamma_i$ . However, in general  $y_i$  is just a point within distance  $r_1$  from  $y^{\text{out}}$ . Therefore, the angle  $\alpha_s$  between the segments  $y^{\text{out}} s'_2$  and  $y_i s'_2$  is at most  $\arcsin(r_1 / r_2)$ , which is obtained when  $y^{\text{out}} y_i s'_2$  is a triangle with  $\|y^{\text{out}} y_i\| = r_1$  and a right angle at  $y_i$ . Since  $r_2$  is much larger than  $r_1$ , we have  $\arcsin(r_1 / r_2) = O(r_1 / r_2)$ . Similarly, the angle  $\alpha_t$  between the segments  $y^{\text{out}} t'_2$  and  $y_i t'_2$  is at most  $\arcsin(r_1 / r_2) = O(r_1 / r_2)$ . Note that  $\beta_i = \gamma_i \pm \alpha_s \pm \alpha_t$ , so we get  $\beta_i \in [\gamma_i - O(r_1 / r_2), \gamma_i + O(r_1 / r_2)]$ .

By the *argument* of a line  $\ell$ , we mean the counterclockwise angle from the  $x$ -axis to  $\ell$ . The argument of a line segment  $s$  is the argument of the line containing  $s$ . Assume without loss of generality that  $y^{\text{out}} s_2^{\text{out}}$  is horizontal with  $s_2^{\text{out}}$  to the right of  $y^{\text{out}}$ , so that the argument of any line through  $y^{\text{out}}$  and a point on  $A_2$  is in the range  $[0, \beta]$ . We claim that then the argument of every segment  $y_i w$ , where  $w \in W_i$ , is in the range  $[-O(r_1 / r_2), \beta + O(r_1 / r_2)]$ . To verify the upper bound, note that the argument of  $y_i w$  is maximum if  $w = x_i$  and  $t'_2 = t_2^{\text{out}}$ , see Figure 17 (bottom). By an argument as the one used in the previous paragraph, we get that the argument can be at most  $O(r_1 / r_2)$  larger than  $\beta$ . The lower bound follows in a similar way.

We now observe that each of the segments  $y_i s'_1$  and  $y_i t'_1$  has length at most  $r_1 + O(r_1^2 / r_2)$ , as follows. See Figure 18 (left). Since  $\beta \leq \pi/2$ , the longest segment  $\ell_1$  in  $D_1$  with an argument



**Figure 18:** Left: Longest segments in  $D_1$ . The segment  $\ell_1$  shows the case that the argument is in  $[0, \beta]$ , and then the longest segment has length  $r_1$ . The segment  $\ell_2$  shows the case where the argument is in  $(\beta, \beta + O(r_1/r_2)]$ , and then the segment has length  $r_1 + O(r_1^2/r_2)$ . Right: Figure to show that  $\text{area}(D_1 \cap W_i) \leq r_1^2 \gamma_i / 2 + O(r_1^3/r_2)$ . The segments  $y_i s_1'$  and  $y_i t_1'$  are assumed to have the same length  $r_1 + O(r_1^2/r_2)$ , and the angle  $\beta_i$  at  $y_i$  is  $\gamma_i + O(r_1/r_2)$ . We consider the point  $y_i'$  such that  $\|y_i' s_1'\| = \|y_i' t_1'\| = r_1$ . Then the angle at  $y_i'$  is likewise  $\gamma_i + O(r_1/r_2)$ , so the area of the blue triangle is  $r_1^2 \gamma_i / 2 + O(r_1^3/r_2)$ . The white triangles have area at most  $O(r_1^3/r_2)$ , so the total area of  $D_1 \cap W_i$  is at most  $r_1^2 \gamma_i / 2 + O(r_1^3/r_2)$ .

in  $[0, \beta]$  connects  $y^{\text{out}}$  to a point on  $A_1$  and has length  $r_1$ . The longest segment  $\ell_2$  in  $D_1$  with an argument in  $(\beta, \beta + O(r_1/r_2)]$  connects  $t_1^{\text{out}}$  to a point  $p$  on  $y^{\text{out}} s_1^{\text{out}}$ . We then get

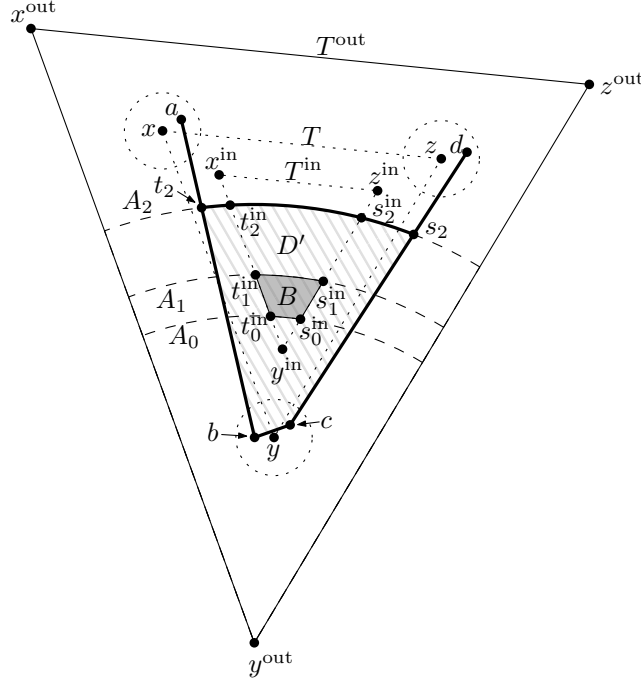
$$\begin{aligned} \|\ell_2\| &= \|t_1^{\text{out}} p\| \leq \|t_1^{\text{out}} y^{\text{out}}\| + \|y^{\text{out}} p\| \leq r_1 + r_1 \tan(O(r_1/r_2)) = r_1 + r_1 \frac{\sin(O(r_1/r_2))}{\cos(O(r_1/r_2))} \\ &\leq r_1 + r_1 \frac{O(r_1/r_2)}{1 - O(r_1/r_2)} = r_1 + O\left(\frac{r_1^2}{r_2 - r_1}\right) = r_1 + O(r_1^2/r_2), \end{aligned}$$

where the last equality follows since  $r_2$  is much larger than  $r_1$ . Similarly, the longest segment in  $D_1$  with an argument in  $[-r_1/r_2, 0)$  connects  $s_1^{\text{out}}$  to a point on  $y^{\text{out}} t_1^{\text{out}}$  and has length  $r_1 + O(r_1^2/r_2)$ . Hence,  $r_1 + O(r_1^2/r_2)$  is also an upper bound on the length of  $y_i s_1'$  and  $y_i t_1'$ .

We get an upper bound on  $\text{area}(D_1 \cap W_i)$  in the case that  $\beta_i$  and the edges  $y_i s_1'$  and  $y_i t_1'$  all reach the upper bounds. This might not be realizable, but still provides an upper bound. See Figure 18 (right). If the edges have length  $\|y_i s_1'\| = \|y_i t_1'\| = r_1$ , the area is  $r_1^2(\gamma_i + O(r_1/r_2))/2 = r_1^2 \gamma_i / 2 + O(r_1^3/r_2)$ . Extending the edges to  $\|y_i s_1'\| = \|y_i t_1'\| = r_1 + O(r_1^2/r_2)$ , we are adding two triangles each of which has area at most  $r_1 \cdot O(r_1^2/r_2) = O(r_1^3/r_2)$ , and the desired bound (7) follows.  $\square$

We want to apply Lemma 50 to a set of pieces covering parts of  $D_1$ . See Figure 19. Let  $s_i^{\text{in}}$  and  $t_i^{\text{in}}$  be the intersection points of  $A_i$  with  $y^{\text{in}} z^{\text{in}}$  and  $x^{\text{in}} y^{\text{in}}$ , respectively. Let  $B \subset D_1 \cap T^{\text{in}}$  be the region bounded by segments  $s_0^{\text{in}} s_1^{\text{in}}$ ,  $t_0^{\text{in}} t_1^{\text{in}}$ , and the arcs  $A_0 \cap T^{\text{in}}$  and  $A_1 \cap T^{\text{in}}$ . We consider only pieces that cover a part of  $B$ . The reason we do not consider all pieces covering a part of  $D_1$  is that a piece covering a part of  $D_1$  but not  $B$  might violate the assumptions of Lemma 50. In particular, such a piece might not have an interior disjoint from  $t_2^{\text{out}} y^{\text{out}}$  and  $y^{\text{out}} s_2^{\text{out}}$ , as is seen in case (ii.a) in Figure 21. Cases (i.b) and (ii.b) in Figures 20 and 21, respectively, show the possibilities of a piece covering a part of  $B$ , and here the piece fits the assumptions of Lemma 50. The following lemma makes this intuition precise. Conceivably, there may be some pieces that





**Figure 19:** Regions  $B$  and  $D'$ . The region  $D'$  is drawn with a pattern of falling gray lines. The fat part of  $A_2$  is the arc  $A'_2$  that bounds  $D'$ . A piece covering part of  $B$  has edges crossing one or both of  $A'_2$  and  $bc$ . The figure is not to scale—in practice  $B$  will cover almost all of the region  $D_1$  below the arc  $A_1$ .

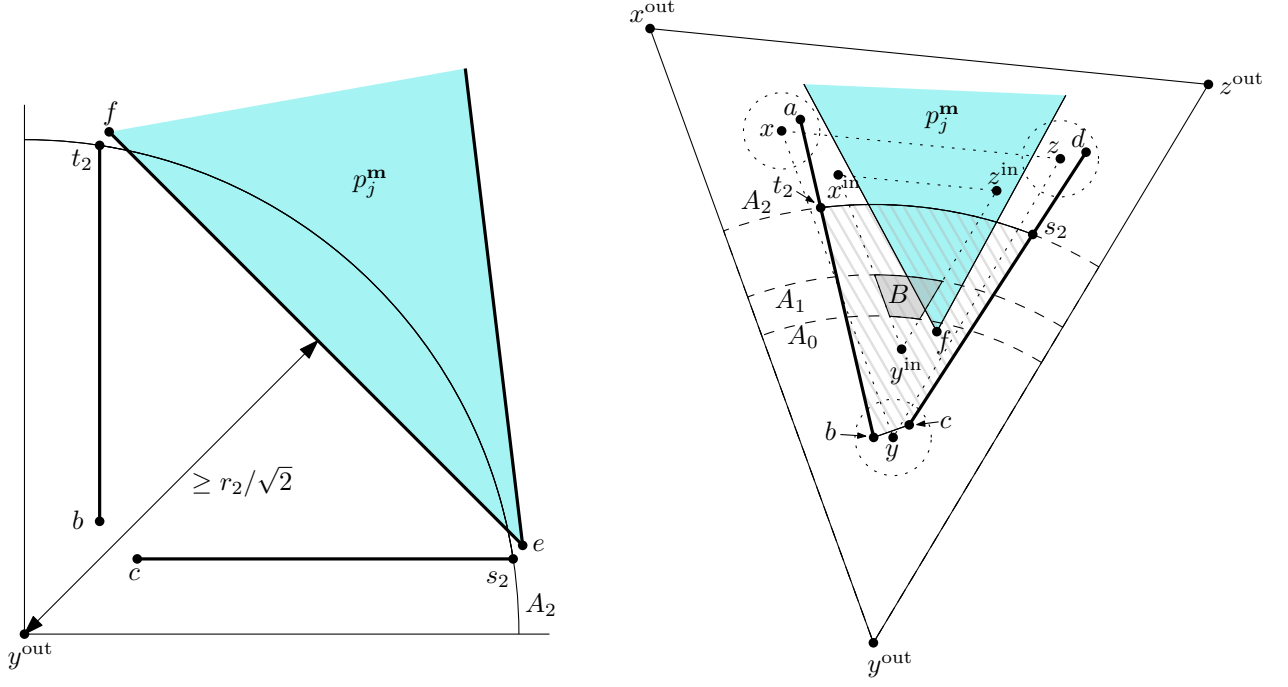
fulfill the conditions of Lemma 50 but do not cover a part of  $B$ . However, even considering only pieces covering a part of  $B$ , we will be able to arrive at our desired conclusion. Recall that the segments  $ab$  and  $cd$  are bounding some pieces (or the container  $C$ ) in the valid motion  $\mathbf{m}$ , so these segments act as obstacles that restrict the placement of a piece  $p_j^{\mathbf{m}}$  covering a part of  $B$ .

**Lemma 51.** *A piece  $p_j^{\mathbf{m}}$  covering a part of the interior of  $B$  has the following properties:*

- *There is a corner  $v^{\mathbf{m}}$  of  $p_j^{\mathbf{m}}$  contained in  $D_1$ .*
- *The edges of  $p_j^{\mathbf{m}}$  adjacent to  $v^{\mathbf{m}}$  cross  $A_2$ .*

*Proof.* Let  $s_2$  and  $t_2$  be the intersection points of  $A_2$  with segment  $cd$  and  $ab$ , respectively, as shown in Figure 19. Let  $A'_2$  be the part of  $A_2$  from  $s_2$  counterclockwise to  $t_2$ . Let  $D'$  be the region bounded by segments  $s_2c$ ,  $bc$ ,  $t_2b$ , and the arc  $A'_2$ . Then  $B \subset D' \subset D$ . Since  $r_2 < 1/2$ , the diameter of  $D$  is less than 1. Since  $p_j^{\mathbf{m}}$  covers a part of the interior of  $B$ , there is one or more edges of  $p_j^{\mathbf{m}}$  that cross the boundary of  $D'$ . An edge of  $p_j^{\mathbf{m}}$  can only cross the boundary of  $D'$  at a point on the segment  $bc$  or the arc  $A'_2$ , since the segments  $cs_2$  and  $bt_2$  are bounding some other pieces. We divide into the following cases, which are also shown in Figures 20 and 21, respectively:

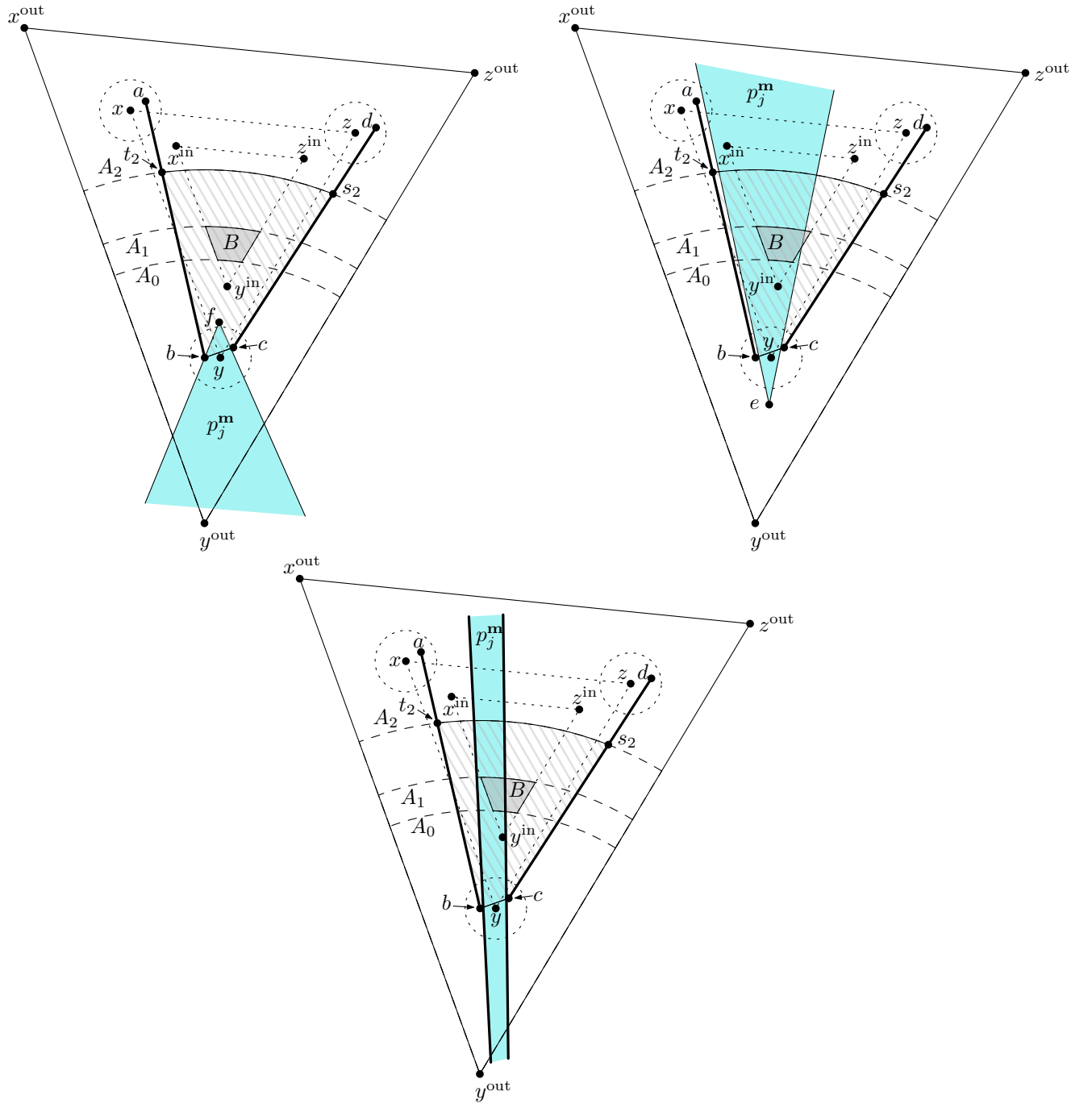
- Case (i): No edge of  $p_j^{\mathbf{m}}$  crosses  $bc$ . Then there is an edge  $ef$  crossing  $A'_2$ . We have the following two cases:
  - Case (i.a): The edge  $ef$  crosses  $A'_2$  twice. Since  $\beta \leq \pi/2$ , we get that the distance from  $y^{\text{out}}$  to  $ef$  is at least  $r_2/\sqrt{2}$ . Since  $r_1$  is much smaller, this edge cannot contribute to covering a part of  $B$ , so there must be some edges of  $p_j^{\mathbf{m}}$  crossing the boundary of  $D'$  that do not belong to this case.



**Figure 20:** Cases from the proof of Lemma 51. Left: Case (i.a). In this case, the piece  $p_j^m$  is too far from  $y^{\text{out}}$  to cover any of  $B$ . Right: Case (i.b). This case agrees with the statement of the lemma.

- Case (i.b): One of the endpoints  $e$  and  $f$  is inside  $D'$  while the other is outside. Assume without loss of generality that  $f$  is inside. It follows that the succeeding edge  $fg$  likewise intersects  $A_2$  due to the minimum length of the edges, and the claim holds.
- Case (ii): An edge  $ef$  of  $p_j^m$  crosses  $bc$ . Suppose that as we follow  $ef$  from  $e$  to  $f$ , we enter  $D'$  as we cross  $bc$ . In particular  $e \notin D'$ . There must likewise be another edge  $gh$  of  $p_j^m$  crossing  $bc$ , since otherwise, the interior of  $p_i^m$  would intersect  $ab$  or  $cd$ . We have the following cases depending on whether an endpoint of  $ef$  coincides with one of  $gh$ :
  - Case (ii.a):  $f$  coincides with an endpoint of  $gh$ . Assume without loss of generality that  $f = g$ . By Lemma 49 part (1), we have  $\|y^{\text{out}}y^r\| \leq \lambda\zeta(\alpha_{\min})^2$ , and by part (2), we have  $\|y^rf\| \leq \lambda\zeta(\alpha_{\min})$ . Therefore  $\|y^{\text{out}}f\| \leq \|y^{\text{out}}y^r\| + \|y^rf\| \leq r_0$ . But then the edges  $ef$  and  $gh$  do not get far enough into  $D'$  so that the wedge they form can cover a part of  $B$ , as every point in  $B$  has distance at least  $r_0$  to  $y^{\text{out}}$ . Therefore, there must be some edges of  $p_j^m$  crossing the boundary of  $D'$  that do not belong to this case.
  - Case (ii.b):  $e$  coincides with an endpoint of  $gh$ . Assume without loss of generality that  $e = g$ . Because the angle at  $e$  is at least  $\alpha_{\min}$ , it follows from Lemma 49 part (2) that  $\|y^re\| \leq \lambda\zeta(\alpha_{\min})$ . Therefore,  $e$  is contained in  $D$ . It then follows that  $ef$  and  $gh$  both cross  $A_2$ , since they must exit  $D$ , and the claim of the lemma thus holds.
  - Case (ii.c): No endpoint of  $ef$  coincides with one of  $gh$ . Since  $\|bc\| \leq 2\lambda < \mu$  and both segments  $ef$  and  $gh$  cross  $\|bc\|$ , we conclude that the fatness condition is violated in this case.

□



**Figure 21:** Cases from the proof of Lemma 51. Top left: Case (ii.a). In this case,  $p_j^{\mathbf{m}}$  cannot cover any of  $B$ . Top right: Case (ii.b). This case agrees with the statement of the lemma. Bottom: Case (ii.c). This case violates the fatness assumption of the pieces.

Here, we give an informal description of the following three lemmas. Lemma 52 states that the area of  $B$  grows quadratically in  $r_1$  while  $D_1 \setminus B$  grows only linearly. Lemma 53 says that almost all of  $B$  must be covered by pieces, as the uncovered area will otherwise be larger than  $\mu$ . We are then able to conclude in Lemma 54 that almost all of  $D_1$  must be covered by the pieces covering  $B$ , as  $B$  has asymptotically the same area as  $D_1$ . This eventually makes it possible to apply Lemma 50 in the proof of Lemma 45.

**Lemma 52.** *We have*

- $\text{area}(D_1 \setminus B) = O(r_0^2 + \lambda r_1)$ .
- $\text{area}(B) = \Omega(r_1^2 - r_0^2)$ .

*Proof.* The points in  $D_1 \setminus B$  are either within distance  $r_0$  from  $y^{\text{out}}$  or within distance  $\lambda(1 + \zeta(\alpha_{\min})) = O(\lambda)$  from one of the line segments  $y^{\text{out}}s_1^{\text{out}}$  or  $y^{\text{out}}t_1^{\text{out}}$ , each of length  $r_1$ . It then follows that  $\text{area}(D_1 \setminus B) = O(r_0^2 + \lambda r_1)$ .

We thus have  $\text{area}(B) = \text{area}(D_1) - \text{area}(D_1 \setminus B) = \Omega(r_1^2) - O(r_0^2 + \lambda r_1) = \Omega(r_1^2 - r_0^2)$ .  $\square$

Let  $Q := \{p_j | j \in \{i, \dots, n\} \text{ and } p_j^{\text{m}} \cap B \neq \emptyset\}$ , and let  $\mathcal{Q} := \bigcup_{p_j \in Q} p_j^{\text{m}}$ .

**Lemma 53.** *By choosing  $r_1 := \Omega(\lambda/\sigma + \sqrt{\mu/\sigma})$ , where  $\Omega$  hides a sufficiently large constant, we get  $\text{area}(B \cap \mathcal{Q}) \geq (1 - \sigma/4)\text{area}(B)$ .*

*Proof.* Recall that the pieces  $p_1^{\text{m}}, \dots, p_{i-1}^{\text{m}}$  are interior disjoint from  $T^{\text{in}}$ , as  $T^{\text{in}} \subset E_i^{\text{m}}$ . Since

$$r_1 = \Omega\left(\lambda/\sigma + \sqrt{\mu/\sigma}\right) = \Omega\left(r_0 + \sqrt{\frac{\mu}{\sigma}}\right) = \Omega\left(\sqrt{r_0^2 + \frac{\mu}{\sigma}}\right),$$

we get from Lemma 52 that

$$\text{area}(B) = \Omega(r_1^2 - r_0^2) = \Omega(\mu/\sigma).$$

Now, if the constant hidden in the  $\Omega$ -notation is large enough, we have  $\text{area}(B) \geq \frac{\mu}{\sigma/4}$ , or equivalently,  $\sigma/4 \cdot \text{area}(B) \geq \mu$ . This means that the area of  $B$  covered by the pieces in  $Q$  is at least  $(1 - \sigma/4)\text{area}(B)$ , as otherwise the uncovered part would be larger than  $\mu$ .  $\square$

**Lemma 54.** *By choosing  $r_1 := \Omega(\lambda/\sigma + \sqrt{\mu/\sigma})$ , where  $\Omega$  hides a sufficiently large constant, we get  $\text{area}(D_1 \cap \mathcal{Q}) \geq (1 - \sigma/2)\text{area}(D_1)$ .*

*Proof.* Note that  $r_1 = \Omega(\lambda/\sigma) = \Omega(r_0/\sqrt{\sigma} + \lambda/\sigma)$ . We get  $r_1^2 = \Omega\left(\frac{r_0^2 + \lambda r_1}{\sigma}\right)$ , where we can choose the constant hidden in the  $\Omega$ -notation as big as needed. Since  $r_1 = \Omega(r_0)$ , we then get  $r_1^2 - r_0^2 = \Omega\left(\frac{r_0^2 + \lambda r_1}{\sigma}\right)$ . Now, if we choose the constant big enough, we get from Lemma 52 that  $\sigma/4 \cdot \text{area}(B) \geq \text{area}(D_1 \setminus B)$  and thus

$$\frac{\text{area}(D_1)}{\text{area}(B)} = \frac{\text{area}(B) + \text{area}(D_1 \setminus B)}{\text{area}(B)} \leq 1 + \sigma/4.$$

It follows that

$$\frac{\text{area}(B)}{\text{area}(D_1)} = \frac{\text{area}(B)}{\text{area}(B) + \text{area}(D_1 \setminus B)} \geq \frac{1}{1 + \sigma/4} \geq \frac{1 - \sigma/2}{1 - \sigma/4}.$$

Hence we have that

$$(1 - \sigma/4)\text{area}(B) \geq (1 - \sigma/2)\text{area}(D_1).$$

The claim now follows from Lemma 53 as

$$\text{area}(D_1 \cap \mathcal{Q}) \geq \text{area}(B \cap \mathcal{Q}) \geq (1 - \sigma/4)\text{area}(B) \geq (1 - \sigma/2)\text{area}(D_1).$$

$\square$

We are now ready to prove Lemma 45. We rephrase the lemma as follows.

**Lemma 55.** *By choosing  $r_2 := \Omega(r_1/\sigma)$ , where  $\Omega$  hides a sufficiently large constant, we get that  $Q$  consists of just one piece  $p_j$ , and  $p_j$  has a corner  $y_j$  such that the angle of  $y_j$  is in  $[\beta - \sigma, \beta + \sigma]$  and  $y_j^{\mathbf{m}} \in D_1$ . In particular,  $\|yy_j^{\mathbf{m}}\| \leq 2r_1 = O(\lambda/\sigma + \sqrt{\mu/\sigma})$ .*

*Furthermore, let  $x_j, z_j$  be the corners preceding and succeeding  $y_j$ , respectively. Then the angle between  $y_j^{\mathbf{m}}x_j^{\mathbf{m}}$  and  $yx$  is  $O(\lambda/\sigma + \sqrt{\mu/\sigma})$ , as is the angle between  $y_j^{\mathbf{m}}z_j^{\mathbf{m}}$  and  $yz$ .*

*Proof.* By Lemma 51, each piece  $p_j \in Q$  has a corner  $y_j$  such that  $y_j^{\mathbf{m}}$  is contained in  $D_1$ , and the two adjacent edges cross  $A_2$ . For each piece  $p_j \in Q$ , we consider the triangle  $W_j := x_jy_jz_j$ , such that  $x_jy_j$  and  $y_jz_j$  are the edges adjacent to  $y_j$ . The triangles  $W_j$  now fit in the setup of Lemma 50. Let  $\rho$  be the fraction of  $A_2$  covered by  $Q$ . We then get by Lemma 54 and Lemma 50 that

$$1 - \sigma/2 \leq \frac{\text{area}(D_1 \cap Q)}{\text{area}(D_1)} \leq \rho + O(r_1/r_2).$$

Lemma 50 furthermore yields that the sum  $S$  of angles of the corners  $y_j$  is in the range  $[\beta\rho - O(r_1/r_2), \beta\rho + O(r_1/r_2)]$ . Since  $1 - \sigma/2 - O(r_1/r_2) \leq \rho \leq 1$ , we get

$$\beta\rho - O(r_1/r_2) \geq (1 - \sigma/2 - O(r_1/r_2))\beta - O(r_1/r_2) \geq \beta - \sigma\pi/4 - O(r_1/r_2), \text{ and} \quad (8)$$

$$\beta\rho + O(r_1/r_2) \leq \beta + O(r_1/r_2). \quad (9)$$

If we now choose  $r_2 = \Omega(r_1/\sigma)$ , where  $\Omega$  hides a sufficiently large constant, we get  $S \in [\beta - \sigma, \beta + \sigma]$ . We then get from the unique angle property that  $Q$  consists of just one piece  $p_j$ .

Since  $\|yy_j^{\mathbf{m}}\| = O(r_1)$  and  $\|xa\| \leq \lambda = O(r_1)$  and  $r_1$  is much smaller than  $\|xy\| = 1$ , we get that the angle between  $y_j^{\mathbf{m}}x_j^{\mathbf{m}}$  and  $yx$  is  $O(r_1/\|yx\|) = O(r_1)$ , and likewise for the angle between  $y_j^{\mathbf{m}}z_j^{\mathbf{m}}$  and  $yz$ .  $\square$

## 6.4 Generalization to curved polygons

Let  $\gamma: [0, L] \rightarrow \mathbb{R}^2$  be a simple curve parameterized by arc-length and of length  $L \geq 1$ . We say that  $\gamma$  is a *curved segment* if

- the prefix  $\gamma([0, 1])$  and suffix  $\gamma([L - 1, L])$  are line segments (each of length 1),
- $\gamma$  is differentiable,
- the *mean curvature* of  $\gamma$  at most some constant  $\kappa = O(1)$ , i.e., for all  $s_1, s_2 \in (0, L)$ , we have

$$\|\gamma'(s_1) - \gamma'(s_2)\| \leq \kappa|s_1 - s_2|.$$

As an example, consider a simple curve  $\gamma$  satisfying the first condition and which is the concatenation of line segments and circular arcs. Then  $\gamma$  is a curved segment as long as each circular arc has radius at least  $\kappa$  and each transition from one line segment or circular arc to the next is tangential.

We say that a compact set  $P \subset \mathbb{R}^2$  is a *curved polygon* if the boundary of  $P$  is a closed simple curve consisting of a finite number of curved segments. We claim that the above results on fingerprinting also hold when the pieces are curved polygons. The other requirements to the pieces described in the beginning of this section (lower and upper bounds on interior angles, bounded diameter, and fatness) should still be satisfied.

We first check that Lemma 51 still holds. The only place where the curved segments make a difference as compared to straight segments is in Case (i.a), where the piece can cover a bit

more of  $D'$ . However, since the mean curvature is at most  $\kappa = O(1)$ , it is still impossible that the piece can cover anything of  $B$  in this case if we choose  $\lambda$  small enough. In our application of the fingerprinting technique (Lemma 48), we will have  $\lambda \rightarrow 0$  as  $n \rightarrow \infty$ , so this will be satisfied for large enough  $n$ .

Now, since the prefix and suffix of each curved segment are line segment of length 1, we can again apply the Lemma 50 (the geometric core lemma) in the proof of Lemma 45.

## 7 Linear gadgets

In this section we are describing four types of gadgets called *anchor*, *swap*, *split*, and *adder*. They all work with convex polygonal pieces, a polygonal container, and translations. They also work when rotations are allowed and can thus be used for all packing variants studied in the paper. For every gadget we will define canonical placements and verify the five required lemmata of Section 2. Some of the steps will be very similar for all the gadgets. In order to avoid unnecessary repetition, we will go in more detail with the anchor than the subsequent gadgets.

### 7.1 Anchor

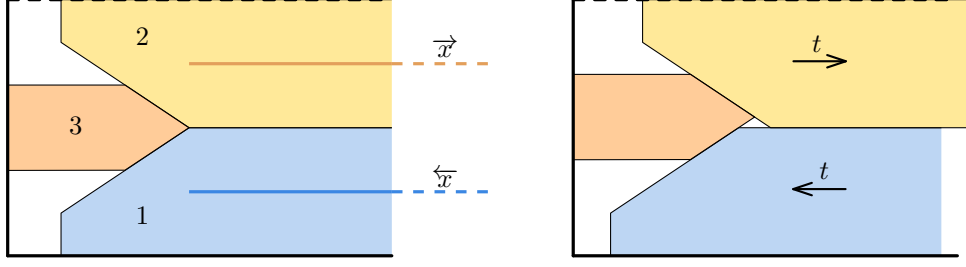
Recall that each variable  $x$  is represented by two wires  $\vec{x}$  and  $\overleftarrow{x}$  in the wiring diagram of the instance  $\mathcal{I}$  of WIRED-INV which we reduce to a packing instance. Furthermore, the left endpoints of the wires occupy neighbouring diagram lines  $\ell$  and  $\ell'$ , as do the right endpoints. In our packing instance, we cover each wire with variable pieces that can slide back and forth and thus encode the value of  $x$ , and the pieces covering one wire are called a *lane*. In order to make the value represented by the lane on  $\vec{x}$  consistent with that of the lane on  $\overleftarrow{x}$ , we make an *anchor* at both ends, which will propagate a push from one lane to the other. Most of this section will be about the anchors at the left ends of the wires. The anchors at the right ends will be handled in the end of the section.

When we use an anchor in our construction, we also define part of the boundary of the container. Two of the three introduced pieces are variable pieces that will extend out through the right side of the gadget, and the remaining part of those will be defined as part of another gadget farther to the right, which will be described in other parts of the paper. It is a general convention in our figures of gadgets that if a part of the boundary of the gadget is drawn with thick full segments, it will be part of the container boundary. If part of the boundary is drawn with thick dashed segments, it means that the segments can be either part of the container boundary or part of the boundary of other pieces that have been introduced to the construction in earlier steps.

**Simplified anchor.** The anchor is meant to be a connection between the two lanes that represent a variable  $x$ ; see Figure 22 for an illustration. The gadget consists of part of the boundary of the container and three pieces: orange, yellow, and blue. The yellow and blue pieces are the two leftmost pieces on the lanes of  $\vec{x}$  and  $\overleftarrow{x}$ , respectively. The orange piece functions as a connection between the two lanes. The idea is that if we move the blue piece to the left by  $t$ , then we have to move the yellow piece to the right by at least  $t$  as well, and vice versa.

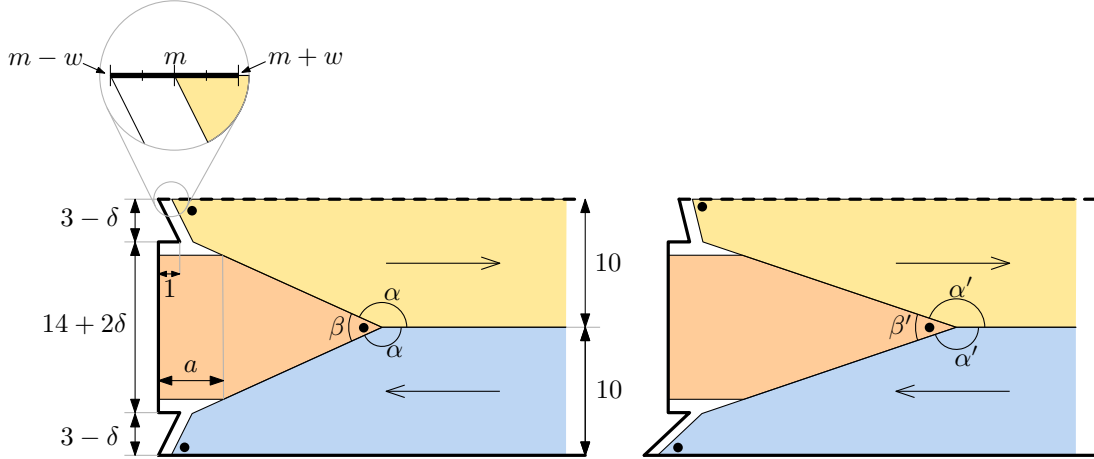
The segment bounding the gadget from below is part of the container boundary. The segment bounding the gadget from above is part of the boundary of a piece introduced in an earlier anchor, except for the very first anchor, which will be bounded from above by the container boundary.

**The actual anchor.** See Figure 23 for an illustration of the following description. Recall that we need the slack added by each gadget to be only  $O(\delta)$ . We therefore design the boundary of the anchor to follow the pieces closely. The yellow and blue piece are fingerprinted on the boundary, as indicated by the dots. The orange piece is fingerprinted in the wedge created by the yellow and blue pieces.



**Figure 22:** Left: A simplified illustration of the anchor and how it is placed on top of the two wires representing a variable  $x$ . Right: If the blue piece is pushed to the left, the yellow piece must move by an equal amount to the right, and vice versa. Color codes: 1 blue, 2 yellow, 3 orange.

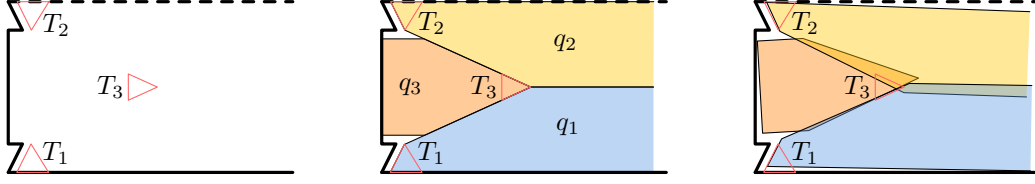
Lines that appear axis-parallel must be axis-parallel; those are important for the alignment. The height of the orange piece is 14. The angle  $\alpha$  is in the range  $[3\pi/4, 7\pi/8]$ . The lower bound ensures that a range of size at most  $2\delta$  is needed for the orange piece, while the upper bound ensures that the length  $a$  is only  $1 + O(\delta)$ . The angle  $\alpha$  and the angles where the yellow and blue pieces are fingerprinted are not fixed, and we therefore have flexibility to choose the angles of the fingerprinted corners freely to obtain the unique angle property; two different choices of angles are shown in Figure 23.



**Figure 23:** Left: An illustration of the anchor gadget. The placement of the pieces corresponds to the value  $x = m$ . The arrows show the orientation of the pieces, and the dots show the fingerprinted corners. The magnifying glass shows a scale of the correspondence between placements of the yellow piece and the encoded value of the variable  $x$ . The length  $a$  is  $1 + O(\delta)$  and depends on  $\alpha$ . Right: Another instance of the gadget with other angles chosen.

**Canonical placements and solution preservation.** As the next step, we define the set of canonical positions for the three pieces. Recall that together with the variable  $x$  is also given an interval  $I(x) \subset [1/2, 2]$  of the form  $[m - w, m + w]$  for some  $m \in [1/2, 2]$  and  $w \leq \delta$ . The yellow and blue pieces are variable pieces, and in the placement shown in Figure 23, both pieces encode the value  $x = m$ . The gadget is constructed so that the blue and yellow pieces each has room to slide exactly  $w$  to the left. By definition, the canonical placements of each are all placements obtained by sliding the piece to the left or right by distance at most  $w$  from the placement shown. Recall that a placement of all pieces of a gadget is canonical if it is (1) valid,





**Figure 24:** The three triangles  $T_1, T_2, T_3$  (shown a bit larger than they should be for clarity) are a witness that the intended placements (middle) are  $O(\delta)$ -sound. We can therefore conclude that the pieces have an almost-canonical placement, as shown to the right (ignore here that the shown placement is not a valid placement).

(2) canonical for each variable piece, and (3) have certain extra properties defined for each gadget individually. For the anchor, we specify point (3) as having edge-edge contacts between the pieces and the container boundary as shown in the figure.

We are now ready to prove that the reduction preserves solutions, for the anchor gadget, as stated in Lemma 6.

*Proof of Lemma 6 for the anchor.* Suppose that for a given solution to the ETR-INV formula  $\Phi$ , there exists a canonical placement of the previously introduced pieces  $\mathbf{p}_{i-1}$  that encodes that solution. To extend the placement to the pieces  $\mathbf{p}_i$ , i.e., with the yellow, blue, and orange piece of this anchor included, we place the yellow and blue pieces so that they represent the value of  $x$  in the solution to  $\Phi$ . This leaves room for the orange piece to be placed with the required edge-edge contacts to the blue and yellow pieces.  $\square$

**Fingerprinting and almost-canonical placement.** We start with proving Lemma 10. Recall that in Lemma 10, we assume that the previous pieces  $\mathbf{p}_{i-1}$  have an aligned  $(i-1)\mu$ -placement and we want to conclude that the new pieces  $\mathbf{p}_i \setminus \mathbf{p}_{i-1}$ , i.e., the three pieces of this anchor, must have an almost-canonical placement.

*Proof of Lemma 10 for the anchor.* Since the pieces  $\mathbf{p}_{i-1}$  have an aligned  $(i-1)\mu$ -placement, the gadget is bounded from above by an earlier introduced piece (unless  $i = 1$ , in which case it is bounded by the boundary of the container). We want to use Lemma 48 (Multiple Fingerprints) to prove that the three pieces have an almost-canonical placement. For this we need to point out intended placements that are  $O(\delta + (i-1)\mu)$ -sound; recall Definition 46. We choose the placement shown in Figure 23. To certify that the intended placements are  $O(\delta + (i-1)\mu)$ -sound, we need to point out three triangles  $T_1, T_2, T_3$ , such that  $E_j^s$  is  $O(\delta + (i-1)\mu)$ -bounding  $T_j$  for  $j \in \{1, 2, 3\}$ . Here  $E_j^s$  is the empty space left by the pieces  $\mathbf{p}_{i-1}$  and the intended placements of the pieces  $q_1, \dots, q_{j-1}$ , where  $q_1, q_2, q_3$  are the blue, yellow, and orange piece, respectively. We choose the triangles as the tips of fingerprinted corners, as shown in Figure 24. The placements of the blue and yellow pieces are  $\delta$ -sound because the boundary of the container or the pieces of  $\mathbf{p}_{i-1}$  follow the relevant edges of the respective triangles  $T_1$  and  $T_2$  within distance  $\delta$ . The placement of the orange piece is 0-sound since the boundaries of the blue and yellow pieces contain the edges of  $T_3$ . It is then clear that the intended placements are  $O(\delta)$ -sound. We conclude using Lemma 48 (Multiple Fingerprints) that the displacement is  $O(n^{-48})$ , so the three pieces must have an almost-canonical placement.  $\square$

**Aligned placement.** We show now Lemma 11, which assumes that the pieces in the anchor are almost-canonical and all previous pieces  $\mathbf{p}_{i-1}$  have an aligned  $(i-1)\mu$ -placement. The goal is to conclude that the pieces of this gadget have an aligned  $i\mu$ -placement, which requires the

variable pieces to be correctly aligned and encode values at most  $i\mu$  away from the middle value of  $x$ .

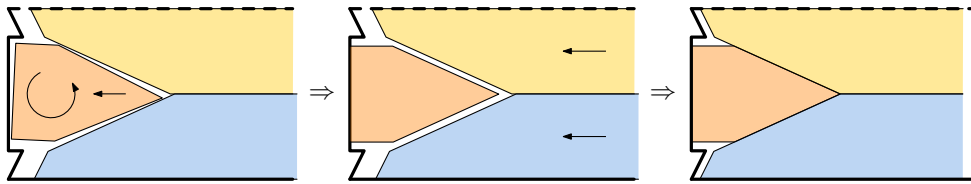
*Proof of Lemma 11 for the anchor.* Consider a valid placement where the pieces  $\mathbf{p}_{i-1}$  have a aligned  $(i-1)\mu$ -placement and the pieces  $\mathbf{p}_i \setminus \mathbf{p}_{i-1}$ , i.e., the yellow, blue, and orange pieces of this anchor, have almost-canonical placements; see Figure 25. We consider the alignment segment  $\ell$  which has length 20. Since the placements are almost-canonical, it follows that  $\ell$  crosses both of the parallel edges of the yellow and the blue pieces. Since the distance between the segments in each pair is 10, it follows that the segments must be horizontal.



**Figure 25:** The parallel edges of the yellow and blue pieces must intersect the alignment segment  $\ell$ . Therefore, the segments must be horizontal.

In order to show that the pieces  $\mathbf{p}_i$  have an aligned  $i\mu$ -placement, it remains to bound the horizontal displacement of the yellow and blue pieces as compared to the placements encoding the middle value  $m$  of the interval  $I(x)$ . Consider the yellow piece  $p$ , the argument for the blue piece is similar. We need to prove  $\langle p \rangle \in [m - i\mu, m + i\mu]$ . We will actually show the stronger statement that  $\langle p \rangle \in [m - w, m + \mu] \subset [m - i\mu, m + i\mu]$ .

Recall that the  $p$  is right-oriented. The constraint that  $p$  must be inside  $C$  ensures that  $\langle p \rangle \geq m - w$ . Since the pieces have an almost-canonical placement by assumption, we know that the displacement as compared to the situation in Figure 23 is at most  $n^{-1}$ . It therefore follows that not other pieces than the orange piece can fit in the region to the left of the yellow and blue pieces. We consider a canonical placement and analyse how much  $p$  can slide to the right before too much empty space has been made in the region. Observe that sliding  $p$  to the right by  $t$  creates empty space of area  $10t$ , since the height of the piece is 10. It therefore follows that we must have  $t \leq \mu/10$ . This translates to  $\langle p \rangle \leq m + w + \mu/10 \leq m + \mu$ , and we are done.  $\square$



**Figure 26:** If the pieces do not have a canonical placement, there is room for the orange piece to be oriented in the canonical way and get a vertical edge-edge contact with the container. Then the blue and yellow pieces can be pushed to the left to obtain a canonical placement, which will decrease the value encoded by the yellow piece and increase the value encoded by the blue piece.

**Edge inequalities.** Recall that Lemma 13 states that for any edge  $(p_1, p_2)$  in the dependency graph  $G_x$ , we have the inequality  $\langle (\cdot) p_x \rangle \leq \langle p_y \rangle$ . We show this lemma now for the anchor.

*Proof of Lemma 13 for the anchor.* Denote by  $p_1$  and  $p_2$  the blue and yellow piece, respectively. The pieces induce the edge  $(p_1, p_2)$  in  $G_x$  and we have to show  $\langle p_1 \rangle \leq \langle p_2 \rangle$ . We have that  $\langle p_1 \rangle = \langle p_2 \rangle$  when the pieces have an edge-edge contact with the orange piece, as shown in Figure 23. We have to show that it is not possible that  $\langle p_1 \rangle > \langle p_2 \rangle$ . This could only potentially happen if the piece do not have a canonical placement. However, some straightforward rotation arguments show that in this case we even have  $\langle p_1 \rangle < \langle p_2 \rangle$ , see Figure 26. It follows that  $\langle p_1 \rangle \leq \langle p_2 \rangle$ .  $\square$

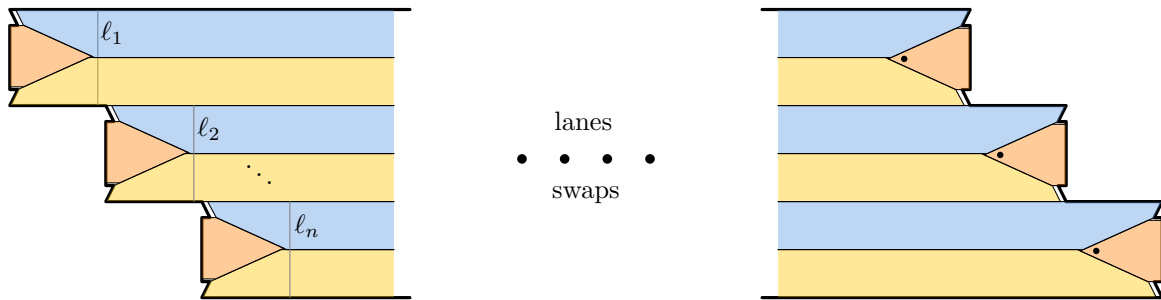
**Range Constraints.** It is claimed in Lemma 14 that all variables are within the range  $[1/2, 2]$ . Here, we show this claim, assuming that every variable is consistently represented.

To see that the range  $[1/2, 2]$  is respected, note that in the situation for  $x = m$  shown in Figure 23, neither the yellow nor the blue piece can move further to the left than  $w$ . Thus as the yellow piece is right-oriented, we get that  $x \geq m - w \geq 1/2$ . Similarly, as the blue piece is left-oriented, we get that  $x \leq m + w \leq 2$ . Hence, we have  $x \in [1/2, 2]$ .

**Valid placements are canonical.** In this paragraph, we show that the pieces of the anchor have a canonical placement in every valid placement. We can assume that we already know soundness as stated in Lemma 7 and that every valid placement is an aligned  $g\mu$ -placement (Lemma 8).

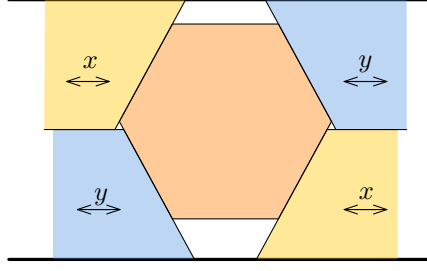
*Proof of Lemma 20 for the anchor.* By Lemma 7, we can assume that all variable pieces are in a canonical placement and they must encode the same value. Now from Figure 26, we conclude that if the orange piece did not have edge-edge contacts with the yellow and blue pieces then the yellow and blue piece would encode different values. That contradicts Lemma 7 and we conclude that the pieces have a canonical placement.  $\square$

**Staircases of achors.** As the next step, we describe how we organize all the anchors of the construction. Recall that the wires of the wiring diagram appear and disappear in the order  $(\vec{x}_1, \overleftarrow{x}_1), \dots, (\vec{x}_n, \overleftarrow{x}_n)$  from left to right in a staircase-like fashion. Therefore, we also stack the anchors onto one another as displayed in Figure 27, so that the boundary of each stack appears similar to a staircase. The rest of the construction will be in between these two staircases. Anchors in the right staircase are treated in the following paragraph.



**Figure 27:** Anchors are placed one on top of the other to form two staircases. The alignment segments  $\ell_1, \dots, \ell_n$  are used to align the blue and yellow pieces of the anchors in this order. The dots in the orange pieces in the right staircase mark the fingerprinted corners.

**Anchors in the right staircase.** For an anchor in the right side, the entering yellow and blue variable pieces have been started in other gadgets farther to the left, and we only add



**Figure 28:** The simplified swap. The yellow pieces representing  $x$  are either both right- or both left-oriented. Likewise for the blue pieces representing  $y$ . For color codes, see Figure 29.

the orange piece. We define the canonical placements in an analogous way as for the left anchors. The proof of Lemma 6 (solution preservation) is trivial since no new variable pieces are introduced. The orange piece in a right anchor is fingerprinted as in the left anchors, and Lemma 10 follows. Lemma 11 is trivial since no new variable pieces are introduced. The edge inequality of Lemma 13 is proven as for the left anchors, as is Lemma 20 that a valid placement is canonical.

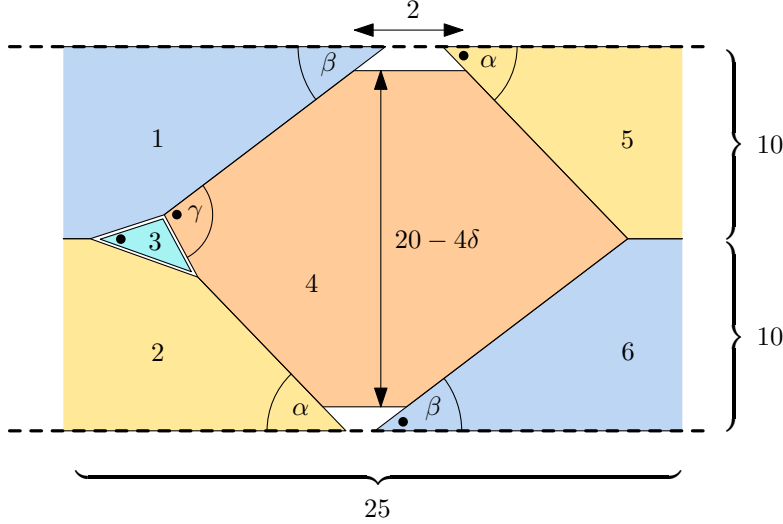
## 7.2 Swap

**Idea.** Recall that in the wiring diagram, the wires may cross each other (see Figure 14). On top of such a crossing, we build a swap. The purpose of the swap is thus to make a crossing of two neighbouring lanes of pieces. To get intuition about how the gadget works, consider Figure 28. The yellow pieces encode a variable  $x$  and the blue pieces encode a variable  $y$ . It is possible that  $x = y$ , which will happen only when the two wires  $\vec{x}, \overleftarrow{x}$  cross each other. Therefore, the yellow pieces will have the opposite orientation of the blue pieces in this special case.

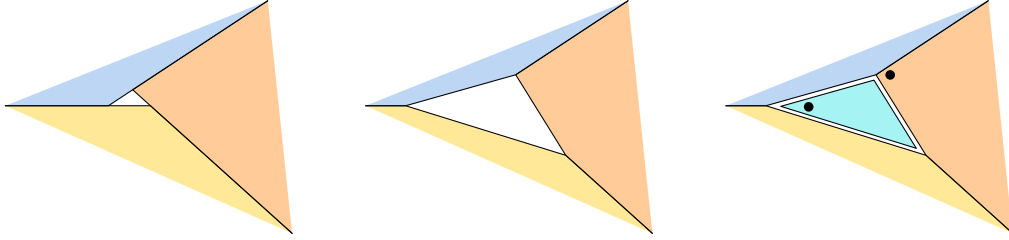
We want to show that when the pieces have edge-edge contacts to the orange piece, the variables are encoded consistently, so that the lanes have been swapped. The key observation is that if the left blue piece pushes to the right and the yellow pieces are fixed, then the orange piece will slide along the yellow pieces and push the right blue piece by an equal amount. Similarly, if the left yellow piece pushes to the right, then the orange piece will slide along the blue pieces, and will push the right yellow piece by an equal amount. For this to work the two opposite edges of the orange piece in contact with the blue pieces must be parallel and similarly the two other edges in contact with the yellow pieces must be parallel as well. The conclusion is that for all placements of the orange piece where it has edge-edge contacts to all yellow and blue pieces, the horizontal distance between the two yellow pieces is the same, as is the distance between the two blue pieces.

**The actual swap.** See Figure 29 for the following description. The swap consists of six pieces. Those are the left and right yellow piece, the left and right blue piece, the orange piece and the turquoise piece.

The left yellow and blue pieces extend outside the gadget to the left, where they have been introduced in other gadgets added earlier to the construction. Likewise, the right yellow and blue pieces extend outside the gadget to the right, where their ends will be defined in other gadgets added later to the construction. The gadget is bounded by horizontal segments from above and below, and these are either part of the container boundary or the boundary of other pieces that have been added earlier and can be assumed to be placed there. As is seen from the figure, the yellow pieces have corners with the same angle  $\alpha$ , and the blue pieces have corners



**Figure 29:** The actual swap. Color codes: 1 blue, 2 yellow, 3 turquoise, 4 orange, 5 yellow, 6 blue.



**Figure 30:** Left: the construction without the turquoise piece. Middle: We remove part of the pieces, leaving a triangular empty space with edges of length more than 1. Right: The turquoise piece is designed to fit in the triangle of empty space, but it is surrounded by empty space of thickness  $\delta$  in every direction. This leaves enough wiggle room for the other pieces to encode all solutions to  $\Phi$ .

with the same angle  $\beta$ . We require  $\alpha$  and  $\beta$  to be in the interval  $[30^\circ, 40^\circ]$ . The precise value of those angles is chosen freely for the fingerprinting. Similarly, the orange and turquoise piece have a corner with a flexible angle. The angle  $\gamma$  is in the interval  $[60^\circ, 80^\circ]$  and is also chosen freely for fingerprinting. The orange piece has a horizontal top and bottom edge of length 2.

For the way we construct the turquoise piece, we refer the reader to Figure 30. The role of the turquoise piece is solely to be able to fingerprint the orange piece. It has no direct use in the functionality of the swap. If we avoid using the turquoise piece and instead use pieces as in the simplified Figure 28, the left corner of the orange piece, that we want to fingerprint in the wedge between the left yellow and blue pieces, has angle  $\alpha + \beta$ , and thus the unique angle property is violated; indeed, the right yellow and blue pieces can cover the wedge equally well. The left endpoints of the horizontal segments of the orange piece cannot be used for fingerprinting, because the angles are more than  $\pi/2$ . It may be tempting to believe that one could avoid the turquoise piece, but we could not find such a way using only convex pieces. Note that we have only two degrees of freedom without the turquoise piece, as certain edges must be parallel. This is not enough to choose three angles freely for fingerprinting.

**Canonical placements and solution preservation.** Recall that the yellow and blue pieces represent the variables  $x$  and  $y$ , respectively. In Figure 29, all variable pieces encode the middle value of their respective interval  $I(x)$  or  $I(y)$ , and this defines their canonical placements. For a placement of the six pieces to be canonical, we require that the yellow and blue pieces have edge-edge contacts to the orange piece as shown and that the turquoise piece is enclosed by the left yellow and blue pieces and the orange piece as shown.

We prove now Lemma 6, about solution preservation, for the swap.

*Proof of Lemma 6 for the swap.* Suppose that for a given solution to the ETR-INV formula  $\Phi$ , there exists a canonical placement of the previously introduced pieces  $\mathbf{p}_{i-1}$  that encodes that solution. To extend the placement to the pieces  $\mathbf{p}_i$ , i.e., with the yellow, blue, turquoise and orange pieces of this swap included, we place the yellow and blue pieces so that they represent the value of  $x$  in the solution to  $\Phi$ . This leaves room for the orange piece to be placed with the required edge-edge contacts to the blue and yellow pieces. The turquoise piece has enough wiggle room to be placed correctly as well.  $\square$

**Fingerprinting and almost-canonical placement.** Here we are less detailed in the application of Lemma 48 (Multiple Fingerprints) than in the section about the anchor. The reason is simply that the arguments repeat almost exactly to the letter and we want to avoid unnecessary repetition.

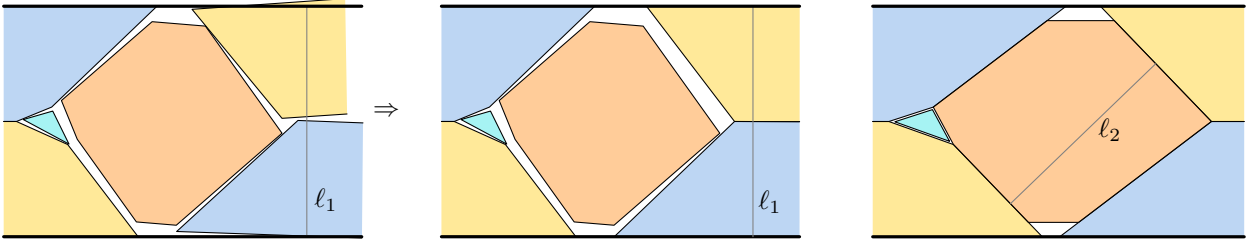
Recall that in Lemma 10, we assume that the previous pieces  $\mathbf{p}_{i-1}$  are in an aligned  $(i-1)\mu$ -placement and we want to conclude that the new pieces  $\mathbf{p}_i$  have an almost canonical placement.

*Proof of Lemma 10 for the swap.* Recall that  $\mathbf{p}_{i-1}$  consists of all pieces introduced previously, including the left blue and left yellow pieces, whereas  $\mathbf{p}_i$  additionally includes the orange, turquoise and the right blue and yellow pieces. We now fingerprint the turquoise, orange, right blue, and right yellow pieces in this order. We use the intended placements of the those pieces shown in Figure 29 (corresponding to the case where the variables have their middle values) and fingerprint the corners marked with dots. These intended placements are  $O(\delta + (i-1)\mu)$ -sound for any aligned  $(i-1)\mu$ -placement of the pieces  $\mathbf{p}_{i-1}$ , since the empty space has thickness  $O(\delta)$  and the left blue and left yellow pieces have displacement of at most  $(i-1)\mu$  compared to the shown placement, by the assumption of Lemma 10. We conclude using Lemma 48 (Multiple Fingerprints) that the displacement is  $O(n^{-48})$ , so the pieces must have an almost-canonical placement.  $\square$

### Aligned placement.

*Proof of Lemma 11 for the swap.* Consider a valid placement where the pieces  $\mathbf{p}_{i-1}$  have an aligned  $(i-1)\mu$ -placement and the pieces of this swap have an almost-canonical placement; see left of Figure 31. We consider the alignment segment  $\ell_1$  which has length 20. Since the placements are almost-canonical, it follows that  $\ell_1$  crosses both of the parallel edges of the right yellow and the blue pieces. Since the distance between the segments in each pair is 10, it follows that the segments must be horizontal.

In order to show that the pieces  $\mathbf{p}_i$  have an aligned  $i\mu$ -placement, it remains to bound the horizontal displacement of the right yellow and blue pieces as compared to the placements encoding the middle values of their intervals  $I(x)$  and  $I(y)$ . Consider the yellow piece, the argument for the blue is similar. Let  $p_1$  be the left yellow piece and  $p_2$  the right one. By assumption, we have  $\langle p_1 \rangle \in [m - (i-1)\mu, m + (i-1)\mu]$ , where  $m$  is the middle value of  $I(x)$ , and we need to prove  $\langle p_2 \rangle \in [m - i\mu, m + i\mu]$ . Suppose that the yellow pieces are right-oriented;



**Figure 31:** Left: Due to the alignment segment  $\ell_1$ , the right yellow and blue pieces must be axis-parallel. Right: Due to the alignment segment  $\ell_2$ , the orange piece must also be in a canonical placement.

the other case is similar. From the proof of Lemma 13 for the swap, we have that  $\langle p_1 \rangle \leq \langle p_2 \rangle$ , so we just need to show  $\langle p_2 \rangle \leq m + i\mu$ . It is therefore sufficient to show  $\langle p_2 \rangle \leq \langle p_1 \rangle + \mu$ .

Since the pieces have an almost-canonical placement by assumption, we know that the displacement as compared to the situation in Figure 29 is  $n^{-1}$ . It therefore follows that not other pieces than the orange and turquoise can fit in the region between the left yellow and blue pieces and the right yellow and blue pieces. We consider the case where  $\langle p_1 \rangle = \langle p_2 \rangle$  and analyse how much  $p_2$  can slide to the right before too much empty space has been made in the region. Observe that sliding  $p_2$  to the right by  $t$  creates empty space of area  $10t$ , since the height of the piece is 10. It therefore follows that we must have  $t \leq \mu/10 \leq \mu$ . This translates to  $\langle p_2 \rangle \leq \langle p_1 \rangle + \mu$ , and we are done.  $\square$

### Edge inequalities.

*Proof of Lemma 13 for the swap.* In the swap, the yellow pieces induce an edge in the graph  $G_x$  and the blue induce an edge in  $G_y$ . In the special case that  $x = y$ , the blue and yellow pieces have opposite orientations, so according to the rule about when to add edges to the dependency graph  $G_x$ , there will also be an edge between the left pieces and one between the right pieces. We make an exception to the rule and do not add these edges to the dependency graph.

We now prove the edge inequality for the edge between the yellow pieces; the argument for the blue pieces is analogous. Suppose that the yellow pieces are right-oriented and let  $p_1$  be the left and  $p_2$  be the right, so that they induce the edge  $(p_1, p_2)$  of  $G_x$ . The argument is analogous if they are left-oriented. Recall that  $\langle p_1 \rangle = \langle p_2 \rangle$  exactly when the pieces have the horizontal distance shown in Figure 29, where the orange piece has edge-edge contacts with both yellow pieces. Since the pieces have an almost-canonical placement by assumption, the displacement of the orange piece is at most  $n^{-1}$ . It therefore follows that the same pair of parallel edges of the orange piece will prevent the yellow pieces from being closer than in the figure, so we have  $\langle p_1 \rangle \leq \langle p_2 \rangle$ .  $\square$

**Valid placements are canonical.** In this paragraph, we show that the pieces of the swap have a canonical placement in every valid placement. We can assume that we already know soundness as stated in Lemma 7 and that every valid placement is an aligned  $g\mu$ -placement (Lemma 8).

*Proof of Lemma 20 for the swap.* By Lemma 7, we can assume that all variable pieces are in a canonical placement and they must encode the same value. Now consider alignment-segment  $\ell_2$  in the right of Figure 31. we conclude that if the orange piece did not have edge-edge contacts with the two yellow pieces then the two yellow pieces would encode different values of the

same variable. Which contradicts Lemma 7 and we conclude that also the orange piece is in a canonical placement.  $\square$

### 7.3 Split

The purpose of the split is to make an extra lane representing a variable  $x$ . This will be needed in order to lead lanes into the gadgets for the addition and inversion inequalities.

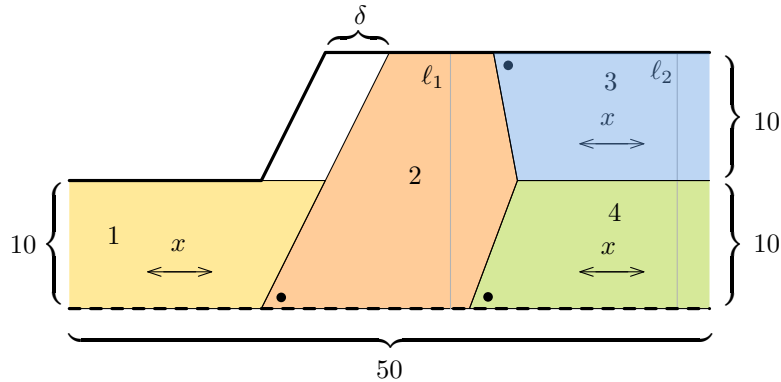
**Description.** See Figure 32 for an illustration of the split. We always split the topmost lane in the construction, so that there is room to expand above with one more lane. Therefore, the split is bounded from above by the boundary of the container and from below by pieces in the second-highest lane, which have been added to the construction earlier.

The yellow piece extends outside the gadget to the left, where it has been introduced to the construction in an earlier step. The yellow piece is in contact to the right with an orange piece with height 20, i.e., twice the height of a lane. The orange piece is in contact to the right with the blue and green pieces, which extend outside the gadget to the right, where they will enter other gadgets defined later in the construction. Each of the orange, blue, and green piece has a corner with an angle that can be freely chosen for fingerprinting.

**Canonical placements and solution preservation.** The yellow, blue, and green pieces are all variable pieces encoding a variable  $x$ . The position as indicated in Figure 32 show the situation where they all encode the middle value of the interval  $I(x)$ . The placement of all four pieces is canonical if they have the shown edge-edge contacts. In the placement shown in Figure 32, the pieces encode middle value of  $x$ . Lemma 6 (solution preservation) follows trivially.

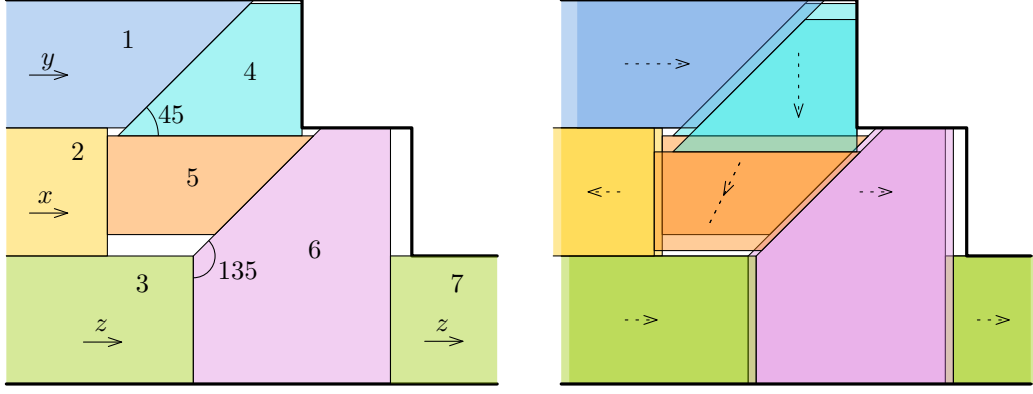
**Fingerprinting and almost-canonical placement.** The proof of Lemma 10 for the split is completely analogous to the one for the swap.

**Aligned placement.** All pieces must be aligned because of the container boundary and the edge of a piece from  $\mathbf{p}_{i-1}$  bounding the gadget from below. As for the swap, to get Lemma 11 for the split, we need to verify that the blue and green piece encodes a value that is at most  $\mu$  larger than that encoded by the yellow piece. The proof is analogous as the one for the swap.



**Figure 32:** The split. The yellow, blue, and green pieces represent the variable  $x$  and are either all right-oriented or all left-oriented. Color codes: 1 yellow, 2 orange, 3 blue, 4 green.





**Figure 33:** Left: The simplified adder. Right: The variable  $x$  is increased by two units. The variable  $y$  is decreased by one unit. Thus the variable  $z$  is increased by one unit. Color codes: 1 blue, 2 yellow, 3 green, 4 turquoise, 5 orange, 6 pink, 7 green.

**Edge inequalities.** In the split, we get two edges in the dependency graph. If the pieces are right-oriented, we have edges from the yellow to green and to the blue pieces. Otherwise, we have edges from green to yellow and blue to yellow. That the edges satisfy the edge inequality (Lemma 13) follows by construction, since the orange piece restricts how close the yellow piece can get to the green and blue pieces.

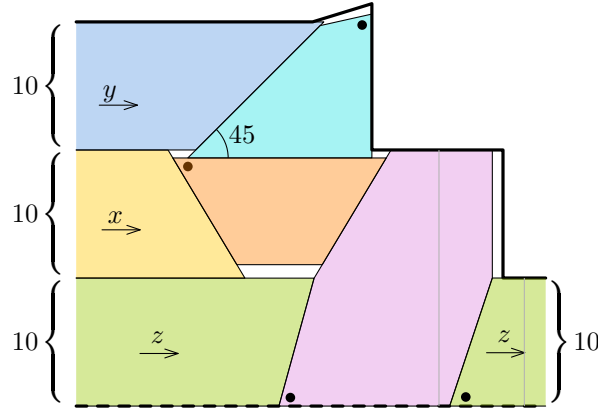
**Valid placements are canonical.** In this paragraph, we show that the pieces of the split have a canonical placement in every valid placement. We can assume that we already know soundness as stated in Lemma 7 and that every valid placement is an aligned  $g\mu$ -placement (Lemma 8).

*Proof of Lemma 20 for the split.* By Lemma 7, we know that all variable pieces encode the same value. We already know that the orange piece is aligned correctly. It remains to show that the orange piece has edge-edge contacts with the other pieces. Since the other pieces encode  $x$  consistently, there is clearly only one way to place the orange piece, and it will have the needed contacts.  $\square$

## 7.4 Adder

**Idea.** For the following description see Figure 33. Here we explain the principle behind the adder for  $x + y \leq z$ . The adder for  $x + y \geq z$  is identical, but has the entering variable pieces for  $x, y, z$  oriented to the left instead of to the right. The adder has three entering variable pieces (yellow, blue, left green), representing three variable ( $x, y, z$ ). There is also one exiting green variable piece representing  $z$ . In addition to this, there are three pieces that are not variable pieces (turquoise, orange, pink). The role of the turquoise piece is transform horizontal motion to the right of the blue piece to downwards vertical motion. Motion of the orange piece downwards or to the right both make the pink piece move to the right by an equal amount. Therefore, when the blue and yellow pieces push to the right, the pink piece will be pushed to the right by the sum of the two motions.

**Actual description.** The actual adder is shown in Figure 34. The figure shows the situation where the yellow and blue pieces encode the middle values  $m_x$  and  $m_y$  of the intervals  $I(x)$  and  $I(y)$ , while the green pieces encode the value  $m_x + m_y$  which is in general not the middle value of the interval  $I(z)$ . The actual adder varies in several points from the simplified version



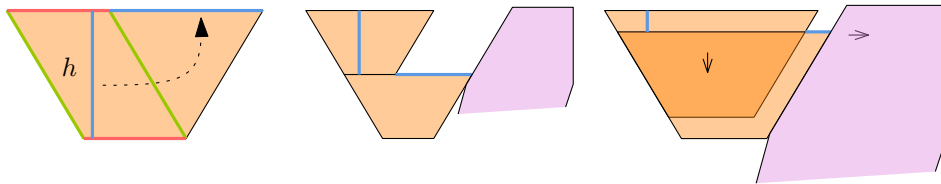
**Figure 34:** The actual adder.

in Figure 33 which are needed in order to use fingerprinting. The orange, turquoise, pink, and right green pieces must be fingerprinted, so they cannot have only nice angles as in the simplified gadget. The turquoise piece can easily be fingerprinted using the top right corner. The orange piece is fingerprinted at the upper left corners. The pink and right green pieces are fingerprinted at their lower left corners. In each case, the angle can be chosen freely by changing the slope of the edge-edge contact with the piece to left.

As a consequence of changing the angle on the bottom left of the orange piece to something else than  $45^\circ$ , we also have to change the angle of the bottom right corner of the orange piece. See Figure 35 for an illustration of the following. First we describe how to construct the orange piece and then we explain why it actually works. The orange piece is a trapezoid with horizontal bottom and top edges and height  $10 - 10\delta$ . The left edge of the orange piece is parallel to the right edge of the yellow piece. The length of the top edge should be at least as long as the bottom edge of the turquoise piece. The length of the bottom piece is the length of the top edge minus the height  $10 - 10\delta$ . The right edge is determined by the description of all the other edges.

We need to explain why pushing the blue piece to the right by some amount  $t > 0$  will push the pink piece to the right by  $t$  as well; see Figure 35. It is helpful to consider the case where  $t$  equals the height  $h$  of the orange piece (even though there is not room for pushing the pieces so much). This push of the blue piece will push the orange piece down by  $h$ . Since the length of the top edge of the orange piece equals the length of the bottom edge plus  $h$ , the pink piece will be pushed to the right by  $h$  as well. All the pieces move linearly, so it will also be the case for smaller values of  $t$ .

We furthermore want the property that for each of the top corners of the turquoise piece,



**Figure 35:** In each of these three pictures, thick segments drawn with the same color are equally long. Left: The construction of the orange piece. Middle: Pushing the orange piece down by its height makes it push the pink piece by the same amount. Right: This also holds when pushing less.

the line through the corner and perpendicular to the diagonal of the corner is a tangent to the piece. The same must hold for the bottom corners of the orange piece; see Figure 36. It is easy to choose the fingerprinted angles so that the pieces have this property.

**Canonical placements and solution preservation.** The canonical placements are defined as the placements with the edge-edge contacts as shown in Figure 34. That there is a canonical placement encoding any given solution to  $\Phi$  (Lemma 6) follows by construction.

**Incorporating the gadget.** In order to incorporate the adder into the construction, we use two splits and eight swaps in order to organize the in-going and out-going lanes to the gadget; see Figure 37 for a schematic illustration.

**Fingerprinting and almost-canonical placement.** The proof of Lemma 10 for the adder is completely analogous to the one for the swap.

**Aligned placement.** The right green piece must be aligned because of the container boundary and the edge of a piece from  $\mathbf{p}_{i-1}$  bounding the gadget from below. As for the swap, to get Lemma 11 for the adder, we need to verify that the right green piece encodes a value that is at most  $\mu$  larger than that encoded by the left green piece. The proof is analogous as the one for the swap.

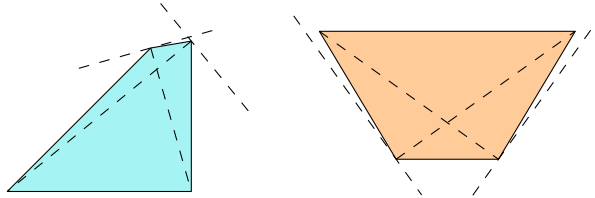
**Edge inequalities.** In the adder, the left and right green edges induce an edge in the dependency graph. That the edge satisfies the edge inequality (Lemma 13) is proven as for the swap.

**The adder works.** In this paragraph we prove Lemma 15. Here we are considering an aligned  $g\mu$ -placement, and we need to prove that for every addition constraint  $x + y = z$  of  $\Phi$ , we have  $\langle K_x \rangle + \langle K_y \rangle = \langle K_z \rangle$ .

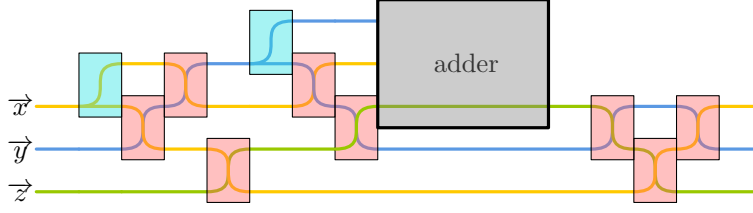
*Proof of Lemma 15.* We prove the inequality  $\langle K_x \rangle + \langle K_y \rangle \leq \langle K_z \rangle$ . The other inequality follows from analogous arguments about the gadget for  $x + y \geq z$ . Let  $p_x, p_y, p_{z1}$  be the yellow, blue, and left green pieces, and  $p_{z2}$  be the right green piece.

Note first that due to the way we incorporate the adder, there are paths  $P_x$  and  $P_y$  in  $G_x$  and  $G_y$  attached to and directed away from the cycles  $K_x$  and  $K_y$ , and the vertices farthest away from the cycles are the pieces  $p_x$  and  $p_y$ . Furthermore, the pieces  $p_{z1}$  and  $p_{z2}$  are two consecutive vertices on the cycle  $K_z$ , so by Lemma 14, we have  $\langle p_{z1} \rangle = \langle p_{z2} \rangle = \langle K_z \rangle$ .

We argue that if  $\langle p_x \rangle + \langle p_y \rangle = \langle K_z \rangle$ , the only way to place the pieces is the canonical way. This excludes the situation  $\langle p_x \rangle + \langle p_y \rangle > \langle K_z \rangle$ , since there the turquoise, orange, and pink pieces have strictly less space. Consider first the turquoise piece. It is straightforward to



**Figure 36:** The lines through corners and perpendicular to diagonals are disjoint from the interiors.



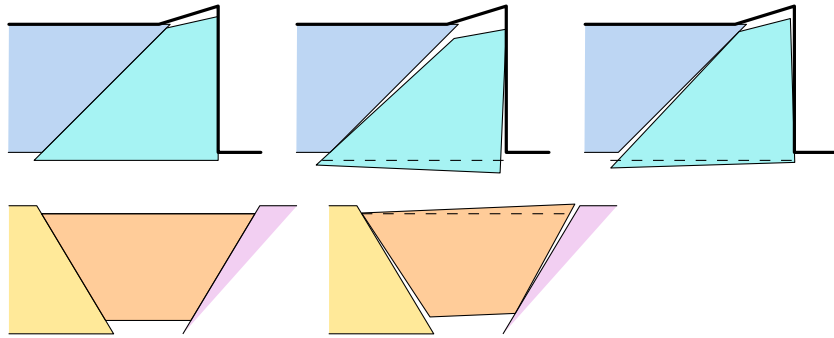
**Figure 37:** Incorporation of the adder. Splits are marked in turquoise, swaps are marked red.

check that if it does not have edge-edge contacts to the blue piece and the container boundary, then the lower edge will be strictly below the placement of the edge where these contacts were present, in the sense that every point on the segment will have a placement with a smaller  $y$ -coordinate. This can be seen in Figure 38 and is due to the property that the lines through corners perpendicular to diagonals are tangents, as shown in Figure 36. Similarly for the orange piece, if it does not have edge-edge contacts with the yellow and pink pieces, the top edge is strictly above the edge in the placement where it does have these contacts. In the canonical placements, the bottom edge of the turquoise piece is contained in the top edge of the orange piece. Therefore, in any other placement of the turquoise and orange pieces, there will be points on the turquoise edge below the orange edge, which makes the placement invalid. We can now conclude that in general, we must have  $\langle p_x \rangle + \langle p_y \rangle \leq \langle K_z \rangle$ .

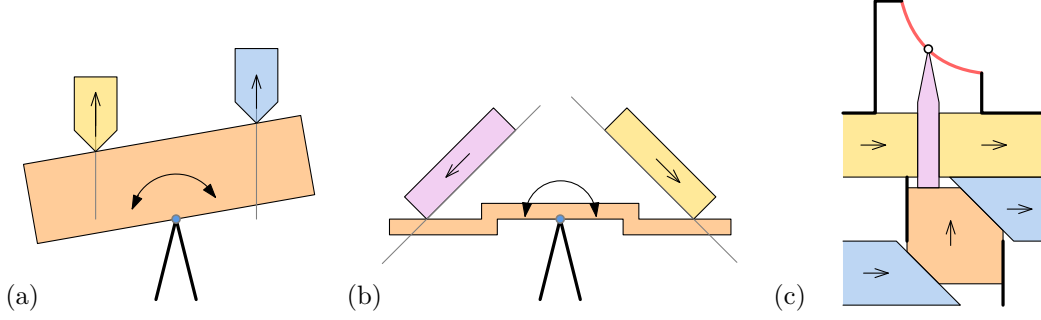
To finish the prove, note that since the paths  $P_x$  and  $P_y$  are directed away from the cycles  $K_x$  and  $K_y$ , we get from the edge inequalities (Lemma 13) that

$$\langle K_x \rangle + \langle K_y \rangle \leq \langle p_x \rangle + \langle p_y \rangle \leq \langle K_z \rangle. \quad \square$$

**Valid placements are canonical.** It was already shown in the proof of Lemma 15 for the adder that in every aligned  $g\mu$ -placement, the pieces of the adder have a canonical placement.



**Figure 38:** Top: If the turquoise piece does not have edge-edge contacts to the blue piece and the boundary, then all points of the lower edge have strictly smaller  $y$ -coordinates than otherwise. Bottom: If the orange piece does not have edge-edge contacts to the yellow and pink pieces, then the top edge is strictly higher than otherwise. The dashed segments are the edges in the canonical situations shown to the left.



**Figure 39:** Displayed are three principles on how an inversion constraint can be constructed. We call them (a) *teeter-totter*, (b) *seesaw*, and (c) *gramophone*. Those ideas use different types of pieces (convex/polygonal/curved), different types motions (rotation/translation) and different properties of the container (curved/polygonal) and result in different types of constraints ( $x \cdot y \geq 1$  /  $x \cdot y \leq 1$ ).

## 8 Inversion gadgets

We are going to construct three different types of inversion gadgets, see Figure 39. Furthermore, we will describe four variants of the last type called the *gramophone*. The figure shows simplified drawings of the gadgets to highlight the principles that make them work and the actual gadgets may at first appear to be considerably different. This is for four reasons. First, we have to construct gadgets so that each gadget adds only  $O(\delta)$  to the slack of the complete construction. Thus we have to fill the empty space in an appropriate way. Second, we will use the fingerprinting technique to ensure that all the pieces will indeed be inside the gadget and not somewhere else in the container, so we need to design the gadgets so that they fit the setup of the fingerprinting technique. Third, we need the part of the boundary of the container which bounds gadgets from above to be an  $x$ -monotone chain, which will be important in order to carry out the reduction to the case where the container is a square in Section 9. Fourth, each inversion gadget has to be connected to the other parts of the overall construction. In particular this leads to a  $90^\circ$  degree rotation in counterclockwise direction of the teeter-totter and seesaw.

Table 2 shows which inversion gadgets we can choose for each type of packing problem. In the following, we will briefly describe each of the three fundamental types.

Two of the gadgets, the teeter-totter and the seesaw, are reminiscent of the levers of the same names, found in parks and playgrounds, consisting of a fulcrum supporting a beam with a seat in each end such that two kids can take turns lifting their side by pushing the feet against the ground. The first inversion gadget (teeter-totter) enforces the constraint  $x \cdot y \geq 1$ . It is built from convex polygonal pieces, and it can therefore be used in all our reductions to packing problems where rotation is allowed.

The second inversion gadget (seesaw) uses polygonal pieces that are *not* all convex. The orange piece rotates around the blue pivot point. It enforces the constraint  $x \cdot y \leq 1$ . The underlying principle of the gadget has been used to build inversion gadgets in hardness proofs of problems related to graph drawing and polytope nesting [20, 21, 43].

The third inversion gadget (gramophone) only needs translations of the pieces, but also work when rotations are allowed. One special pink piece is translated in  $x$ - and  $y$ -direction by the yellow and the blue pieces, respectively. The pink piece is bounded from above by a curve, which translates to a dependency between the yellow and blue pieces. By adjusting the curve and the orientations of the entering lanes, we can make  $\leq$ -gramophones and  $\geq$ -gramophones, for inequalities  $x \cdot y \leq 1$  and  $x \cdot y \geq 1$ , respectively. Furthermore, we can choose whether the

	gadget for $x \cdot y \leq 1$			gadget for $x \cdot y \geq 1$	
	seesaw	curved $\leq$ -gram.	poly. $\leq$ -gram.	teeter-totter	curved $\geq$ -gram.
<b>Pack</b> ( $\square \rightarrow \sqcup, \odot +$ )		X		X	X
<b>Pack</b> ( $\triangleright \rightarrow \triangleright, \odot +$ )	X			X	
<b>Pack</b> ( $\sqsupset \rightarrow \triangleright, \odot +$ )			X	X	
<b>Pack</b> ( $\square \rightarrow \sqcup, +$ )		X			X

**Table 2:** The inversion gadgets we can use for each type of packing problem.

curved part should be on the boundary of the container (a *curved* gramophone) or on a piece in the gramophone (a *polygonal* gramophone). We will use three different types of gramophones, depending on the version of packing we are reducing to.

For the inversion gadgets the intervals  $I(x)$  for each value  $x$  (promised to contain the solutions to the ETR-INV formula  $\Phi$  we are reducing from) also become important, recall Definition 2. From the definition, we know that for a constraint  $x \cdot y = 1$ , we will have either  $I(x) = I(y) = [1 - \delta, 1 + \delta]$  or  $I(x) = [2/3 - \delta, 2/3 + \delta]$  and  $I(y) = [3/2 - \delta, 3/2 + \delta]$ . In the former case, we say that the *middle values* of  $(x, y)$  are  $(1, 1)$ , and in the latter they are  $(2/3, 3/2)$ . The precise inversion gadgets will depend on the actual case.

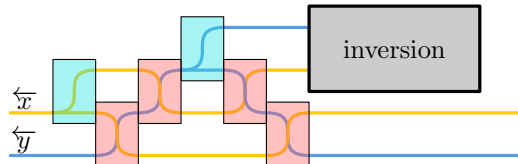
**Installation of the gadgets.** Similarly to the adder, we will place each inversion gadget on the top of the entire construction at a place corresponding to an inversion constraint box of the wiring diagram. We use splits and swaps to organize the lanes correctly, which is done differently for the gramophone than for the teeter-totter and seesaw; see Figure 40 for the organization of the latter ones.

### 8.1 Teeter-Totter

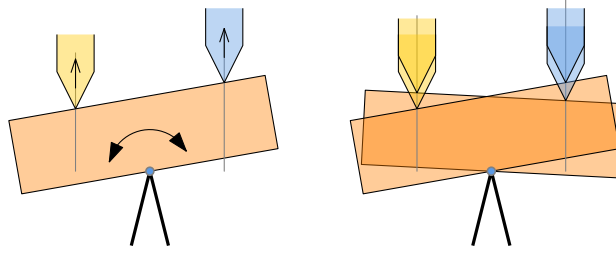
In the teeter-totter, there is an orange piece that can rotate around a pivot point. There are two pieces (yellow and blue), which are “sitting” on the orange piece, see Figure 41.

**Principle.** For the following argument, see Figure 42 and the notation therein. In the simplified teeter-totter, there is an orange rectangular piece of width 1 which can rotate around a pivot point  $p$ . A yellow and blue piece have a fixed rotation and horizontal placement, but can slide vertically up and down. The lower corners  $c_x$  and  $c_y$  of the pieces are bounded from below by the orange piece, and they are always on vertical lines at distance 1 to the left and to the right of  $p$ , respectively. The  $y$ -coordinates of these corners encode the values of  $x$  and  $y$ , respectively. We now prove that  $x \cdot y \geq 1$ .

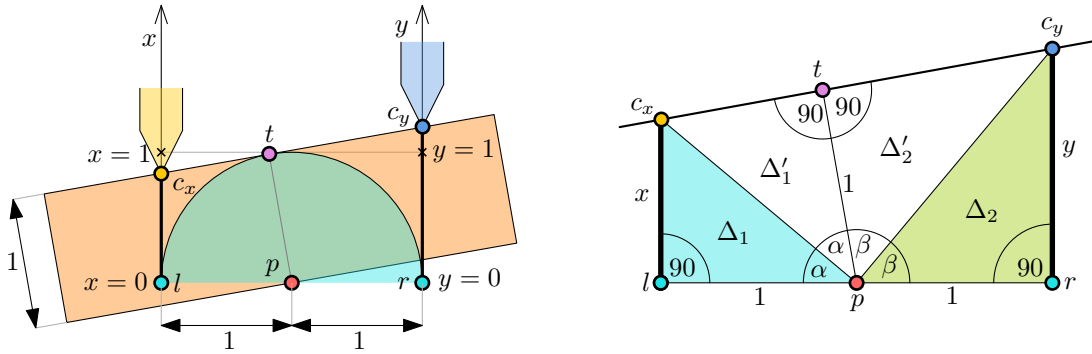
For this we consider the extreme situation that the yellow and blue piece are touching the orange piece at the corners  $c_x$  and  $c_y$ , since otherwise the product  $x \cdot y$  is only larger. As shown



**Figure 40:** The installation of a teeter-totter or a seesaw using swaps and splits. The wires should be  $\overleftarrow{x}, \overleftarrow{y}$  for the teeter-totter (as shown) and  $\overrightarrow{x}, \overrightarrow{y}$  for the seesaw.



**Figure 41:** Left: The simplified teeter-totter. Right: Different motions of the pieces.



**Figure 42:** Left: The teeter-totter with a unit disk around the pivot point  $p$ . The upper edge of the orange piece is always tangent to that unit disk. The turquoise points  $l, r$  correspond to the values  $x = 0$  and  $y = 0$ . Right: The quadrilateral  $lrc_y c_x$  is partitioned into four triangles.

in the figure, we consider the two triangles  $\Delta_1$  and  $\Delta_2$  and want to show that they are similar with  $\alpha = 90^\circ - \beta$ , since this implies

$$\frac{x}{1} = \frac{1}{y} \quad \Leftrightarrow \quad x \cdot y = 1.$$

Note first that the triangles  $\Delta'_1$  and  $\Delta_1$  are congruent: They both have one right angle, they share the hypotenuse and they both have one leg of length 1. By the same reasoning the triangles  $\Delta'_2$  and  $\Delta_2$  are congruent. We define  $\alpha$  as the angle of  $\Delta_1$  at  $p$  and we define  $\beta$  as the angle of  $\Delta_2$  at  $p$ . Due to the similarity discussed before it holds that

$$2\alpha + 2\beta = 180^\circ \quad \Leftrightarrow \quad \alpha = 90^\circ - \beta,$$

and we are done.

**Actual description.** Note first that we have two versions of the teeter-totter: One for the middle values  $(1, 1)$  and one for the middle values  $(2/3, 3/2)$ ; see Figure 43. We describe in this paragraph both versions, but only point out where the constructions differ. Note that the gadget is rotated counterclockwise by  $90^\circ$  compared to the simplified version.

The gadget consists of a yellow and a blue variable piece, encoding the variables  $x$  and  $y$ , respectively. We describe the gadget in the situation where the yellow and a blue piece encode the middle values of  $x$  and  $y$ . The blue and yellow piece extends outside the gadget to the left, where they are fingerprinted in gadgets added earlier in the construction. Then we have an orange and a turquoise piece, which are fully contained inside the gadget. The top right corner of the turquoise piece is fingerprinted such that exactly the turquoise piece fits, without any empty space. The turquoise piece has 5 corners, the leftmost is a corner  $p$  that acts as



a pivot point around which the orange piece can rotate. The orange piece has width 1 and a vertical height in the range  $[21, 22]$ . On the top of the boundary of the gadget is a spike of vertical height in the range  $[1 + 50\delta, 2 + 50\delta]$ , where we fingerprint the topmost corner of the orange piece. We can change the angle of the fingerprinted corner by extending the edge touching the pivot point  $p$  and the height of the spike accordingly. The spike is built in a way that allows the orange piece to rotate a bit and at the same time, we keep the empty space limited to thickness  $O(\delta)$ . The blue and yellow piece have corners  $c_x, c_y$  which are in contact with an edge of the orange piece. For the middle values  $(1, 1)$  those corners are the points  $c_x = p + (-1, -1, )$  and  $c_y = p + (-1, 1, )$ . For the middle values  $(3/2, 2/3)$  those corners are the points  $c_x = p + (-2/3, -1, )$  and  $c_y = p + (-3/2, 1, )$ .

**Canonical placements and solution preservation.** A placement of the four pieces of the gadget is canonical if (i) the turquoise piece placed with edge-edge contacts to the boundary of  $C$  as shown in Figure 43, and (ii) the orange piece separates the yellow and blue pieces from the turquoise piece in the following sense. We require that the horizontal lines through the corners  $c_x$  and  $c_y$  cross first the yellow or blue piece, then the long parallel edges of the orange piece, and then the turquoise piece in order from left to right.

*Proof of Lemma 6 for the teeter-totter.* Suppose that for a given solution to the ETR-INV formula  $\Phi$ , there exists a canonical placement of the previously introduced pieces  $\mathbf{p}_{i-1}$  that encodes that solution. The placement of the yellow and blue piece is then fixed. We need to verify that there is enough empty room such that the orange piece can be placed in the gadget. We place it as shown in Figure 43 with the longest contact in contact to the pivot point  $p$ . The corners  $c_x$  and  $c_y$  can slide at most  $\delta$  to the left and right and are at vertical distance 1 from the pivot point  $p$ . The top and bottom corners of the orange piece have vertical distance at most 12 to the pivot point  $p$ . The orange piece can therefore sweep from side to side in a range of size at most  $12 \cdot 2\delta = 24\delta$ . Since we have made room of thickness  $25\delta$ , there is enough space for the piece to rotate.  $\square$

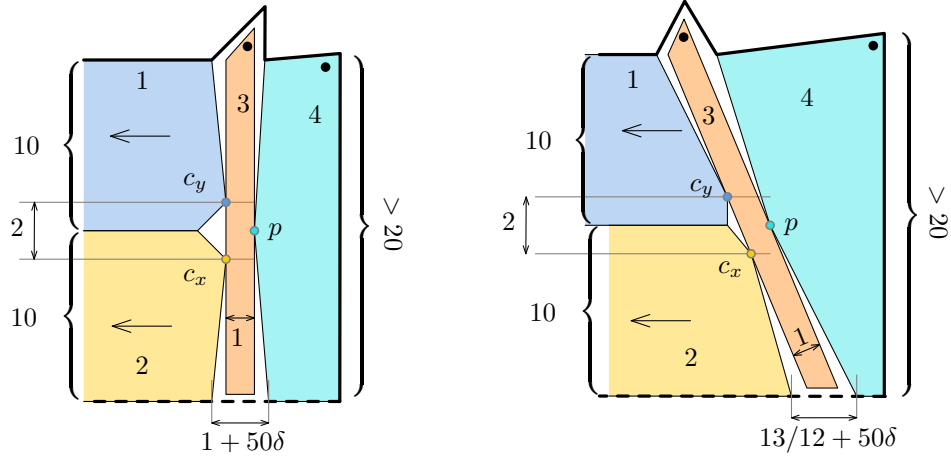
**Fingerprinting and almost-canonical placement.** The proof of Lemma 10 for the teeter-totter follows exactly as for the anchor. We first fingerprint the orange and then the turquoise piece.

**Aligned placement.** Lemma 11 holds vacuously for the teeter-totter as there are no exiting variable pieces in this gadget.

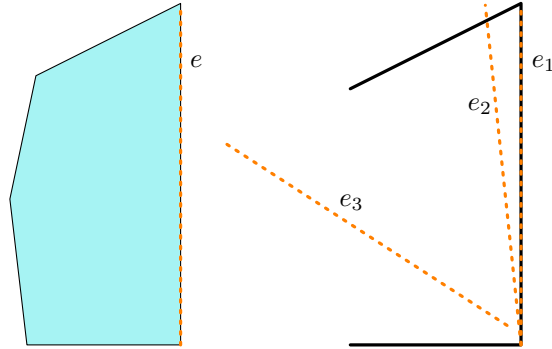
**Edge inequalities.** The pieces of the teeter-totter induce no edges in the dependency graphs, so there are no edge inequalities to verify.

**The teeter-totter works.** In this paragraph we prove the part of Lemma 16 that the teeter-totter is responsible for, namely that in a given aligned  $g\mu$ -placement, the teeter-totter used for the variables  $x$  and  $y$  implies that  $\langle K_x \rangle \cdot \langle K_y \rangle \geq 1$ .

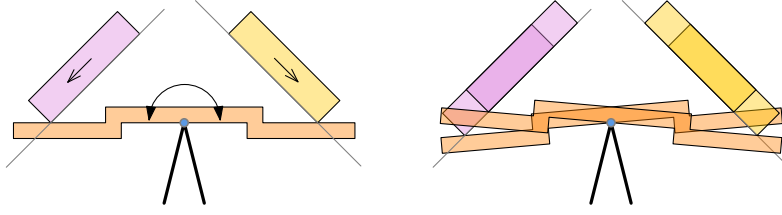
*Lemma 16 for the teeter-totter.* We first point out that the turquoise piece must be placed as in a canonical placement because the edge  $e$  only fits at one position, see Figure 44. Now, since we consider an aligned  $g\mu$ -placement, the orange piece separates the yellow and blue pieces from the pivot point  $p$  as in the simplified teeter-totter. We then get from the principle behind the gadget (described in the beginning of this section) that  $\langle p_x \rangle \cdot \langle p_y \rangle \geq 1$ , where  $p_x$  and  $p_y$  are the yellow and blue piece, respectively. We note that there are paths  $P_x$  and  $P_y$  in  $G_x$  and  $G_y$



**Figure 43:** Actual teeter-totters. The solid boundary segments are part of the boundary of the container, whereas the dashed segments bounding the gadgets from below is on the boundary of a piece that has been added to the construction earlier. Left: Teeter-totter for the middle values  $(1,1)$ . Right: Teeter-totter for the middle values  $(2/3, 3/2)$ . Color codes: 1 blue, 2 yellow, 3 orange, 4 turquoise.



**Figure 44:** The segments  $e_1, e_2, e_3$  show three potential placements of the edge  $e$  of the turquoise piece. The placement  $e_2$  can be excluded since it crosses with the boundary. The placement  $e_3$  can be excluded since it is not almost-canonical, which is an assumption here. We exaggerated the angle of the fingerprinted corner to make the difference better visible.



**Figure 45:** A simplified drawing of the seesaw. To the right is shown two different positions.

attached to and directed towards the cycles  $K_x$  and  $K_y$ , and the vertices farthest away from the cycles are the yellow and blue pieces  $p_x$  and  $p_y$ . In particular  $\langle K_x \rangle \geq \langle p_x \rangle$  and  $\langle K_y \rangle \geq \langle p_y \rangle$ . Hence,  $\langle K_x \rangle \cdot \langle K_y \rangle \geq 1$   $\square$

**Valid placements are canonical.** In this paragraph, we show that the pieces of the teeter-totter have a canonical placement in every valid placement. We can assume that we already know that every valid placement is an aligned  $g\mu$ -placement (Lemma 8).

*Proof of Lemma 20 for the teeter-totter.* We already know from the proof of Lemma 16 for the teeter-totter that the turquoise piece is placed as in the canonical placements. We observe that for all almost-canonical placements of the orange piece, it separates the yellow and blue pieces from the pivot point  $p$  as required, since there are not other places in the gadget where it can fit. Hence, the placement is canonical.  $\square$

## 8.2 Seesaw

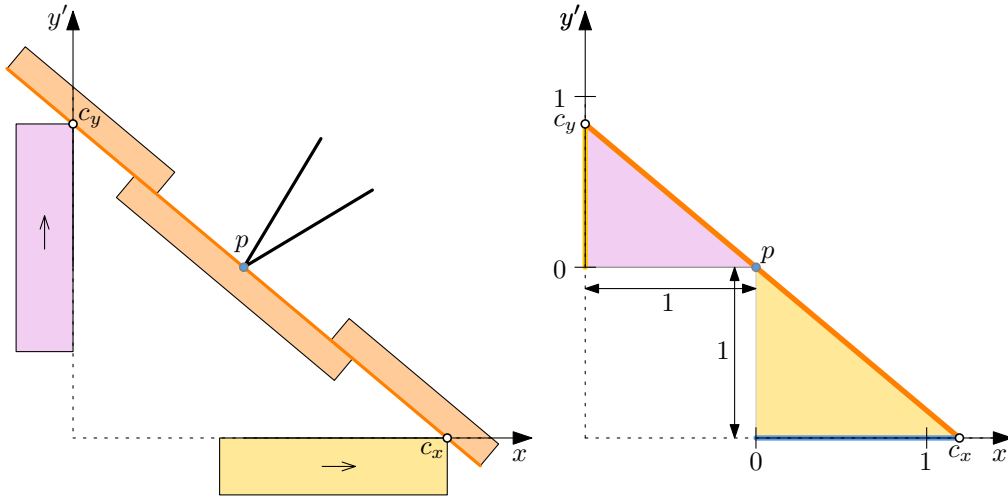
The principle behind the seesaw is very simple and can be considered folklore. See Figure 45 for a simplified sketch of the gadget. It uses one polygonal non-convex piece which rotates around a pivot point.

To principle behind the seesaw was already used in other  $\exists\mathbb{R}$ -hardness reductions [20, 21, 43]. We first repeat the principle, then we explain how to realize the principle as a gadget in our framework. As for the teeter-totter, there are two versions of the seesaw, for the middle values  $(1, 1)$  and  $(3/2, 2/3)$ . We focus our attention on the gadget for the middle value pair  $(1, 1)$ , as all arguments for the other gadget are identical.

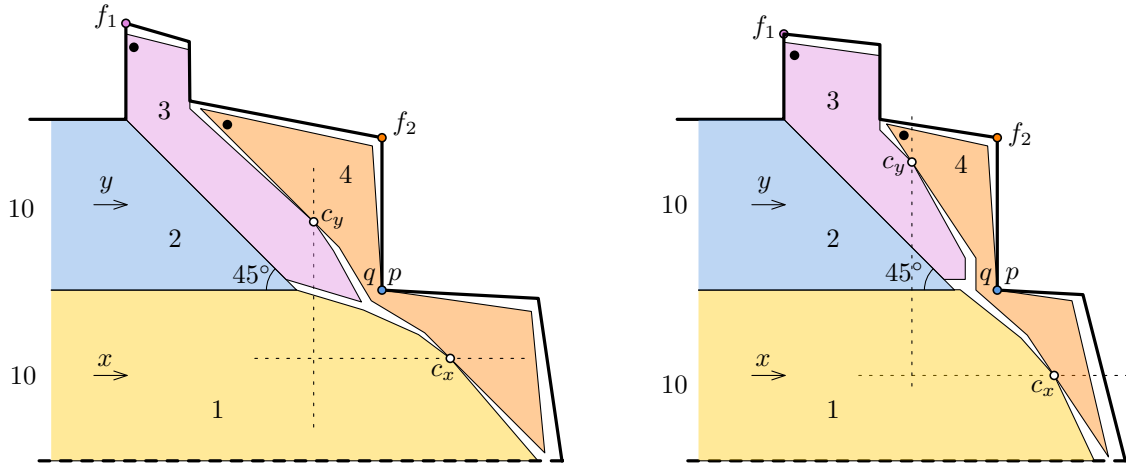
**Principle.** For the following description, we refer to Figure 46. We assume that the yellow and pink pieces are moving by horizontal and vertical translation, respectively, so that the corner-segment contact points  $c_x$  and  $c_y$  to the orange piece are always on the axes. Note that the distance of the pivot point  $p$  to both axes is 1. It is indicated how we interpret the values  $x$  and  $y'$  of the positions of the yellow and the pink piece. We can now identify the pink and yellow triangle and observe that they are similar, by construction. This implies that

$$\frac{1}{x} = \frac{y'}{1} \Leftrightarrow x \cdot y' = 1.$$

**Actual gadget.** For the following description, we refer to Figure 47. The gadget consists of four pieces. The yellow and blue pieces extend outside the gadget to the left, where they have been introduced in other gadgets introduced earlier in the construction. The orange piece plays the role of the orange piece as in Figure 46, however it has a different shape in order to fill out most of the space to have little slack. Crucially, it has two edges and a concave corner  $q$  on a common line. The pink piece transforms the horizontal motion of the blue piece to a vertical



**Figure 46:** The principle behind the seesaw. The two triangles are similar implying  $x \cdot y' = 1$ , where  $x, y'$  are the values represented by  $c_x, c_y$ , respectively.



**Figure 47:** A more accurate drawing of the seesaw. The solid boundary segments are part of the boundary of the container, whereas the dashed segments bounding the gadgets from below is on the boundary of a piece that has been added to the construction earlier. Some distances are exaggerated for the purpose of readability. The concave corner  $q$  of the orange piece is coincident with the concave pivot point  $p$  of the container. Left: Core values equal  $(1, 1)$ . Right: Core values equal  $(2/3, 3/2)$ . Color codes: 1 yellow, 2 blue, 3 pink, 4 orange.

motion. The orange and the pink pieces are fingerprinted at the corners indicated by dots. The angles of the fingerprinted corners can be changed continuously by moving the corners  $f_1$  and  $f_2$  of the container boundary vertically up and expanding the pieces accordingly. We make the boundary of the container so that the orange piece has room to rotate around the pivot point  $p$  as the pink and yellow pieces move up/down and left/right at a distance of  $\delta$ .

**Canonical placements and solution preservation.** The yellow and blue pieces are the variable pieces encoding the variables  $x$  and  $y$ , respectively.

A placement of the four pieces of the gadget is canonical if (i) the pink piece has vertical edge-edge contacts with the boundary as shown, and (ii) the orange piece separates the pink and blue pieces from the pivot corner  $p$  in the following sense. Let  $d$  be the segment of the orange piece defining its diameter, i.e., the segment that connects the topmost and bottommost corners of the piece in Figure 47. We require that the horizontal line through the corner  $c_x$  crosses  $d$  to the right of  $c_x$ . Similarly, we require that the vertical line through the corner  $c_y$  crosses  $d$  above  $c_y$ .

Even though the pink piece is not a variable piece, it also represents a value  $y'$  as shown in Figure 46.

*Proof of Lemma 7 for the seesaw.* Suppose that in all canonical placements of the previously introduced pieces  $\mathbf{p}_{i-1}$ , variables are encoded consistently and in a way that satisfies the respective addition and inversion inequalities. It is trivial that consistency of variable encodings extends to the pieces  $\mathbf{p}_i$  where this gadget is included: Each of the variables  $x$  and  $y$  are represented by one piece in the gadget, and the piece is also in  $\mathbf{p}_{i-1}$ , so the encoding is consistent by assumption.

It is left to verify that in all canonical placements, we have  $x \cdot y \leq 1$ , where  $x$  and  $y$  are the variables represented by the yellow and blue piece, respectively. The vertical placement of the pink piece corresponds to a value  $y'$ , as defined in Figure 46. The gadget is constructed such that  $y \leq y'$ . Since the diametral segment of the orange piece is separating  $c_x$  and  $c_y$  from  $p$ , we then get  $x \cdot y \leq x \cdot y' \leq 1$ , where the latter inequality follows from the principle behind the gadget.  $\square$

*Proof of Lemma 6 for the seesaw.* Suppose that for a given solution to the ETR-INV formula  $\Phi$ , there exists a canonical placement of the previously introduced pieces  $\mathbf{p}_{i-1}$  that encodes that solution. The placement of the yellow and blue piece is then fixed. We place the pink piece so that it has edge-edge contact to the yellow piece. The orange piece is placed with the corner  $q$  coincident to the pivot point  $p$  on the container boundary. The boundary of the container has been constructed so that there is enough room to place the orange piece in this way.  $\square$

**Fingerprinting and almost-canonical placement.** The proof of Lemma 10 for the seesaw follows exactly as for the swap. We first fingerprint the pink and then the orange piece.

**Aligned placement.** Lemma 11 holds vacuously for the seesaw as there are no exiting variable pieces in this gadget.

**Edge inequalities.** The pieces of the seesaw induce no edges in the dependency graphs, so there are no edge inequalities to verify.

**The seesaw works.** In this paragraph we prove the part of Lemma 16 that the seesaw is responsible for, namely that in a given aligned  $g\mu$ -placement, the seesaw used for the variables  $x$  and  $y$  implies that  $\langle K_x \rangle \cdot \langle K_y \rangle \leq 1$ .

*Lemma 16 for the seesaw.* We first point out that the pink piece must be placed as in a canonical placement because it just fits in between the two vertical edges of the container. Now, since we consider an aligned  $g\mu$ -placement, the orange piece separates the pink and blue pieces from the pivot point  $p$  as in the simplified seesaw. Let  $p_x, p_y, p'_y$  be the yellow, blue, and pink piece, respectively. Although the pink piece is not a variable piece, its vertical placement corresponds to a value, as defined in Figure 46, and we denote as  $\langle p'_y \rangle$ . The value is defined so that when the blue and pink pieces have edge-edge contact, then  $\langle p_y \rangle = \langle p'_y \rangle$ , and otherwise  $\langle p_y \rangle < \langle p'_y \rangle$ . Since the diametral segment of the orange piece is separating  $c_x$  and  $c_y$  from  $p$ , we then get  $\langle p_x \rangle \cdot \langle p_y \rangle \leq \langle p_x \rangle \cdot \langle p'_y \rangle \leq 1$ , where the latter inequality follows from the principle behind the gadget.

We note that there are paths  $P_x$  and  $P_y$  in  $G_x$  and  $G_y$  attached to and directed away from the cycles  $K_x$  and  $K_y$ , and the vertices farthest away from the cycles are the yellow and blue pieces  $p_x$  and  $p_y$ . In particular  $\langle K_x \rangle \leq \langle p_x \rangle$  and  $\langle K_y \rangle \leq \langle p_y \rangle$ . Hence,  $\langle K_x \rangle \cdot \langle K_y \rangle \leq 1$   $\square$

**Valid placements are canonical.** In this paragraph, we show that the pieces of the seesaw have a canonical placement in every valid placement. We can assume that we already know that every valid placement is an aligned  $g\mu$ -placement (Lemma 8).

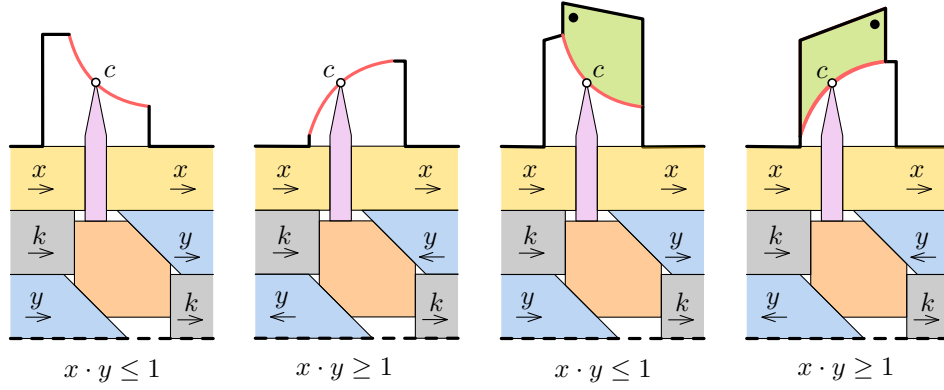
*Proof of Lemma 20 for the seesaw.* We already know from the proof of Lemma 16 for the seesaw that the pink piece is placed as in the canonical placements. We observe that for all almost-canonical placements of the orange piece, it separates the yellow and pink pieces from the pivot point  $p$  as required, since there are not other places in the gadget where it can fit. Hence, the placement is canonical.  $\square$

### 8.3 Gramophone

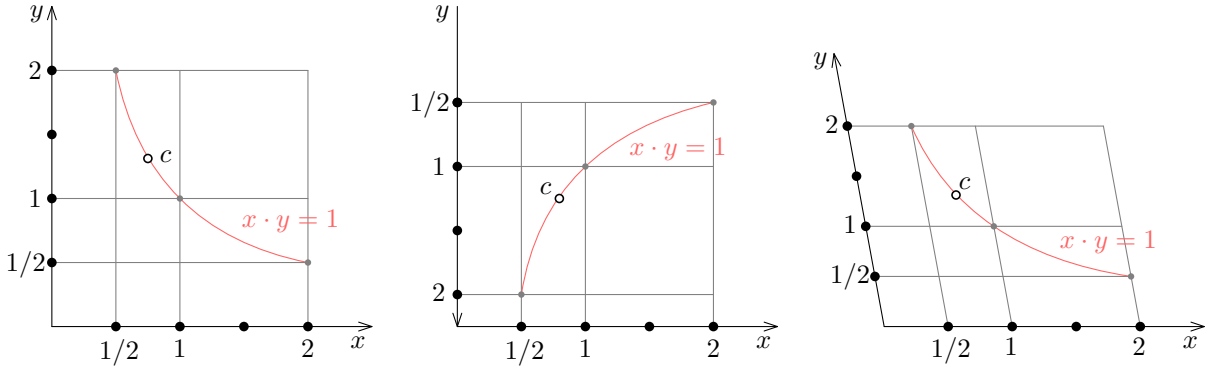
The idea behind the gramophone is to have a special pink piece which is translated horizontally by motions of one lane and translated vertically by motions of another lane; see Figure 48 for an illustration. Therefore, the placement of the piece in a sense encodes two variables at once. The pink piece has a corner  $c$  which is bounded from above by a curve, and that induces a dependency between the two lanes, translating to an inequality of the variables represented by the lanes. The name is chosen since motion of one lane makes the pink piece trace and “read” the curve and thus act as the stylus of a gramophone.

The inequality can be changed by choosing another curve bounding the corner  $c$ . We can therefore make gramophones for both inequalities  $x \cdot y \leq 1$  and  $x \cdot y \geq 1$ , which are called  $\leq$ -gramophones and  $\geq$ -gramophones, respectively. A gramophone either needs the boundary of the container or the boundary of one of its pieces to have a curved segment. If the boundary of the container is curved, we call it a *curved* gramophone and otherwise it is a *polygonal* gramophone. Therefore, there are in total four variants of the gramophone, but we will never use the polygonal  $\geq$ -gramophone. A gramophone for the inequality  $x \cdot y \leq 1$  can be realized with polygonal container boundary and convex curved pieces ( $\sqsupset$ ). However, in the gramophone for the inequality  $x \cdot y \geq 1$ , we need non-convex curved pieces if the container has to be polygonal.

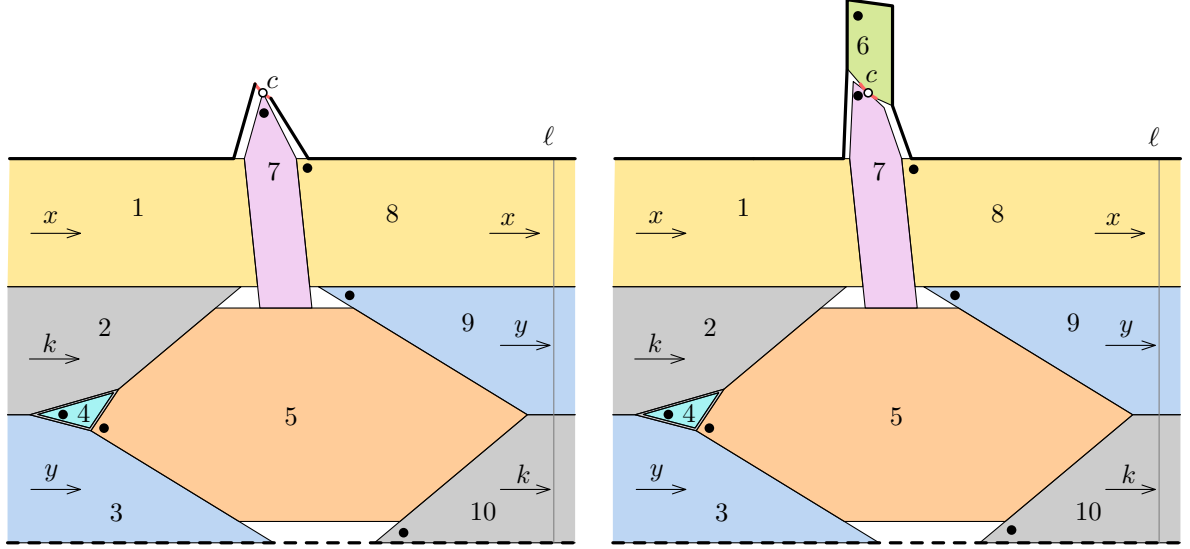
In the following, we will first show that indeed the gramophone allows us to encode the constraints that we intend. Then we describe in more detail how to turn the principle into a gadget that can be installed in our framework.



**Figure 48:** The four variants of the gramophone. The two to the left are *curved* gramophones whereas the two to the right are *polygonal* gramophones. Here, the gray pieces marked with  $k$  cannot move, so these can be thought of as representing a constant  $k$ . The purpose of these is to fix the horizontal placement of the orange piece such that horizontal motion of the blue pieces translates directly to vertical motion of the pink piece. In all cases the gramophone relies on translations only. For the resulting dependency between  $x$  and  $y$  to be non-linear, the curve restricting the corner  $c$  must be non-linear, requiring either the boundary of the container or some pieces to have curved parts. We will never use the right-most variant, the polygonal  $\geq$ -gramophone. For color codes, see Figure 50.



**Figure 49:** All three figures display the curve for the equation  $x \cdot y = 1$ . The drawings differ because of different  $y$ -axes. The middle figure corresponds to the case where the lane for the variable  $y$  is left-oriented. In the other cases, both lanes are right-oriented.



**Figure 50:** The actual gramophone, with curved container boundary (left) and with curved convex pieces (right). The solid boundary bounding the gadgets from above are part of the boundary of the container, whereas the dashed segment bounding the gadgets from below is on the boundary of a piece that has been added to the construction earlier. The gray pieces marked with  $k$  cannot move, so these can be thought of as representing a constant  $k$ . Color codes: 1 yellow, 2 gray, 3 blue, 4 turquoise, 5 orange, 6 green, 7 pink, 8 yellow, 9 blue, 10 gray.

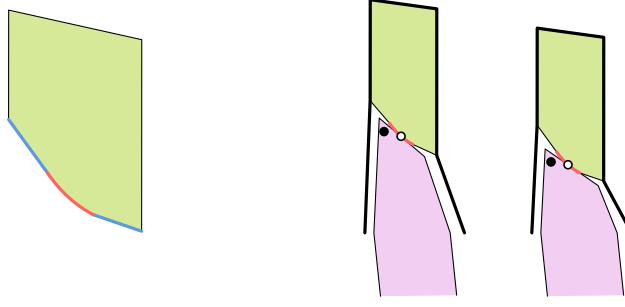
**Principle.** To understand why the gramophone gives the correct constraints, it helps to draw a coordinate system showing the correspondence between the position of the corner  $c$  and the variables  $x$  and  $y$  represented by the two lanes; see Figure 49. Notably, if the orientation of the blue piece (representing  $y$ ) is to the left, the  $y$ -axis flips upside down. To see this note that pushing the left blue piece to the right pushes the pink piece upwards and this corresponds to a linear decrease of  $y$ . The curve restricting the corner  $c$  from above is always the curve described by the equation  $x \cdot y = 1$  in the respective coordinate system. It then follows that gramophones can be made to encode both the constraint  $x \cdot y \leq 1$  and the constraint  $x \cdot y \geq 1$ .

**Actual gadget.** The actual design of the gramophone can be seen in Figure 50 and many details differ from the simplified drawing in Figure 48. We only go through the two variants of  $\leq$ -gramophones. The  $\geq$ -gramophone is similar, except for the curved part and the orientation of the blue pieces. In order to incorporate the gadget into the complete construction, we need to add some swaps and a constant lane, as we will explain below.

Note first that since the ranges  $I(x)$  and  $I(y)$  of the variables  $x$  and  $y$  are at most  $2\delta$ , the curved part needed is likewise of length  $O(\delta)$ , i.e., extremely short. We start with the curved gramophone (where the boundary of the container is allowed to have curved parts); see Figure 50 (left), and will later describe the version where the pieces but not the boundary can have curved parts. The gray, orange, blue and turquoise pieces form a swap. We refer to the details and correctness of the swap to Section 7.2. The gray pieces will have a fixed placement and can therefore be considered as pieces encoding a constant value. A lane for the constant will be started to the left of the gramophone and terminated to the right, which will be explained later.

Above the swap is the yellow lane and a pink piece. The pink piece has edge-edge contacts with the yellow and orange pieces. The top vertex of the pink piece is our special vertex  $c$  that is bounded from above from a curve. In the simplified description, the pink piece had a pair of parallel segments that were fixed at a vertical orientation by the yellow pieces. However, in





**Figure 51:** Fingerprinting the pink piece. By moving the green piece up and down, the fingerprinted corner of the pink piece can be continuously altered.

order to fingerprint the right yellow piece, we rotate the pink piece a bit clockwise (and adjust the edges of the yellow pieces accordingly) so that the angle of the corner where the right yellow piece is fingerprinted can be chosen freely. The gadget is bounded on the top by the container boundary and this part contains a tiny curved part, which corresponds to the curve  $x \cdot y = 1$ , marked red. However, because of the slanted orientation of the pink piece, the  $y$ -axis of the corner  $c$  is now likewise slanted as in Figure 49 (right).

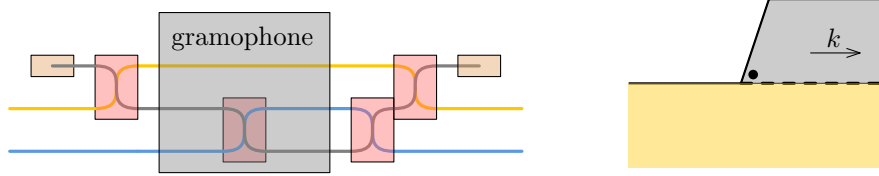
In the simplified construction, the angles were chosen so that horizontal motion of the blue pieces was translated to vertical motion of the orange piece with no scaling involved. In the actual gadget, since we want to fingerprint the right blue piece, we need to choose the slope of the edge-edge contact between the blue and orange pieces freely, and then a horizontal motion of the blue pieces is scaled when transformed to a vertical motion of the orange piece.

These two differences (slanted and scaled  $y$ -axis) result in a linear deformation of the red curve, as compared to the simplified situation. An example of such a deformation can be seen in Figure 49 (right). The curve will however still be contained in a hyperbola. Moving the red curve up and down (where up and down is defined by the transformed  $y$ -axis) makes it possible to freely choose the fingerprinted angle of the pink piece.

We are now going to describe the polygonal gramophone; see Figure 50 (right). In this version, we have an additional green piece which is the only piece that is curved. If we encode the constraint  $x \cdot y \leq 1$  then the green piece is convex. If we encode the constraint  $x \cdot y \geq 1$  the green piece will not be convex. Recall from Section 6.4 that for pieces with curved segments, it is needed that the curvature is bounded and that the curved segments have a straight line segment of length 1 as prefix and suffix. In Figure 51 (left), the red curve and the blue segments together form a curved segment that satisfies the requirements. The pink piece is changed accordingly: In this version of the gramophone, the pink piece has two more corners and the corner on the top left is fingerprinted. It is shown in Figure 51 how the angle of the fingerprinted corner can be changed freely by moving up and down the green piece.

**Installation of the gramophone.** Figure 52 (left) shows how to install the gramophone in the complete construction. We make a new lane representing a constant which is started just to the left of the gramophone and terminated just to the right. See Figure 52 (right) on how a constant lane can start and end. In addition to this, three swaps are needed to organize the lanes in the right way.

**Constant lane of gray pieces.** By inspecting the installation manual in Figure 52 (left), we observe that the gray lane consists of 5 pieces  $p_1, \dots, p_5$  in order from left to right, where pieces  $p_2$  and  $p_3$  are the left and right gray piece in the gramophone itself. We here argue that



**Figure 52:** Left: Installation manual for the gramophone. The gray lane consists of pieces with a fixed placement and can be interpreted as encoding a constant. This lane starts and ends just outside the gramophone. Right: The start of a constant lane consists of a single gray piece, which is fingerprinted at the left corner. The top of the gadget is the container boundary and we assume that the gadget is bounded from below by a yellow piece representing the variable  $x$ , which has been introduced to the construction earlier. The yellow piece is already known to be horizontally aligned, and it then follows that the gray is as well. The lane of the gray pieces is terminated in an analogous way.

these five pieces must have a fixed placement independently of the rest of the construction, so that they can indeed be considered as variable pieces encoding a constant. Let us define the placement of the first piece  $p_1$  shown in Figure 52 to encode the value  $\langle p_1 \rangle = 1$ . We then know that in every placement,  $1 \leq \langle p_1 \rangle$ , since the piece may slide to the right, but not to the left due to the container boundary. In a similar way as for the proof of the edge inequality in Lemma 13, we get that  $1 \leq \langle p_1 \rangle \leq \dots \leq \langle p_5 \rangle \leq 1$ , where the last inequality follows since  $p_5$  is bounded from the right by the container boundary. We then have  $\langle p_1 \rangle = \dots = \langle p_5 \rangle = 1$ .

**Canonical placements and solution preservation.** The variable pieces are the yellow and blue pieces. We define the canonical placements to be placements where the pieces have the edge-edge contacts as in Figure 50 and the turquoise piece is enclosed by the left gray and blue pieces and the orange piece. If the green piece is present, it should have edge-edge contacts with the container boundary as shown.

*Proof of Lemma 7 for the gramophone.* Suppose that in all canonical placements of the previously introduced pieces  $\mathbf{p}_{i-1}$ , variables are encoded consistently and in a way that satisfies the respective addition and inversion inequalities. In a canonical placement of the pieces in the gramophone, the vertical distance between the two yellow pieces is always the same, and hence they encode the value of the variable  $x$  consistently by construction. The same holds for the blue pieces. Hence, the pieces  $\mathbf{p}_i$  also encode variables consistently.

We need to verify that in any canonical placement, the respective inequality,  $x \cdot y \leq 1$  or  $x \cdot y \geq 1$ , is satisfied. We consider the case  $x \cdot y \leq 1$ , since the other is analogous. In the general case, the corner  $c$  is below the curved part (of the boundary of container or the green piece). We can then slide the blue pieces to the right such that the pink piece goes up until  $c$  hits the curve, and this will only make the product  $x \cdot y$  larger. The situation where this contact is made is exactly when  $x \cdot y = 1$  by construction of the curve. Therefore, we initially had the situation  $x \cdot y \leq 1$ .  $\square$

*Proof of Lemma 6 for the gramophone.* Suppose that for a given solution to the ETR-INV formula  $\Phi$ , there exists a canonical placement of the previously introduced pieces  $\mathbf{p}_{i-1}$  that encodes that solution. The placement of the left yellow, gray, and blue piece is then fixed. It is now clear from the construction that the remaining pieces can be placed, since the inequality of the gramophone is satisfied by the solution to  $\Phi$ .  $\square$

**Fingerprinting and almost-canonical placement.** The proof of Lemma 10 for the gramophone follows exactly as for the anchor. We fingerprint the pieces in the order shown in Figure 50 used for color codes.

**Aligned placement.**

*Proof of Lemma 11 for the gramophone.* From the alignment line  $\ell$ , we get that the right yellow, right blue, and right gray pieces are correctly aligned. By arguments similar as for the swap, we get that the pieces encode variables in the correct ranges, i.e., that the placement must be an aligned  $i\mu$ -placement.  $\square$

**Edge inequalities.** We have an edge from the left to the right yellow piece and from the left to the right blue piece. The edge inequalities (Lemma 13) follow in a similar way as for the split (yellow) and swap (blue).

**The gramophone works.** In this paragraph we prove the part of Lemma 16 that the gramophone is responsible for, namely that in a given aligned  $g\mu$ -placement, a  $\leq$ -gramophone used for the variables  $x$  and  $y$  implies that  $\langle K_x \rangle \cdot \langle K_y \rangle \leq 1$  while a  $\geq$ -gramophone implies that  $\langle K_x \rangle \cdot \langle K_y \rangle \geq 1$ . We show the statement for the  $\leq$ -gramophone; the proof for the  $\geq$ -gramophone is analogous.

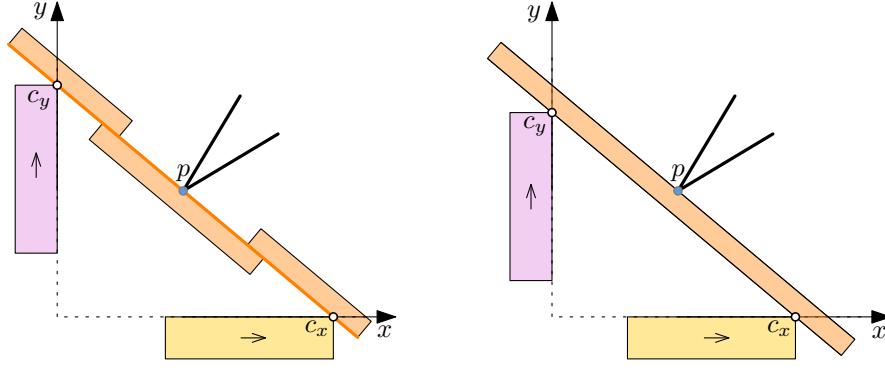
*Proof of Lemma 16 for the  $\leq$ -gramophone.* The yellow pieces are part of the cycle  $K_x$ . Since they encode values consistently by Lemma 14, the rotation of the pink piece is fixed and it has edge-edge contacts with the yellow pieces. Likewise, the blue pieces are part of  $K_y$ , so they also encode the same value of  $y$ . Since the gray pieces encode the same constant, we now get that the orange piece has edge-edge contacts to all blue and gray pieces. We can slide the pink piece down until it gets edge-edge contact to the orange piece. We now consider sliding the blue pieces to the right. This will make the pink piece slide up, and we stop when the corner  $c$  hits the curve bounding it from above. In this situation, we have  $\langle K_x \rangle \cdot \langle K_y \rangle = 1$  by construction. Since we have slid the blue pieces to the right, we started with a placement where  $\langle K_x \rangle \cdot \langle K_y \rangle \leq 1$ .  $\square$

**Valid placements are canonical.** In this paragraph, we show that the pieces of the gramophone have a canonical placement in every valid placement. We can assume that we already know soundness as stated in Lemma 7 and that every valid placement is an aligned  $g\mu$ -placement (Lemma 8). Again, we give the proof for the  $\leq$ -gramophone as the proof for the  $\geq$ -gramophone is analogous.

*Proof of Lemma 20 for the  $\leq$ -gramophone.* We already know from the proof of Lemma 16 for the  $\leq$ -gramophone that we can edge-edge contacts between the pink and the yellow pieces and between the orange and the blue and gray pieces, so it only remains to prove that we have an edge-edge contact between the pink and the orange piece. This follows since  $\langle K_x \rangle \cdot \langle K_y \rangle = 1$ , and we are done.  $\square$

## 8.4 Concluding remarks on inversion

It may be tempting to believe that using the inequality  $x \cdot y \geq 1$  can be used in some indirect way to enforce  $x \cdot y \leq 1$  as well. However, note that  $S_{\geq} := \{(x, y) \in \mathbb{R}^2 : x \cdot y \geq 1, x, y > 0\}$  is convex, whereas  $S_{\leq} := \{(x, y) \in \mathbb{R}^2 : x \cdot y \leq 1, x, y > 0\}$  is not convex. This principle difference indicates the difficulty of the above approach.



**Figure 53:** Left: The seesaw (simplified), using a non-convex rotating orange piece. Right: An alternative to the seesaw using a rotating orange rectangle, enforcing a constraint of the form  $y \leq f(x)$  for a convex function  $f$  depending on the thickness of the rectangle and the coordinates of the pivot point  $p$ .

Recall that the seesaw enforces the inequality  $y \leq 1/x$  using polygonal container and pieces and rotation. However, the rotating piece has to be non-convex in order for the pivot point  $p$  to be on line with the segments pushed by the corners  $c_x, c_y$ . If instead of this non-convex rotating piece, we use a skinny rectangle, we get another constraint of the form  $y \leq f(x)$ , for a more complicated convex function  $f$ ; see Figure 53. We have not been able to use such a constraint to prove  $\exists\mathbb{R}$ -hardness, which leads us to the following paragraph.

**Gadget wanted!** Most interesting to us is whether there exists a gadget encoding  $x \cdot y \leq 1$ , using a polygonal container, convex polygonal pieces, and rotation. Such a gadget would imply  $\exists\mathbb{R}$ -completeness of  $\mathbf{Pack}(\square \rightarrow \square, \circlearrowleft +)$  using the reduction from Section 9, and therefore it would imply  $\exists\mathbb{R}$ -completeness of all the problems with rotation allowed in Table 1. Furthermore, the seesaw would become obsolete. Despite much effort, we could not find such a gadget.

## 9 Square container

Recall from Lemma 18 that when we reduce to problems where the container is a (curved) polygon, the resulting container is 4-monotone (for the definition of 4-monotone, see Definition 17). Let  $\mathcal{I}_1$  be an instance of a packing problem where the container  $C := C(\mathcal{I}_1)$  is a 4-monotone polygon. We show how to make a reduction from  $\mathbf{Pack}(\mathcal{P} \rightarrow \triangleright, \mathcal{M})$  to  $\mathbf{Pack}(\mathcal{P} \rightarrow \square, \mathcal{M})$ . The reduction also works if the container  $C$  is a 4-monotone *curved* polygon. In that case, some of the orange pieces introduced below will be curved pieces, because they will inherit part of the boundary of  $C$ . Therefore, we reduce from  $\mathbf{Pack}(\square \rightarrow \mathbb{L}, \mathcal{M})$  to  $\mathbf{Pack}(\mathbb{L} \rightarrow \square, \mathcal{M})$  in that case.

We show that the instance  $\mathcal{I}_1$  can be reduced to an instance  $\mathcal{I}_2$  where the container is a square  $S$  with corners  $b_1 b_2 b_3 b_4$ . To this end, we introduce some auxiliary pieces that can essentially be placed in only one way in  $S$ . We call these new pieces the *exterior* pieces, whereas we call the pieces of  $\mathcal{I}_1$  the *inner* pieces. The empty space left by the exterior pieces is the 4-monotone polygon  $C$  which act as the container  $C$  of  $\mathcal{I}_1$ . We scale down the container  $C$  and the inner pieces so that  $C$  fits in a  $\varepsilon \times \varepsilon$  square in the middle of  $S$ , for a small value  $\varepsilon = \Theta(1)$  to be defined shortly. Since the original container  $C$  has size  $O(N^4) \times O(N)$ , we scale it down by a factor of  $O(N^4)$ , where  $N$  is the number of pieces.

An example of the construction can be seen in Figure 54, where only the exterior pieces are shown. Our construction is parameterized by a number  $\varepsilon > 0$ , and the container  $S$  is the square  $[0, 1 + \varepsilon] \times [0, 1 + \varepsilon]$ . The blue pieces  $B_1, B_2, B_3, B_4$  are independent of  $\varepsilon$ , but the green, turquoise, and orange pieces depend on  $\varepsilon$ . Only the exterior pieces are shown, but the full instance  $\mathcal{I}_2$  does also include the inner pieces, which are intended to be packed in  $C$ . Each green piece  $G_i$  has a pair of corners  $c_i, d_i$  of interior angle  $\alpha_i$  such that  $\alpha_i \neq \alpha_j$  for  $i \neq j$ . In reality, these angles  $\alpha_i$  are only slightly less than  $\pi/2$ , so that all the eight segments from a point  $c_i$  or  $d_i$  to the closest corner  $b_j$  are almost equally large. The angles  $\alpha_i$  are independent of  $\varepsilon$  and the instance  $\mathcal{I}_1$ .

Each orange piece is a trapezoid, and edges of the orange pieces form the boundary of  $C$ . At the opposite end of the pieces, they meet the green or turquoise pieces. To make sure that they are placed in the right order, they have unique angles so that fingerprinting can be used to argue about their placement. This will be explained in more detail in the end of this section.

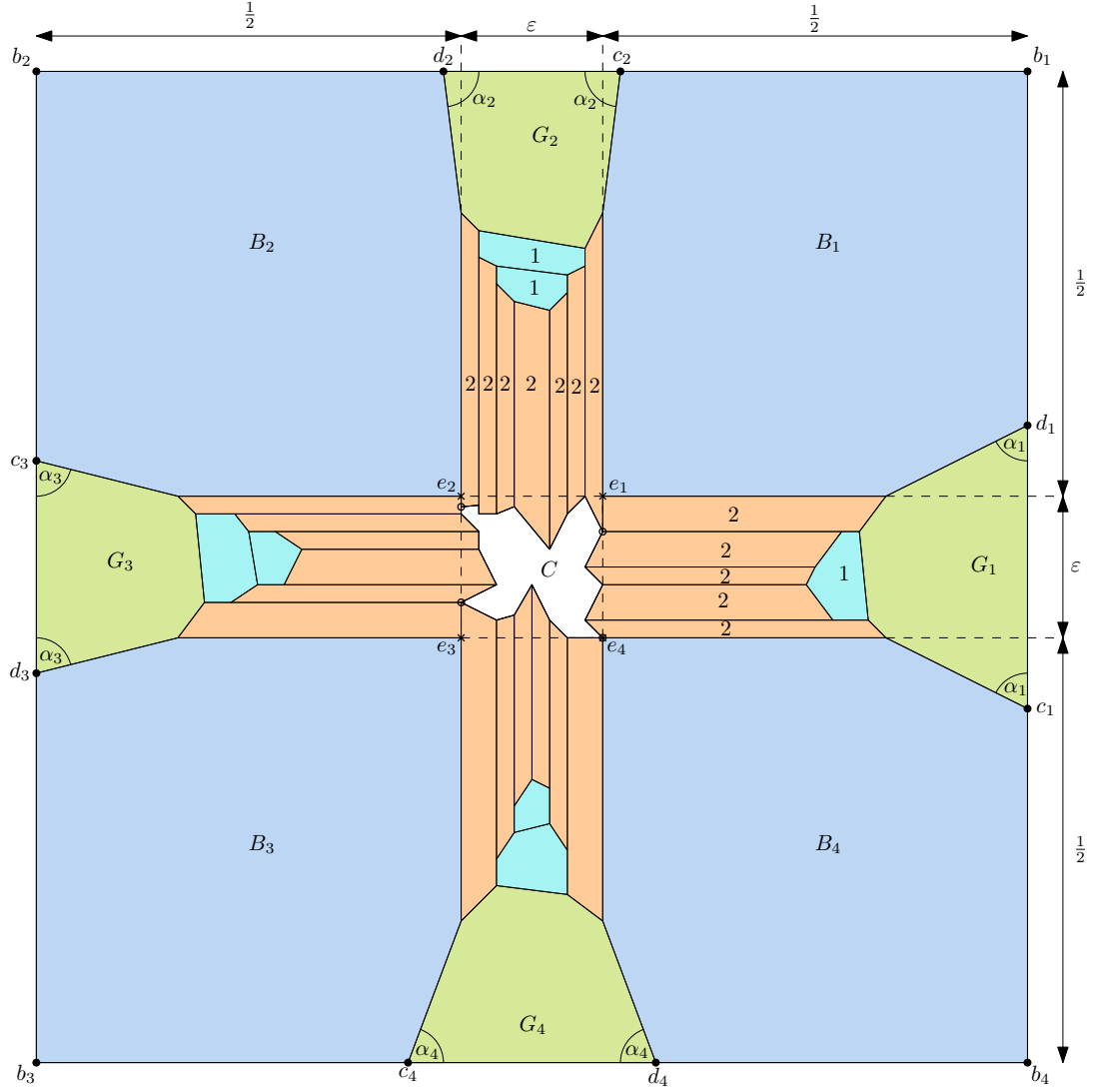
We denote the placement of the exterior pieces shown in Figure 54 to be *canonical*. We also define the placements we get from the figure by sliding the orange and turquoise pieces towards  $C$  to be *canonical*. We aim at proving the following lemma.

**Lemma 56.** *If  $\varepsilon$  is sufficiently small, the following holds. For all valid placement of the pieces in  $\mathcal{I}_2$ , the exterior pieces have a canonical placement.*

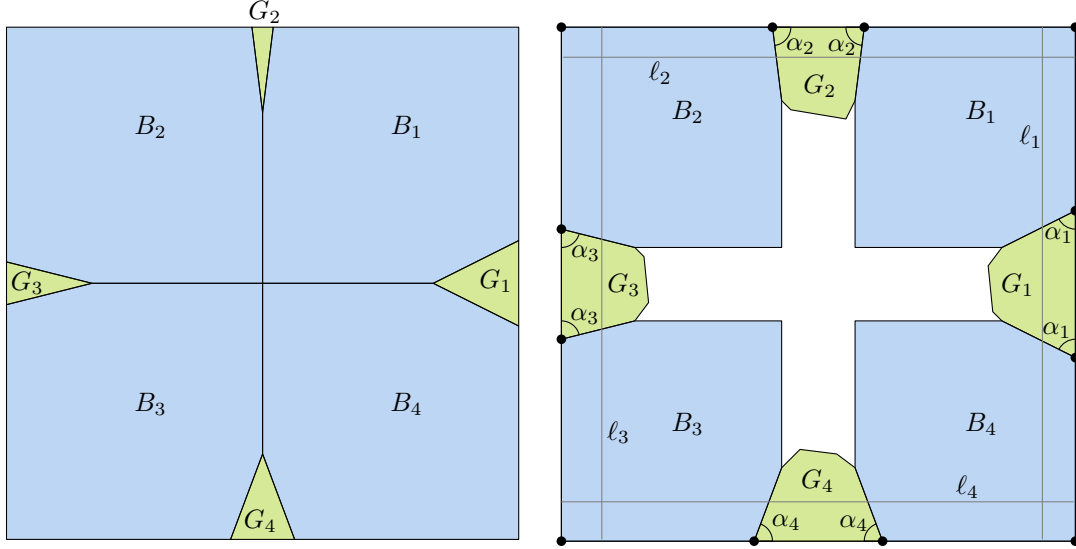
It follows from the lemma that  $\mathcal{I}_1$  has a solution if and only if  $\mathcal{I}_2$  has one, so that the problems are equivalent under polynomial time reductions.

The first step in proving Lemma 56 is to prove that the blue and green pieces, up to a rotation, can only be placed in the canonical way, i.e., even when we disregard the turquoise and orange pieces and the inner pieces. To prove this, we consider the situation when  $\varepsilon$  gets very small, as shown in Figure 55 (left), so that the blue and green pieces cover almost all of  $C$ . Then all the turquoise and orange pieces are skinny, and the 4-monotone polygon  $C$  is very small. When changing  $\varepsilon$ , we keep all angles constant and the blue pieces constant, and  $C$  is scaled appropriately so that it fits in the central square of size  $\varepsilon \times \varepsilon$  (this square is drawn with dashed segments in Figure 54).

**Lemma 57.** *If  $\varepsilon$  is sufficiently small, the canonical placement is the only way to place the blue and green pieces into  $S$ , i.e., even when the turquoise and orange pieces and the inner pieces do*



**Figure 54:** An example of the instance we get from the reduction using a square container for a given 4-monotone polygon  $C$ . In reality, the angles  $\alpha_i$  are just slightly less than  $\pi/2$ , and all the eight segments from a point  $c_i$  or  $d_i$  to the closest corner  $b_j$  have length almost  $1/2$ . Color codes:  $B_1, \dots, B_4$  are blue,  $G_1, \dots, G_4$  are green, 1 is turquoise, 2 is orange.



**Figure 55:** Left: The situation from Figure 54 in the limit  $\varepsilon = 0$ . Right: The canonical placement of the green and blue pieces. For some sufficiently small  $\varepsilon$  must  $Q_m$  be the shown placement. We have four alignment segments  $\ell_1, \ell_2, \ell_3, \ell_4$ .

*not have to be placed. (When rotations are allowed, the three rotations of this packing by angles  $\pi/2, \pi, 3\pi/2$  are also possible.)*

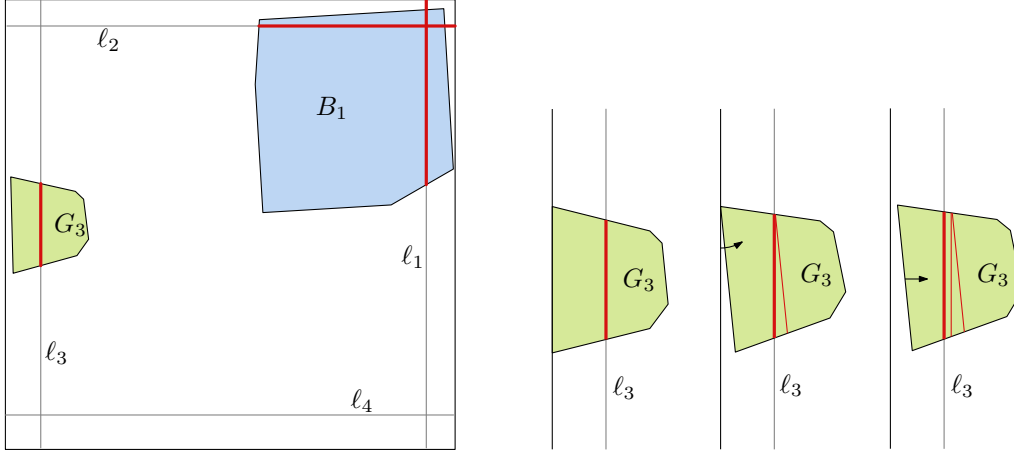
*Proof.* Suppose for the purpose of contradiction that for arbitrarily small  $\varepsilon > 0$ , there are other ways in which the eight pieces can be placed. For every  $m \in \mathbb{N}$ , let  $Q_m$  be such a placement for some  $\varepsilon \in (0, 1/m)$ . Recall that the blue pieces are independent of  $\varepsilon$ , and note that as  $m \rightarrow \infty$ , the shape of the green pieces converge to the pieces shown in Figure 55. Note that the pieces are compact sets in the plane, and recall that the Hausdorff distance turns the set of non-empty compact sets into a compact metric space in its own right. By passing to a subsequence, we may therefore assume that for each piece  $p$ , the placement of  $p$  according to  $Q_m$  is likewise converging with respect to the Hausdorff distance.

We are going to apply the Single Fingerprint Lemma 45 to the corner  $b_1$  of  $G_1$ , and we want to prove that in the limit placement, a right corner of a blue piece coincides with  $b_1$ . For the following consider the notation of Lemma 45. We define the triangle  $T$  so that  $x \in b_1b_4$ ,  $y = b_1$ , and  $z \in b_1b_2$ , and we set  $u := 0$ . Choose  $\sigma$  so small that the eight blue and green pieces have the unique angle property. We get that a blue piece must be placed such that one of its right corners  $v$  is within distance  $O(\sqrt{\mu/\sigma})$  from  $b_1$ . Now, as  $m \rightarrow \infty$ ,  $\mu$  gets arbitrarily small, and therefore we get that  $v$  coincides with  $b_1$  in the limit.

We likewise get that corners with right angles of the other blue segments are placed at the other corners  $b_2, b_3, b_4$  of  $S$ .

Conceivably, the blue pieces can be placed incorrectly in two ways: (i) their cyclic order around the boundary of  $S$  can be different from  $B_1, B_2, B_3, B_4$  and (ii) one of the right corners  $e_i$  which is supposed to be placed in the interior of  $S$  can be placed at a corner of  $S$ . Due to the difference in the angles  $\alpha_1, \dots, \alpha_4$ , it is clear that in each of these cases, the green pieces cannot be placed. Hence, the pieces must be placed as shown in Figure 55 (left) in the limit.

We conclude that by choosing  $m$  sufficiently large (and thus  $\varepsilon$  sufficiently small), the difference between each piece of  $Q_m$  and the packing of Figure 55 (left) can be made arbitrarily small. We now prove that if the difference is sufficiently small, the placement  $Q_m$  must be the canonical placement. Intuitively, this means that the canonical placement is “locked” in



**Figure 56:** Left: The red segments show the parts of the alignment segments that is occupied by the pieces  $B_1$  and  $G_3$ . Right: The fat red segments show the parts of the alignment segment  $\ell_3$  that is occupied by the piece  $G_3$  in three different situations. The thin red segments are the parts occupied in the preceding situations. First is shown the canonical situation from Figure 55 (right). The middle situation shows that as  $G_3$  is rotated, it occupies more. The last situation shows that when  $G_3$  is translated, it occupies even more.

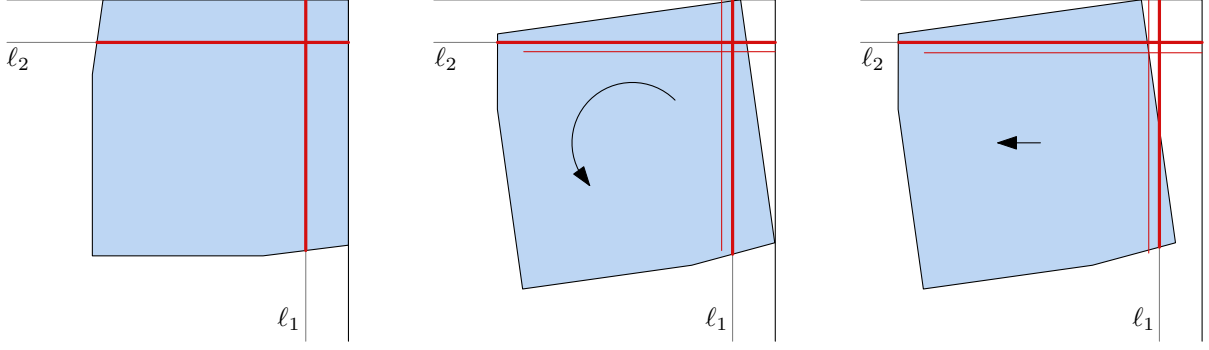
the sense that it is not possible to move the pieces just a little bit and obtain another valid placement.

In order to argue about the precise placement, we make an alignment argument using four alignment segments  $\ell_1, \ell_2, \ell_3, \ell_4$  simultaneously. For each edge of  $S$ , we have an alignment segment  $\ell_i$  parallel to and close to the edge, as shown in Figure 55 (right). For each of the eight blue and green pieces  $p$ , we measure how much  $p$  occupies of each alignment segment, and we take the sum of all these measures and show that it is strictly minimum in the canonical placement. In the placement, the segments are fully covered by the pieces, which means that there cannot be any other placement since they would occupy more of the segments than what is available.

Note that as we consider a placement that is close to the canonical placement, we get that the blue piece  $B_1$  only intersects the segments  $\ell_1$  and  $\ell_2$ , and the other blue pieces likewise only intersect two segments each. Each green piece  $G_i$  only intersects  $\ell_i$ . We now define the occupied parts of the alignment segments as follows, see Figure 56 for an illustration. Each green piece  $G_i$  occupies the part  $G_i \cap \ell_i$  of the segment  $\ell_i$  and nothing of the other segments. The piece blue piece  $B_1$  occupies the part of  $\ell_1$  from the upper endpoint of  $\ell_1$  to the lowest point in  $B_1 \cap \ell_1$ . Similarly,  $B_1$  occupies the part of  $\ell_2$  from the right endpoint to the leftmost point in  $B_1 \cap \ell_2$ . Each of the other pieces  $B_2, B_3, B_4$  occupies parts of the two segments it intersects, defined in the analogous way. It follows that the parts of a segment  $\ell_i$  occupied by two different pieces are interior-disjoint: This is trivial for the parts covered by pieces, but a blue piece  $B_j$  can also occupy parts that it does not cover close to the boundary of  $S$ . However, these parts of the alignment segments are close to the corner  $b_j$ , and the other pieces are too fat to cover such a part of a segment without colliding with  $B_j$ , since the displacement of  $B_j$  can be made arbitrarily small.

Let  $L$  be the sum of lengths of the occupied parts. Since the occupied parts are interior-disjoint, we get that  $L$  is at most  $4 \cdot (1 + \varepsilon)$ , i.e., the sum of lengths of  $\ell_1, \dots, \ell_4$ . We now show that  $L$  has a strict local minimum in the canonical placement. To this end, we observe that starting with the canonical placement, any small movement of one of the pieces makes





**Figure 57:** The fat red segments show the parts of the alignment segments  $\ell_1$  and  $\ell_2$  that is occupied by a piece in three different situations. The thin red segments are the parts occupied in the preceding situation.

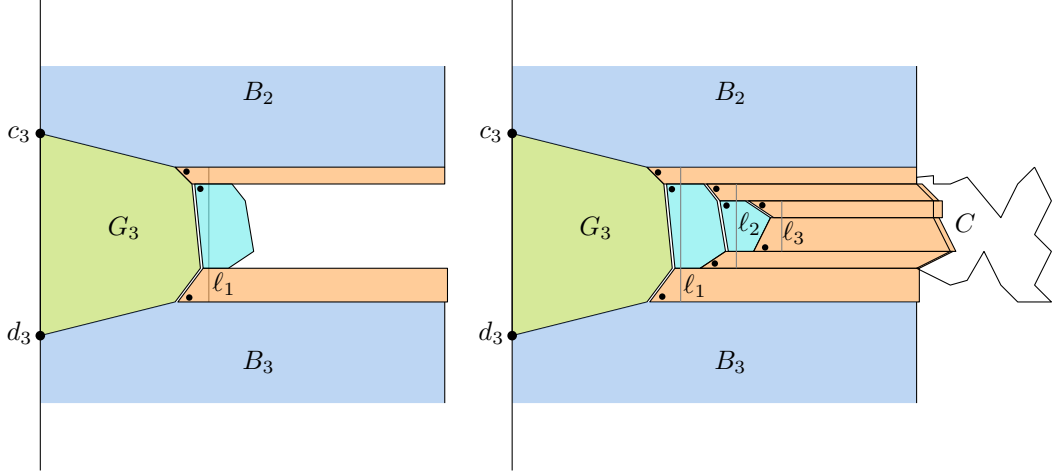
$L$  increase. This is seen for a green piece  $G_3$  in Figure 56 (right). For a blue piece, consider the blue piece in Figure 58. First is shown the canonical placement. The middle figure shows a situation where the piece is rotated slightly while keeping it as far up and to the right as possible. We see that it occupies more of both alignment segments. The last situation shows that when the piece is translated to the left, the part occupied of  $\ell_2$  increases as much as the translation, while the part occupied of  $\ell_1$  slightly decreases (*slightly* since the piece has been only slightly rotated and the angles  $\alpha_i$  are close to  $\pi/2$ ). In total, the piece occupies more of  $\ell_1$  and  $\ell_2$ . The occupied amount likewise increases when the piece is translated down. It then follows that moving the piece from the canonical placement by any small movement (rotation and translation combined) will strictly increase the occupied amount of the alignment segments.

To sum up, choosing  $m$  sufficiently big, the packing  $Q_m$  can be made arbitrarily close to the canonical packing, but this implies that it must be identical to the packing, as it would otherwise occupy more of the alignment segments  $\ell_1, \dots, \ell_4$  than what is possible. This contradicts that every  $Q_m$  is different from the canonical placement. Hence, when  $\varepsilon$  is small enough, the eight blue and green pieces can only be placed in the canonical way.  $\square$

We now argue about the fixed placement of the orange and turquoise pieces. The use of fingerprinting and aligning used here is similar as how we argued about the gadgets. We consider the piece  $G_3$  as an example, and refer to Figure 58 for an illustration of the process. We fix the pieces in layers, so that there are a constant number of pieces in each layer. We first fingerprint the pieces touching  $G_3$  in the canonical packing. We then align them. This may leave a bit of empty space to the right of  $G_3$  and to the left of the orange and turquoise pieces, but that is allowed in the canonical placements, and the empty space will be too small for any piece to fit there. We then fingerprint the pieces touching the first turquoise piece, and repeat. This leads to a canonical placement of the exterior pieces, proving Lemma 56.

Recall that the (unscaled) instance  $\mathcal{I}_1$  has  $\mu = \Theta(n^{-296})$  and size  $O(N^4) \times O(N)$ . We scale it down to be contained in a square of size  $\varepsilon \times \varepsilon$ , where  $\varepsilon = \Theta(1)$ , so we get that the slack of our created instance  $\mathcal{I}_2$  has  $\mu = \Theta(N^{-304})$ , which is polynomial. The reason that we use the turquoise pieces is that if instead all orange pieces were adjacent to the green pieces, we would need to fingerprint a superconstant number of pieces at once, and then we would need  $\mu$  to be smaller than polynomial, as mentioned in Section 2.

As mentioned above, the empty space to the left of the orange and turquoise pieces sticking out from  $G_3$  is too small that any pieces can fit there. We can therefore without loss of generality slide the pieces to the left so that they create all the edge-edge contacts shown in Figure 54. Similarly, those sticking out from  $G_4$  can be pushed down, etc. After pushing all the orange and



**Figure 58:** Left: Fixing the alignment of the first layer of pieces. The three pieces are fingerprinted and then aligned. The empty space between  $G_3$  and the three pieces is so small that no piece can fit in there. Right: The three layers which together fix all the orange and turquoise pieces. Note that the empty space between the exterior pieces leaves less room in  $C$  for the inner pieces (refer to Figure 54).

turquoise pieces towards their green piece, the empty area left for the inner pieces is exactly the container  $C$ . We conclude that there is a solution to the created instance  $\mathcal{I}_2$  with a square container if and only if there is a solution to the given instance  $\mathcal{I}_1$ . To sum up, we have proven the following theorem.

**Theorem 19.** *The problems  $\text{Pack}(\mathcal{P} \rightarrow \square, \mathcal{M})$  are  $\exists\mathbb{R}$ -hard, where*

$$(\mathcal{P}, \mathcal{M}) \in \{(\mathbb{L}, \odot +), (\mathbb{D}, \odot +), (\mathbb{L}, +)\}.$$

The following definition will be important for the proof of Lemma 20, which will be used in Section 10 about universality-type theorems. We say that a placement of all pieces (exterior and inner) is *canonical* if the inner pieces are placed in  $C$  in a canonical way and the exterior pieces are also placed in a canonical way. From the above discussion, we get a proof of Lemma 20, namely that all valid placements are canonical.

## 10 Universality-type theorems

**Algebraic universality.** Here we state and prove a form of algebraic universality of the packing problems. The proofs given rely on a strengthened solution preservation lemma. See Lemma 6 for comparison. Recall that  $n$  denotes the number of variables in our RANGE-ETR-INV instance  $\mathcal{I}$  and  $N$  denotes the number of pieces as the output of our reduction.

**Lemma 58** (Algebraic Solution Preservation). *Let  $(\mathbf{p}, C)$  be a packing instance that results from the reduction described in Theorem 4 from a RANGE-ETR-INV instance  $\mathcal{I} = [\Phi, \delta, (I(x_1), \dots, I(x_n))]$ . Let  $\mathbb{F} \subset \mathbb{R}$  be an algebraic field extension of  $\mathbb{Q}$  and  $x \in V(\Phi) \cap \mathbb{F}^n$ . Then there exists a canonical motion  $\mathbf{m}_x \in \mathbb{F}^{6N}$  of all the pieces  $\mathbf{p}$ .*

*Proof.* By applying Lemma 6 inductively there is a canonical placement of all the pieces  $\mathbf{p}$  where the variable pieces encode  $x \in V(\Phi)$  consistently.

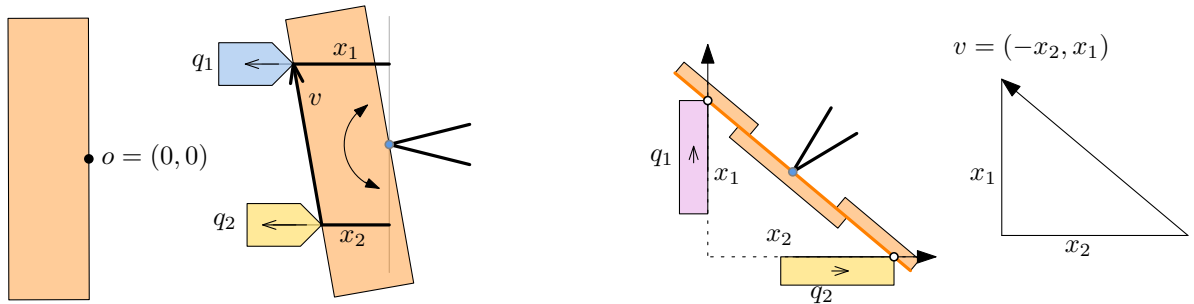
For the packing versions with a square container, we can place all exterior pieces in the way as described in Section 9. All of those placements can be described by rational motions  $m \in \mathbb{Q}^6$ . For the remainder of this proof, we focus only on interior pieces.

To be more specific, for every variable piece  $p$ , we have  $\langle p \rangle \in \mathbb{F}$ , and therefore also  $m \in \mathbb{F}^6$ , where  $m$  is the motion of  $p$ . (The piece is not rotated and only translated.) We need to argue that the placement of pieces that are not variable pieces can also be done such that their motion is in the field  $\mathbb{F}$ . To this end, we consider five types of pieces:

- fixed pieces,
- pieces whose placement is defined by two non-parallel edge-edge contacts,
- pieces that have wiggle room in two directions (so-called rattlers),
- pieces that can slide in one direction,
- pieces that can rotate.

First, pieces with a fixed position are only the turquoise piece in the teeter-totter and the gray pieces and the green piece in the gramophone. All of their placements can actually be described by a rational motion  $m \in \mathbb{Q}^6$ .

Second, we consider pieces  $p$  that have edge-edge contacts with two other pieces or one piece and the container boundary. Most of these pieces have edge-edge contacts with two variable pieces or a variable piece and the boundary of the container, and then their motion is clearly



**Figure 59:** Left: The rotation of the orange piece in the teeter-totter. Right: The rotation of the orange piece in the seesaw.

in  $\mathbb{F}$ . The exception is the orange piece in the adder, which has an edge-edge contact to two of the former kind, so that motion is also in  $\mathbb{F}$ .

Third, we consider a piece that has some wiggle room in two directions, which is only the turquoise piece in the swap and the gramophone. We are actually in the comfortable situation that this piece always has a valid placement with rational coordinates.

Fourth, we consider pieces that can slide. One such piece that can slide is the orange piece in the teeter-totter. As this piece can also rotate, we treat it in the next paragraph.

Fifth, we consider pieces that can rotate. These are the orange pieces in the teeter-totter and the seesaw. Those pieces are in corner-edge contact with two variable pieces and those two variable pieces  $q_1, q_2$  are defining the rotation  $M$  of the orange piece  $p$ .

We deal first with the orange piece in the teeter-totter. Recall that there is a special point  $o$  on the right edge that we intend to coincide with the pivot point in the canonical placements. When we construct the piece, we make sure that  $o$  is in the origin. We first describe a rotation  $M$  and argue that it can be realized with entries in  $\mathbb{F}$ . Note that this rotation matrix maps  $o$  to itself, even after a normalization. Then we apply the translation that takes the origin to the pivot point. As this pivot point is rational, so is the translation.

Let us denote with  $x_1 := \langle q_1 \rangle \in \mathbb{F}$  and  $x_2 := \langle q_2 \rangle \in \mathbb{F}$  the values encoded by the pieces that touch the orange piece. We show that if  $x_1, x_2 \in \mathbb{F}$  then the rotation can also be described by a matrix  $M$  with entries in  $\mathbb{F}$ . Consider Figure 59 (left) for the following description. We first note that the motion  $m_1, m_2$  for  $q_1, q_2$  are in  $\mathbb{F}$  if and only if the values  $x_1, x_2$  that they represent are in  $\mathbb{F}$ . Define  $v_1 := x_1 - x_2$ ,  $v_2 := 2$ , and the vector  $v := (v_1, v_2) \in \mathbb{F}^2$ . We now observe that the rotation of the orange piece can be described by the matrix

$$M := \begin{pmatrix} v_1 & -v_2 \\ v_2 & v_1 \end{pmatrix}.$$

This matrix is a non-normalized rotation matrix with entries in  $\mathbb{F}$ .

We now consider the orange piece of the seesaw. Let us denote by  $x_1 := \langle q_1 \rangle \in \mathbb{F}$  and  $x_2 := \langle q_2 \rangle \in \mathbb{F}$  the values encoded by the pieces that touch the orange piece. Consider Figure 59 (right) for the definition of the vector  $v := (-x_2, x_1)$ . We observe that the rotation of the orange piece in the seesaw can be described by the matrix

$$M := \begin{pmatrix} v_1 & -v_2 \\ v_2 & v_1 \end{pmatrix}.$$

This matrix also has entries in  $\mathbb{F}$ . □

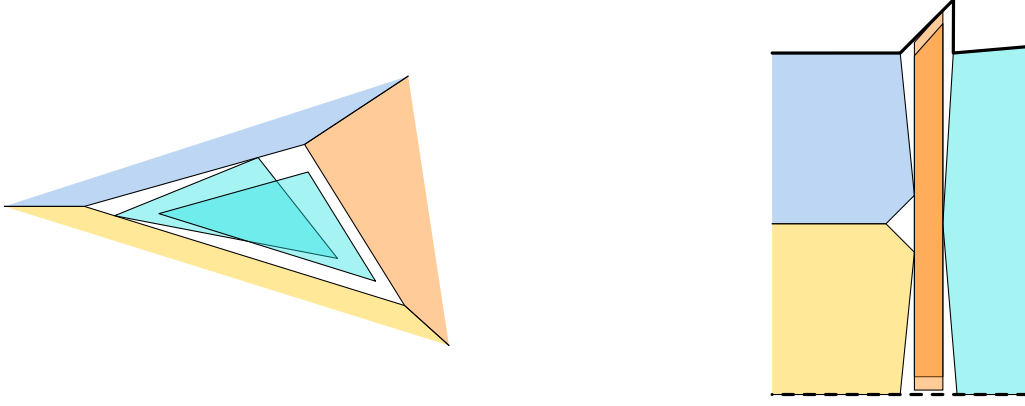
**Theorem 21.** *Let  $P$  be one of the packing problems indicated as  $\exists\mathbb{R}$ -complete in Table 1. Let  $\mathbb{F}_1, \mathbb{F}_2$  be algebraic field extensions of  $\mathbb{Q}$  such that  $\mathbb{Q} \subseteq \mathbb{F}_1 \subsetneq \mathbb{F}_2 \subset \mathbb{R}$ . Then there exists an instance  $(\mathbf{p}, C)$  of  $P$  that has a solution in  $\mathbb{F}_2$ , but none in  $\mathbb{F}_1$ .*

*Proof.* Let  $p \in \mathbb{Z}[x]$  be a univariate polynomial and  $[a, b]$  be an interval such that  $\{t : p(t) = 0, t \in [a, b]\} \cap \mathbb{F}_2 \neq \emptyset$ , but  $\{t \in [a, b] : p(t) = 0\} \cap \mathbb{F}_1 = \emptyset$ . We construct the ETR formula  $\Psi(x)$  as  $p(x) = 0 \wedge a \leq x \wedge x \leq b$ .

Then according to Theorem 29 there is an instance  $\mathcal{I}$  of RANGE-ETR-INV with ETR-INV formula  $\Phi$  such that  $V(\Phi)$  is rationally equivalent to  $V(\Psi)$ . Thus  $V(\Phi) \cap \mathbb{F}_1^n = \emptyset$  and  $V(\Phi) \cap \mathbb{F}_2^n \neq \emptyset$ , where  $n$  is the number of variables of  $\Phi$ .

Let  $(\mathbf{p}, C)$  be a packing instance that results from the reduction described in Theorem 4. Due to Lemma 58, we know that there is a canonical motion  $\mathbf{m}_2 \in \mathbb{F}_2^{6N}$  of all the pieces.

For the other direction, suppose for the purpose of contradiction that there is a valid motion  $\mathbf{m}_1 \in \mathbb{F}_1^{6N}$ . Due to Lemma 20, it holds that  $\mathbf{m}_1$  is canonical. By Lemma 7, the variable pieces encode a solution to  $\Phi$  which must then be in  $\mathbb{F}_1^n$ . This is a contradiction to  $\mathbb{F}_1^n \cap V(\mathcal{I}) = \emptyset$ . □



**Figure 60:** Left: The set of valid motions of the turquoise piece in the swap can be contracted to a single point. Right: The set of valid motions of the orange piece in the teeter-totter can be contracted to a single point.

### Topological universality.

**Lemma 59.** *Let  $T$  be a compact semi-algebraic set. Then there is an instance  $\mathcal{I} = [\Phi, \delta, (I(x_1), \dots, I(x_n))]$  of RANGE-ETR-INV such that the solution space  $V(\Phi)$  is homotopy equivalent to  $T$ .*

*Proof.* This follows directly from Theorem 29, as rational equivalence is stronger than homotopy equivalence.  $\square$

**Theorem 22.** *Let  $T$  be a compact semi-algebraic set, and let  $P$  be one of the packing problems indicated as  $\exists\mathbb{R}$ -complete in Table 1. Then there is an instance  $(\mathbf{p}, C)$  of  $P$  such that  $T$  is homotopy equivalent to the solution space  $V(\mathbf{p}, C)$ .*

*Proof.* Due to Lemma 59, we can assume that  $T$  is described by a RANGE-ETR-INV instance  $\mathcal{I} = [\Phi, \delta, (I(x_1), \dots, I(x_n))]$ . Using the transformation from Theorem 4, we get a packing instance  $\mathcal{I}' = (\mathbf{p}, C)$  of  $P$ . Due to Lemma 6, we know that all valid placements are canonical. In particular, the proof of Lemma 6 defines for every  $x \in V(\mathcal{I})$  a canonical motion  $f(x) \in V(\mathcal{I}')$ , where we require the rotation matrices encoded by  $f(x)$  to be normalized. As  $x$  changes continuously, the motions of the pieces  $f(x)$  also changes continuously, so  $f$  is continuous. This mapping is not surjective as will be explained in detail below. However, we can define a natural continuous inverse  $f^{-1}: f(V(\mathcal{I})) \rightarrow V(\mathcal{I})$ , so we get that  $V(\mathcal{I})$  is homotopy equivalent to  $f(V(\mathcal{I}))$ .

Recall that Lemma 20 states that every valid placement is also canonical. This implies that the only reasons that  $f$  is not surjective are as follows: 1) There are non-variable pieces that have freedom to move. 2) We allow non-normalized rotation matrices in the solution space  $V(\mathcal{I}')$ . We go through these cases in the following to show that the full solution space  $V(\mathcal{I}')$  is homotopy equivalent to  $f(V(\mathcal{I}))$ .

First, note that the pieces that have freedom to move are the turquoise pieces in the swaps and gramophones, the orange pieces in the teeter-totters and the orange pieces in the exterior construction. In all cases locally, we can contract the part of the solution space representing these placements to a single point. See Figure 60 for an illustration.

Second, we need to show that we can contract the solutions in  $V(\mathcal{I}')$  where the rotation matrices are not normalized to the solutions where they are. For this let us fix some piece  $p$  and a valid placement of all the pieces. The placement of  $p$  is represented by many valid motions, since we do not require rotation matrices to be normalized. By scaling the matrices

continuously to reach a normalized matrix, we can however contract the space of motions of  $p$  to the motion where the matrix is normalized.

We can now conclude that  $f(V(\mathcal{I}))$  is homotopy equivalent to  $V(\mathcal{I}')$ , and hence that  $T$  is homotopy equivalent to  $V(\mathcal{I}')$ .  $\square$

## 11 References

- [1] Zachary Abel, Erik D. Demaine, Martin L. Demaine, Sarah Eisenstat, Jayson Lynch, and Tao B. Schardl. Who needs crossings? Hardness of plane graph rigidity. In *32nd International Symposium on Computational Geometry (SoCG 2016)*, pages 3:1–3:15, 2016.
- [2] Mikkel Abrahamsen, Anna Adamaszek, and Tillmann Miltzow. The art gallery problem is  $\exists\mathbb{R}$ -complete. In *STOC*, pages 65–73, 2018.
- [3] Anna Adamaszek, Tomasz Kociumaka, Marcin Pilipczuk, and Michał Pilipczuk. Hardness of approximation for strip packing. *ACM Trans. Comput. Theory*, 9(3), September 2017.
- [4] Anna Adamaszek and Andreas Wiese. A quasi-PTAS for the two-dimensional geometric knapsack problem. In *Proceedings of the twenty-sixth annual ACM-SIAM Symposium on Discrete Algorithms (SODA 2014)*, pages 1491–1505, 2014.
- [5] Alfred V. Aho, John E. Hopcroft, and Jeffrey D. Ullman. *The design and analysis of computer algorithms*. Addison-Wesley, 1975.
- [6] Helmut Alt. Computational aspects of packing problems. *Bulletin of the EATCS*, 118, 2016.
- [7] Nikhil Bansal and Arindam Khan. Improved approximation algorithm for two-dimensional bin packing. In *Proceedings of the Twenty-Fifth Annual ACM-SIAM Symposium on Discrete Algorithms (SODA 2014)*, pages 13–25, 2014.
- [8] Saugata Basu and Marie-Françoise Roy. Bounding the radii of balls meeting every connected component of semi-algebraic sets. *Journal of Symbolic Computation*, 45(12):1270–1279, 2010.
- [9] Julia Bennell and Jose Oliveira. The geometry of nesting problems: A tutorial. *European Journal of Operational Research*, 184(2):397–415, 2008.
- [10] Julia Bennell and Jose Oliveira. A tutorial in irregular shape packing problems. *Journal of the Operational Research Society*, 60:S93–S105, 2009.
- [11] Marie Louisa Tølbøll Berthelsen and Kristoffer Arnsfelt Hansen. On the computational complexity of decision problems about multi-player Nash equilibria. In *International Symposium on Algorithmic Game Theory*, pages 153–167. Springer, 2019.
- [12] Therese Biedl. Segment representations with small resolution. *Information Processing Letters*, 153:105868, 2020.
- [13] Daniel Bienstock. Some provably hard crossing number problems. *Discrete & Computational Geometry*, 6(3):443–459, 1991.
- [14] John Canny. Some algebraic and geometric computations in PSPACE. In *Proceedings of the twentieth annual ACM symposium on Theory of computing (STOC 1988)*, pages 460–467. ACM, 1988.
- [15] Jean Cardinal. Computational geometry column 62. *SIGACT News*, 46(4):69–78, 2015.
- [16] Jean Cardinal, Stefan Felsner, Tillmann Miltzow, Casey Tompkins, and Birgit Vogtenhuber. Intersection graphs of rays and grounded segments. In *International Workshop on Graph-Theoretic Concepts in Computer Science*, pages 153–166. Springer, 2017.

- [17] Jean Cardinal and Udo Hoffmann. Recognition and complexity of point visibility graphs. *Discrete & Computational Geometry*, 57(1):164–178, 2017.
- [18] Fan Chung and Ron Graham. Efficient packings of unit squares in a large square. *Discrete & Computational Geometry*, 2019.
- [19] Erik D. Demaine, Sándor P. Fekete, and Robert J. Lang. Circle packing for origami design is hard, 2010. Preprint <https://arxiv.org/pdf/1008.1224.pdf>.
- [20] Michael Gene Dobbins, Andreas Holmsen, and Tillmann Miltzow. A universality theorem for nested polytopes. 2019. Preprint, [arxiv.org/abs/1908.02213](https://arxiv.org/abs/1908.02213).
- [21] Michael Gene Dobbins, Linda Kleist, Tillmann Miltzow, and Paweł Rzażewski.  $\forall\exists\mathbb{R}$ -completeness and area-universality. In *Proceedings of the 44th International Workshop on Graph-Theoretic Concepts in Computer Science (WG 2018)*, pages 164–175, 2018.
- [22] Harald Dyckhoff and Ute Finke. *Cutting and packing in production and distribution: A typology and bibliography*. Springer Science & Business Media, 1992.
- [23] Paul Erdős and Ron Graham. On packing squares with equal squares. *Journal of Combinatorial Theory, Series A*, 19(1):119–123, 1975.
- [24] Jeff Erickson. Optimal curve straightening is  $\exists\mathbb{R}$ -complete. *arXiv:1908.09400*, 2019.
- [25] Jeff Erickson, Ivor van der Hoog, and Tillmann Miltzow. A framework for robust realistic geometric computations. *ArXiv*, abs/1912.02278, 2019.
- [26] Fedor V. Fomin and Vladimir V. Podolskii, editors. *Complexity and Inapproximability Results for Parallel Task Scheduling and Strip Packing*, 2018.
- [27] Waldo Gálvez, Fabrizio Grandoni, Sandy Heydrich, Salvatore Ingala, Arindam Khan, and Andreas Wiese. Approximating geometric knapsack via L-packings. In *2017 IEEE 58th Annual Symposium on Foundations of Computer Science (FOCS 2017)*, pages 260–271, 2017.
- [28] Jugal Garg, Ruta Mehta, Vijay V. Vazirani, and Sadra Yazdanbod. ETR-completeness for decision versions of multi-player (symmetric) Nash equilibria. In *Proceedings of the 42nd International Colloquium on Automata, Languages, and Programming (ICALP 2015), part 1*, volume 9134 of *Lecture Notes in Computer Science (LNCS)*, pages 554–566, 2015.
- [29] Thierry Gensane and Philippe Ryckelynck. Improved dense packings of congruent squares in asquare. *DCG*, 34(1):97–109, 2005.
- [30] Thomas Hales. A proof of the Kepler conjecture. *Annals of mathematics*, pages 1065–1185, 2005.
- [31] Rolf Harren, Klaus Jansen, Lars Prädell, and Rob [van Stee]. A  $(5/3 + \varepsilon)$ -approximation for strip packing. *Computational Geometry*, 47(2, Part B):248–267, 2014.
- [32] Sören Henning, Klaus Jansen, Malin Rau, and Lars Schmarje. Complexity and inapproximability results for parallel task scheduling and strip packing. *Theory Comput. Syst.*, 64(1):120–140, 2020.
- [33] Sandy Heydrich and Andreas Wiese. Faster approximation schemes for the two-dimensional knapsack problem. *ACM Transactions on Algorithms (TALG)*, 15(4):1–28, 2019.



- [34] Eva Hopper and Brian Turton. A review of the application of meta-heuristic algorithms to 2D strip packing problems. *Artificial Intelligence Review*, 16(4):257–300, 2001.
- [35] Klaus Jansen and Malin Rau. Closing the gap for pseudo-polynomial strip packing. In *27th Annual European Symposium on Algorithms (ESA 2019)*, pages 62:1–62:14, 2019.
- [36] Klaus Jansen and Roberto Solis-Oba. Rectangle packing with one-dimensional resource augmentation. *Discrete Optimization*, 6(3):310–323, 2009.
- [37] Klaus Jansen and Guochuan Zhang. On rectangle packing: Maximizing benefits. In *Proceedings of the Fifteenth Annual ACM-SIAM Symposium on Discrete Algorithms (SODA 2004)*, pages 204–213, 2004.
- [38] Ross J. Kang and Tobias Müller. Sphere and dot product representations of graphs. In *SoCG*, pages 308–314. ACM, 2011.
- [39] Heuna Kim and Tillmann Miltzow. Packing segments in a simple polygon is APX-hard. In *European Conference on Computational Geometry (EuroCG 2015)*, pages 24–27, 2015. <http://eurocg15.fri.uni-lj.si/pub/eurocg15-book-of-abstracts.pdf>.
- [40] Linda Kleist. *Planar graphs and faces areas – Area-Universality*. PhD thesis, 2018. PhD thesis, Technische Universität Berlin, [dx.doi.org/10.14279/depositonce-7674](https://dx.doi.org/10.14279/depositonce-7674).
- [41] Aline A.S. Leao, Franklina M.B. Toledo, José Fernando Oliveira, Maria Antónia Carravilla, and Ramón Alvarez-Valdés. Irregular packing problems: A review of mathematical models. *European Journal of Operational Research*, 282(3):803 – 822, 2020.
- [42] Joseph Leung, Tommy Tam, Chin Wong, Gilbert Young, and Francis Chin. Packing squares into a square. *Journal of Parallel and Distributed Computing*, 10(3):271–275, 1990.
- [43] Anna Lubiw, Tillmann Miltzow, and Debajyoti Mondal. The complexity of drawing a graph in a polygonal region. In *Proceedings on the 26th International Symposium on Graph Drawing and Network Visualization (GD 2018)*, pages 387–401, 2018.
- [44] Jiří Matoušek. Intersection graphs of segments and  $\exists\mathbb{R}$ . 2014. Preprint, <https://arxiv.org/abs/1406.2636>.
- [45] Colin McDiarmid and Tobias Müller. Integer realizations of disk and segment graphs. *Journal of Combinatorial Theory, Series B*, 103(1):114–143, 2013.
- [46] Nicolai E Mnëv. The universality theorems on the classification problem of configuration varieties and convex polytopes varieties. In Oleg Y. Viro, editor, *Topology and geometry – Rohlin seminar*, pages 527–543. Springer-Verlag Berlin Heidelberg, 1988.
- [47] Giorgi Nadiradze and Andreas Wiese. On approximating strip packing with a better ratio than  $3/2$ . In *Proceedings of the twenty-seventh annual ACM-SIAM Symposium on Discrete Algorithms (2016)*, pages 1491–1510, 2016.
- [48] Jürgen Richter-Gebert and Günter M. Ziegler. Realization spaces of 4-polytopes are universal. *Bulletin of the American Mathematical Society*, 32(4):403–412, 1995.
- [49] Marcus Schaefer. Complexity of some geometric and topological problems. In *Proceedings of the 17th International Symposium on Graph Drawing (GD 2009)*, volume 5849 of *Lecture Notes in Computer Science (LNCS)*, pages 334–344. Springer, 2009.

- [50] Marcus Schaefer. Realizability of graphs and linkages. In János Pach, editor, *Thirty Essays on Geometric Graph Theory*, chapter 23, pages 461–482. Springer-Verlag New York, 2013.
- [51] Marcus Schaefer and Daniel Štefankovič. Fixed points, Nash equilibria, and the existential theory of the reals. *Theory of Computing Systems*, 60(2):172–193, 2017.
- [52] Yaroslav Shitov. A universality theorem for nonnegative matrix factorizations. 2016. Preprint, <https://arxiv.org/abs/1606.09068>.
- [53] Yaroslav Shitov. The complexity of positive semidefinite matrix factorization. *SIAM Journal on Optimization*, 27(3):1898–1909, 2017.
- [54] Peter W. Shor. Stretchability of pseudolines is NP-hard. In Peter Gritzmann and Bernd Sturmfels, editors, *Applied Geometry and Discrete Mathematics: The Victor Klee Festschrift*, volume 4 of *DIMACS – Series in Discrete Mathematics and Theoretical Computer Science*, pages 531–554. American Mathematical Society and Association for Computing Machinery, 1991.
- [55] Paul Sweeney and Elizabeth Ridenour Paternoster. Cutting and packing problems: a categorized, application-orientated research bibliography. *Journal of the Operational Research Society*, 43(7):691–706, 1992.
- [56] László Fejes Tóth. Über die dichteste kugellagerung. *Mathematische Zeitschrift*, 48:676–684, 1942.